Synthesis of silver nanoparticles and their role against a thiazolekinase enzyme from *Plasmodium falciparum*

A thesis submitted in fulfilment of the requirements for the degree of

Master of Science

Department of Biochemistry, Microbiology and Biotechnology

Faculty of Science

Rhodes University

By

Jia Yao

November, 2013

Supervisor: Prof. C. Whiteley

Abstract

Malaria, a mosquito-borne infectious disease, caused by the protozoan *Plasmodium* genus, is the greatest health challenges worldwide. The plasmodial vitamin B_1 biosynthetic enzyme *Pf*ThzK diverges significantly, both structurally and functionally from its counterpart in higher eukaryotes, thereby making it particularly attractive as a biomedical target. In the present study, *Pf*ThzK was recombinantly produced as 6×His fusion protein in *E. coli* BL21, purified using nickel affinity chromatography and size exclusion chromatography resulting in 1.03% yield and specific activity 0.28 U/mg. The enzyme was found to be a monomer with a molecular mass of 34 kDa. Characterization of the *Pf*ThzK showed an optimum temperature and pH of 37 ℃ and 7.5 respectively, and it is relatively stable ($t_{1/2}$=2.66 h). Ag nanoparticles were synthesized by $NaBH_4$/tannic acid, and characterized by UV-vis spectroscopy and transmission electron microscopy. The morphologies of these Ag nanoparticles (in terms of size) synthesized by tannic acid appeared to be more controlled with the size of 7.06±2.41 nm, compared with those synthesized by $NaBH_4$, with the sized of 12.9±4.21 nm. The purified *Pf*ThzK was challenged with Ag NPs synthesized by tannic acid, and the results suggested that they competitively inhibited *Pf*ThzK (89 %) at low concentrations (5-10 μM) with a K_i = 6.45 μM.

Keywords: **Ag nanoparticles, synthesis, methylhydroxyethylthiazolekinase (*Pf*ThzK)**

Declaration

I, Jia Yao, hereby declare that this thesis is my own, unaided work. It is being submitted for the degree of Master of Science at Rhodes University. It has not been submitted before for any other degree or examination in any other university.

_____ _____

Author's Signature Date

Table of Contents

List of Abbreviations

µg	Microgram
µM	Micromolar (µmoles/litre)
µL	Microlitre
µmol	Micromole
6×His-tag	Hexahistidine purification tag
A	Absorbance
Ag	Silver
BCA	Bicinchoninic acid
bp	Base pair
CAM	Chloramphenicol
Da	Dalton
DMSO	Dimethyl sulfoxide
DNA	Deoxyribonucleic acid
E. coli	*Escherichia coli*
EDTA	Ethylenediaminetetraacetic acid
FPLC	Fast protein liquid chromatography
HIV	Human immunodeficiency virus
k_{cat}	Enzyme turn-over number
kDa	Kilodalton
K_i	Inhibitor constant
K_m	Michaelis-Menten constant

NPs	Nanoparticles
PCR	Polymerase chain reaction
PEG	Polyethylene glycol
SEM	Scanning electron microscopy
SDS	Sodium dodecyl sulphate
SDS-PAGE	Sodium dodecyl sulphate polyacrylamide gel electrophoresis
TEM	Transmission electron microscopy
UV-vis	Ultraviolet-visible

Acknowledgements

I would like to acknowledge and thank the following people for their support and contributions during this study:

- My supervisor, Professor Christopher Whiteley, for his unfailing dedication, academic and emotional support.
- Rhodes University and National Research Foundation for financial assistance.
- Our lab manager, Dr Jacqueline van Marwijk, for her scientific contributions and continued support to this work.
- Dr Brendan Wilhelmi, for his support and encouragement.
- Members of Lab 129C, for their assistance, encouragement and friendship.
- Members of the Department of Biochemistry, Microbiology and Biotechnology of Rhodes University, especially to Mrs Margot Brooks and Mr Sagaran Abboo.
- My family, for their endless love and encouragement.

List of outputs

Local conferences proceedings:

Yao, J., van Marwijk, J. and Whiteley, C. G. The role of silver nanoparticles against a thiazolekinase from *Plasmodium falciparum*. *SASBMB 2012 Conference,* Drakensberg, Champagne Sport Resort, 29 January - 01 February.

Chapter 1
Literature review

1.1. Malaria

Malaria, a mosquito-borne infectious disease, caused by the protozoan *Plasmodium* genus, especially by four species, *P. falciparum*, *P. vivax*, *P. malariae* and *P. ovale*, is the greatest health challenges worldwide. Malaria is becoming the most prevalent parasitic disease in the world. In 2006, there were an estimated 247 million malaria episodes causing over 1.25 million deaths, of which 86% were in Africa (Gardella *et al*., 2008). Around 80% of malaria cases in Africa were in 13 countries in 2006, and approximately 109 countries were endemic for malaria in 2008, 45 of which were in Africa. There were an estimated 216 million malaria episodes worldwide in 2010, and 81% of those cases occurred in Africa, followed by South East Asia with 13%, and Eastern Mediterranean regions with 5%. There were an estimated 655 thousand malaria deaths in the world in 2010, and 91% of those were in Africa region, followed by South East Asia with 6% and Eastern Mediterranean with 3%; about 86% of these cases were children under 5 years old (WHO[1], 2012). The reason for such high morbidity and death rate in Africa is because 91% of these cases were due to *P. falciparum*, the most prevalent of the four malarial parasites. As shown in Figure 1.1, Africa, South-East Asia, Eastern Mediterranean and South America regions were the most affected areas in the world by 2011. As people migrated, there was an increase of globalization in business and commerce, and also an increase in travel with more and more people from malaria-free

countries being exposed to the disease. It is reported that every year about 25 thousand travelers return with malaria after visiting endemic countries, and 0.4% of these die from the infection (Gyang, 2009).

The number of global malaria episodes has risen from 223 million in 2000 to 237 million cases in 2005, and the estimation of the world population that is at risk with malaria has recently been challenged using a combination of data (Table 1.1). It was indicated that there were more than 500 million episodes of clinical malaria, from *P. falciparum* in 2002, which was considerably higher than the 400 million cases reported by the World Health Organization (WHO[1], 2012).

Table 1.1. Estimates of malaria cases and deaths by WHO Region, 2011.
Source: World Health Organization 2012.

	Estimated cases ('000s)				Confirmed cases reported	Reported/estimated
Region	Estimate	Lower	Upper	% *P. falciparum*		
Africa	174 000	113 000	239 000	98%	20 000	11%
Americas	1 000	1 000	1 000	34%	1 000	59%
Eastern Mediterranean	10 000	8 000	14 000	82%	1 000	10%
Europe	0.2	0.2	0.2	0%	0.2	87%
South-East Asia	28 000	23 000	35 000	54%	2 000	9%
Western Pacific	2 000	2 000	2 000	77%	257	13%
World	216 000	149 000	274 000	91%	24 000	11%

	Estimated deaths			
Region	Estimate	Lower	Upper	% <5
Africa	596 000	468 000	837 000	91%
Americas	1 000	1 000	2 000	29%
Eastern Mediterranean	15 000	1 000	38 000	60%
Europe	0	0	0	4%
South-East Asia	38 000	28 000	50 000	31%
Western Pacific	5 000	3 000	6 000	41%
World	655 000	537 000	907 000	86%

There are several reasons that contribute to the increasing malarial burden. First, it is the drug resistance. In Africa and part of Southeast Asia, *P. falciparum* is resistant to almost all the antimalarial drugs and *P. vivax* is almost chloroquine resistant. Second, it is insecticide resistance. Third, it is climatic changes. Global warming may contribute to the spread of the malaria vector into some non-endemic countries. Fourth, it is travel. Travel from malaria-free countries to malarial endemic countries is an increasingly important cause of malaria. As every year, in Europe, approximately 7 thousand imported malarial cases have been reported (Behrens *et al*., 2008).

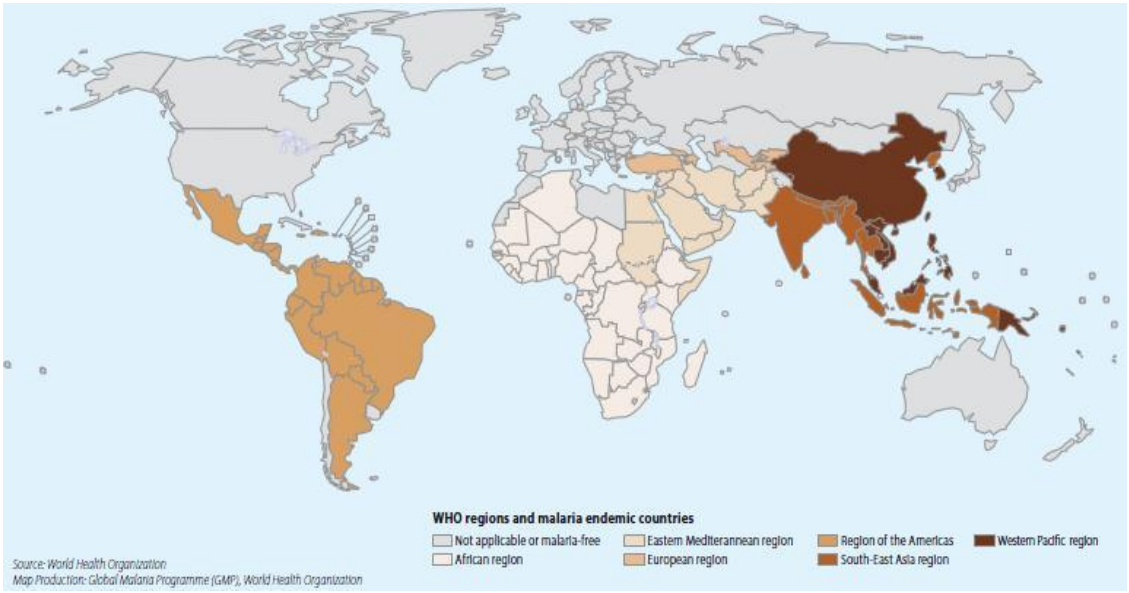

Figure 1.1. Malaria affected countries, prevention of reintroduction countries and malaria-free countries at the end of 2011.
Source: World Health Organization 2012.

1.1.1. Life-cycle of malaria

Malaria is transmitted to humans by the bite of the female *Anopheles* mosquito vector. The female *Anopheles* mosquito injects approximately 15-20 sporozoites each time which

then migrate to the liver within a few minutes and invade the hepatocytes by an unknown mechanism, to form hepatic schizonts (Lindner *et al*., 2012).

A sporozoite of *P. falciparum* generates about 30,000 new parasites, which develop slowly in liver cells into hypnozoites, which remain for months in the tissue. These hypnozoites could induce new relapses of the disease up to two years after the initial infection. Meanwhile, the asexual blood stages (late trophozoites and schizonts) of the parasite are the main etiological agents in malaria, causing the symptoms of the disease to appear about two weeks after the mosquito-vectored sporozoite injection (WHO[2], 2006). These asexual stages are the main target of the antimalarial drugs (Wells *et al*., 2009). The schizonts rupture to form merozoites, which are released into the bloodstream where they enter the red blood cells, and remain relatively inactive metabolically for about 10–15 hours. The parasite then undergoes a rapid growth phase over the next 25 hours, constituting the trophozoite stage, digesting the majority of the hemoglobin and growing to fill more than 50% of the volume of the host cells. It takes 1-2 weeks for hepatic schizonts to rupture, and the young trophozoites to consume the hemoglobin in the red cells and to develop into schizonts and eventually to rupture, and release more merozoites to invade more blood cells, and cause fever symptoms. At the end of the trophozoite stage, the parasite divides several times (the schizont stage) before the host cell lyses to release the newly formed merozoites that continue the cycle (See Figure 1.2). This concerted cell lysis results in the classical malaria symptoms, which are mainly headache, periodically recurrent high fever (every 48–72 hours), myalgia, anemia, hepatitis and splenomegaly (Santos-Magalhaes *et al*., 2010). Moreover, neurological symptoms may occur resulting in death in the case of severe *P. falciparum* infection.

After several asexual life-cycles, certain parasites develop into sexual forms. In *P. falciparum* malaria, it takes approximately 10 days to produce gametocytes. A female *Anopheles* mosquito fuses the male and female gametocytes in their midgut to form a zygote, and the zygote eventually develops new sporozoits to complete the whole life-cycle. In *P. vivax* and *P. ovale* malarias a few of the sporozoites in the liver remain as dormant hypnozoites that may cause a relapse of malaria after several years. In contrast, the *P. malariae* malarias do not have the hypnozoite stages but may remain in the blood for several years.

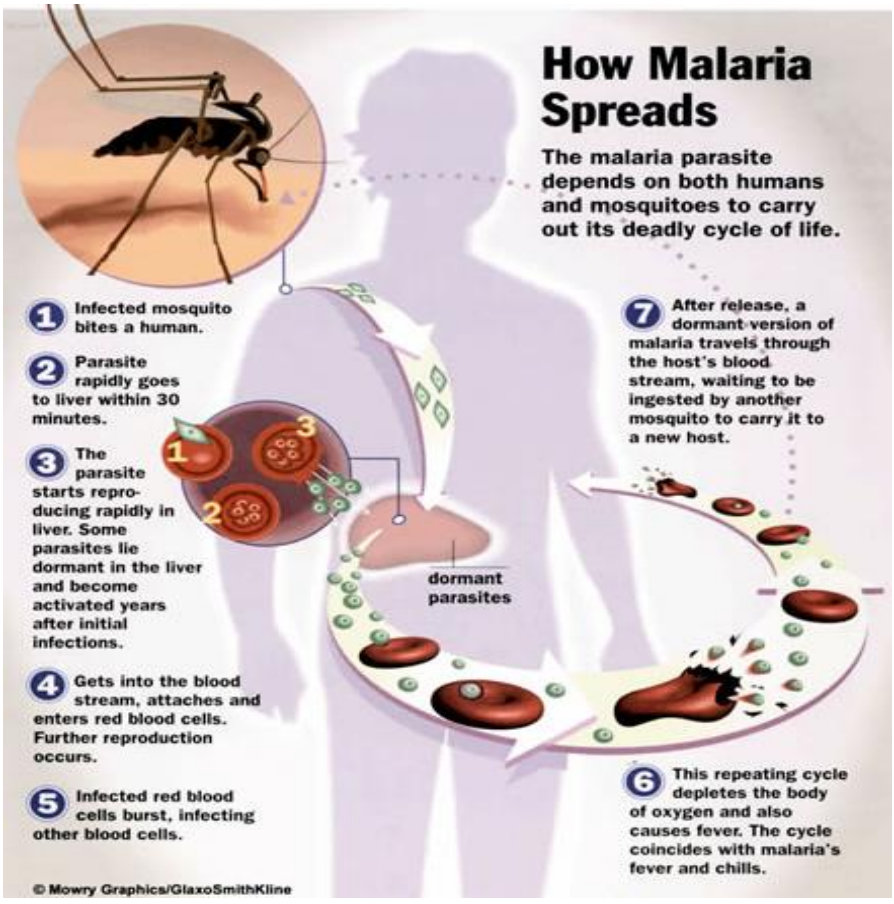

Figure 1.2. Life-cycle of malaria.
Source: http://www.travelhealth.co.uk/diseases/malaria_lifcycle.htm

1.1.2. Strategies for malaria control

Strategy for the control of malaria is to reduce the malaria disease burden to a level, which is no longer a problem to public health. These include vector control with residual insecticide spraying, larva control and personal protection, such as insecticide treated bednets and insect repellent spray (Rozendaal, 1997). Studies on the development of an effective malaria vaccine and a transgenic mosquito which cannot transmit malaria are ongoing but neither is likely to be available soon.

The antimalarial drugs commonly used are classified as 5 compounds: quinolines and aryaminoalcohols, the antifols, the artemisinin derivatives, the hydroxynaphtha-quinones and antibacterial agents.

Quinolines and aryaminoalcohols include amodiaquine, chloroquine, quinine and mefloquine. Quinine is an ancient drug and is used for the treatment of severe malaria especially that from *P. falciparum*. Side-effects, however, are quite common, including hearing impairment (van Huyssteen, 2010), dizziness and vertigo (Croft *et al.*, 2001). Quinine may cause hypoglycaemia and renal failure (Trampuz *et al*., 2003). Chloroquine is especially used against the mature trophozoite stage, but extensive resistant has recently been reported (Olliaro, 2001). Side-effects include headache, hair loss, convulsions (Deen *et al.*, 2008), and it is also known to stimulate psoriasis in some cases (Ferreira, 2010), it is considerably toxic in an overdose and can induce severe cardiac arrhythmias.

Antifols are folate biosynthesis inhibitors, and include pyrimethamine, proguanil, chloroproguanil and trimethoprim. Pyrimethamine and proguanil act as prodrugs to

inhibit plasmodial dihydrofolate reductase (DHFR). Pyrimethamine and proguanil should be used in combination with sulpha drugs because resistance can be developed quickly if it is issued alone (Gregson and Plowe, 2005). Pyrimethamine and proguanil induce abdominal pain, vomiting and diarrhoea (Hatz, 2001).

Artemisinin derivatives include artemisinin, dihydroartemisinin and artesunate. These drugs were originally derived from *Artemisia annua*, and were used in traditional Chinese medicine for fever a thousand years ago. These drugs act fast, and are the most commonly used for the treatment of malaria, nowadays. Side-effects such as mild gastrointestinal disturbances (Sevene *et al*., 2010), dizziness and tinnitus (Ehrhardt and Meyer, 2009), have been reported, but in general these drugs are extremely tolerated. The only weakness of these drugs is that they are only suitable to treat uncomplicated malaria because of the short half-life (Ndiaye *et al*., 2011).

Antibacterial drugs are those with antimalarial activity, such as clindamycin and tetracyclines. These drugs are weak antimalarials that act slowly, and could only be used in combination with other drugs (Nosten *et al*., 2006). They commonly induce gastrointestinal effects, such as vomiting and diarrhoea (van Boxtel, 2001). Rashes and drug fever have been also been reported, along with haemolytic anaemia.

1.1.3. Genomic field for malaria investigation

Due to the complexity of the parasites life cycle and the development of drug resistance (WHO[2], 2008), it is really essential to work out novel drug targets and develop new chemotherapeutics. The publication of the *P. falciparum* genome sequence in 2002 (Gardner *et al*., 2002), and that of *P. vivax* in 2008 (Dharia *et al.*, 2010) opened a new

door with the genomic knowledge to understand the malaria pathogens and also provide new tools to develop malaria therapy. These genome sequences can be investigated to describe biological pathways and also hypothesize possible functions for malaria genes. The database research allow people to identify novel biological pathways present in the parasite and so far give people an idea about interesting targets for subsequent research. The isoprenoids biosynthesis pathway in the parasite was identified by the genomic sequence information (Ralph *et al*., 2004), and subsequently, the *Pfdxr* gene was identified as a target of fosmidomycin resistance (Zhang *et al*., 2011).

According to the predominantly intracellular life cycle of *P. falciparum*, interfering with the salvage system for cofactors and metabolites could be a possible target (Huthmacher *et al*., 2006; Muller *et al*., 2010) with the life cycle of mosquito being disrupted, and the malarial parasite being controlled. One possible target is the thiamine metabolizing enzyme responsible for the synthesis of B group vitamins such as vitamin B_1, B_6 and B_9. Humans cannot synthesize the vitamin and require it as an additive form within their diet. Bacteria, fungi, plants and the malarial parasite, on the other hand, possess a biosynthetic pathway for the vitamin incorporating the thiamine metabolizing enzymes (Muller *et al*., 2009).

Vitamin B_1 exists ubiquitously in all organisms as a cofactor for carbohydrate metabolism (Muller and Kappes, 2007; Knockel, 2008). The biosynthetic pathway of vitamin B_1 in *Escherichia coli* and *Saccharomyces cerevisiae* is fully understood (Sprenger *et al*., 1997; Himmeldirk *et al*., 1998; Settembre *et al*., 2003; Nosaka, 2006). The plasmodial pathway identified three vitamin B_1 biosynthetic enzymes: a) 5-(2-hydroxy-ethyl)-4-methylthiazole (THZ) kinase (ThiM or *Pf*ThzK); b) 4-amino-5-hydroxymethyl-2-

methylpyrimidine (HMP) HMP-P kinase (ThiD) and c) thiaminephosphate synthase (ThiE) (Figure 1.3).

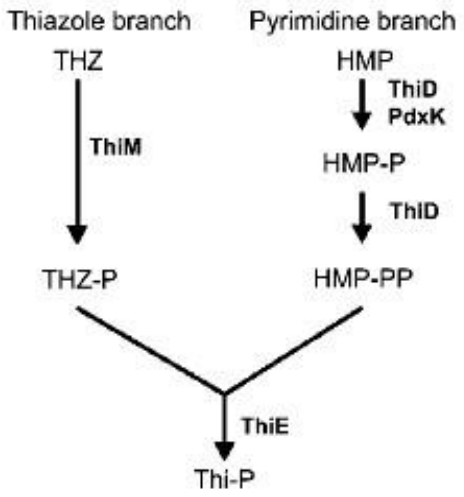

Figure 1.3. Reaction scheme of the enzymes involved in thiamine phosphate biosynthesis.
(Wrenger, 2006)

Two independent synthesis branches are combined in the biosynthesis of thiamine. The biosynthesis of thiamine phosphate is divided into two branches, the thiazole branch and the pyrimidine branch. In *E. coli*, the precursor of pyrimidine branch is 4-amino-5-hydroxymethyl-2-methylpyrimidine (HMP), which has to be phosphorylated in two steps to 4-amino-2-methyl-5-hydroxymethyl pyrimidine diphosphate (HMP-PP) by HMP/HMP-P kinase (ThiD). The first phosphorylation, however, can also be effected by pyridoxine kinase (PdxK), which is involved in the activation of vitamin B_6, as demonstrated for the parasites *Trypanosoma brucei* and *P. falciparum* (Yang *et al*., 1998; Besteiro *et al*., 2002; Cassera *et al*., 2004; Bozdech and Ginsburg, 2005; Rapala-Kozik *et al*., 2007; Knockel *et al*., 2008; Muller *et al*., 2010). HMP itself is synthesized in bacteria

by the HMP biosynthesis enzyme, whereas it has been suggested that in eukaryotes pyridoxine and histidine are possibly bonded to HMP (Webb *et al*., 2007; Jurgenson *et al*., 2009). The thiamine biosynthesis branch starts with 5-(2-hydroxyethyl)-4-methylthiazole (THZ), which is converted by THZ kinase (ThiM) to 4-methyl-5-(2-phosphoethyl)-thiazole (THZ-P). Finally, the thiazole and pyrimidine moieties, HMP-PP and THZ-P, are merged to form thiamine phosphate (Thi-P) by thiamine phosphate synthase (ThiE) (Wrenger *et al*., 2006; Jurgenson *et al*., 2009).

To develop new antimalarial drugs, several rules must be considered. These novel drugs should only target the parasite, with no or harmless effects on the human host. An example of this would be the enzymes involved in vitamin biosynthesis pathways which are absent in the host. One promising target is the thiamine metabolizing enzyme methylhydroxyethylthiazolekinase from *P. falciparum* (*Pf*ThzK), which diverges significantly, both structurally and functionally from its counterpart in higher eukaryotes, thereby making it particularly attractive as a biomedical target (Wrenger *et al*., 2006).

1.2. Nanotechnology

The term ‘nano’ is adapted from the Greek word meaning ‘dwarf’, when used as a prefix, it implies 10^{-9}. A nanometer (nm) is one billionth of a meter, or roughly the length of three atoms side by side. The research of nanotechnology often centres around three primary studies and applied science: nano-materials, nano-instrumentation and nano-medicine. Nanotechnology refers to the study of particles that can be classified as a certain number below sizes of 100 nm, often on a molecular or atomic scale. A DNA molecule is 2.5 nm wide, a protein approximately 50 nm, and a flu virus about 100 nm, a

human hair is approximately 10,000 nm thick. By comparing the scale and size of known objects one is able to grasp the concept of nanotechnological research (Figure 1.4) (Keiper, 2003; Du Mont, 2008; Toumey, 2010). Nanotechnology involves the design, synthesis, and characterization of materials and devices that have a functional organization in at least one dimension on the nanometer scale ranging from a few nm up to 100 nm (Chen and Li, 2007; Tasker *et al*., 2007; Varadan *et al*., 2008; Thakkar *et al*., 2010; Shrestha, 2012).

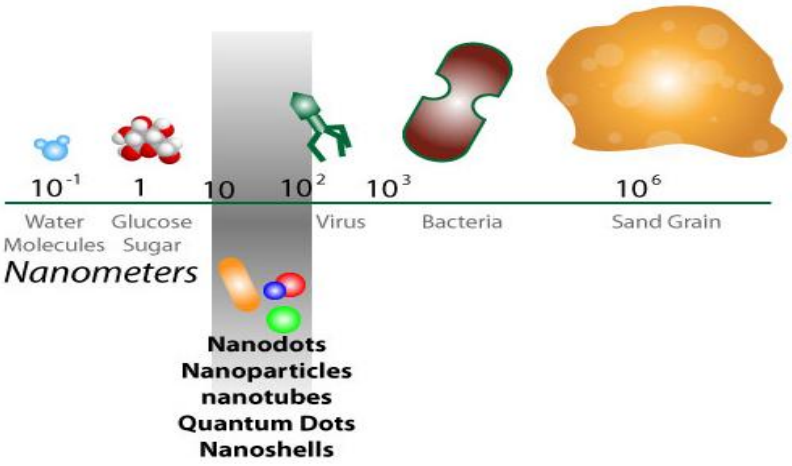

Figure 1.4. Nanoscale and examples of objects of different sizes. (http://angiebiotech.com/nanotechnology-nanoparticle-fight-infection/)

1.2.1. Nanomaterials and nanoparticles

Nanomaterials are those materials with unique physical properties derived from the inherent nanoscale dimensions, and leading to large surface to volume ratio (Barth *et al*., 2005). The term nanoparticle is often mentioned interchangeably with nanomaterial but typically defines the individual molecules that make up the nanomaterial in bulk. Nanoparticles are really of scientific interest because they connect bulk materials and atomic or molecular structures (Martin *et al*., 2006). There are many reasons for this, one

being the fact that nanoparticles possess a very high surface-to-volume aspect ratio. In the case of silver nanoparticles (AgNPs), this allows them to easily interact with other particles and to increase their antibacterial efficiency (Ju-Nam and Lead, 2008; Zhang *et al*., 2008; Veerapandian and Yun, 2011; Wu *et al*., 2011; Wiarachai *et al*., 2012). This effect is extremely robust, and as little as 1 g of AgNPs is known to impart antibacterial properties on hundreds of square meters of substrate material. Recently the most investigated nanomaterials include carbon nanomaterials such as fullerenes, nanotubes and buckyballs; quantum dots (QDs); metal nanoparticles such as gold and silver nanoparticles (Burgess, 2012).

1.2.1.1. Fullerenes

Fullerenes are those hollow-cage molecules composed entirely of carbon atoms, in a form of a sphere, an ellipsoid or a tube. They were discovered as a third form of carbon-based molecules besides diamond and graphite as shown in Figure 1.5 (Smalley and Yakobson, 1998). Due to the unique physical and chemical properties of these forms of carbon molecules, a great deal of research on fullerenes technological applications has been carried out, especially on material science and electronics (Satoh *et al*., 1995; Hodak and Girifalco, 2001; Bosi *et al*., 2003; Hayashi *et al*., 2004), even on medical therapeutics such as tumour diagnostics recently (Bakry *et al.,* 2007; Takagi *et al.*, 2008; Lee *et al.*, 2009; Sharma *et al*., 2011; Chen *et al*., 2012). According to the structural variations, fullerenes can be separated into different types, such as buckyballs, nanotubes, megatubes, polymers, and fullerene rings (Ray, 2012).

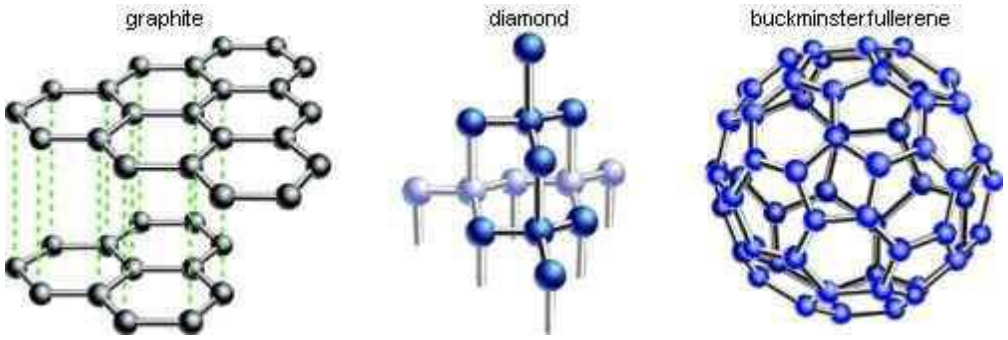

Figure 1.5. The structures of those three different forms of carbon-based molecules: Graphite; Diamond and Fullerene.
(http://www.designanduniverse.com/articles/diamond.php)

The most studied fullerene is C_{60}, also referred to as buckminsterfullerene, which was named after Richard Buckminster Fuller, is the most stable fullerene and also the most abundant in nature (Yadav and Kumar, 2008). The C_{60} fullerene molecule consists of 60 carbon atoms, with a total of 12 pentagons and 20 hexagons, resembles a soccer ball, and all the rings are fused and all double bonds are conjugated. There are 120 symmetrical operations, like the rotations around the axis and reflections in a plane, which makes the C_{60} molecule with the largest symmetrical operations, the most symmetric molecule (Parag and Ashish, 2005). C_{60} fullerene and their derivatives have potential antiviral activity, which has strong implications on the treatment of acquired immunodeficiency syndrome (AIDS), which based on those biological properties including their unique molecular architecture and antioxidant activity (Judd *et al*., 2001; Du Toit *et al*., 2010; Kar and Knecht, 2012). It has been shown that the amino acid derivatives of fullerene C_{60} are potentially to inhibit human immunodeficiency virus (HIV) and human

cytomegalovirus replication (Yu *et al*., 2002; Hegde *et al*., 2006; Bakry *et al*., 2007; Hu *et al*., 2010).

It was reported that fullerenes have potential biological antioxidant property, which is based on the fact that fullerenes possess a great deal of conjugated double bonds and low lying unoccupied molecular orbitals, and easily take up an electron (Mateo-Alonso *et al*., 2006; Witte, 2008; Yeung *et al*., 2011). It was shown that some polar group-derivatized fullerene, such as polyhydroxylated fullerenes and C_{60} tris-acid are able to generate a large amount of oxygen free radicals (Lai *et al*., 2000; Isakovic *et al*., 2006; Markovic and Trajkovic, 2008;), which are necessary to protect cell growth from induced apoptotic injuries (Chen *et al*., 2004; Hu *et al*., 2007; Partha and Conyers, 2009; Rebecca *et al*., 2009; Badireddy *et al*., 2012). Fullerenes have also been investigated for skin cells on cytoprotective action against ultraviolet A radiation recently (Xiao *et al*., 2006; Xiao *et al*., 2010; Saitoh *et al*., 2011).

Carbon nanotubes (CNTs) are carbon sheets rolled up into a nanoscale-tube, including single-wall carbon nanotubes (SWCNTs) and those with additional graphene tubes around the core of an SWCNT named multi-wall CNTs (MWCNTs) shown as Figure 1.6. Three methods were employed to synthesize CNTs so far, including arc-discharge (Hutchison *et al*., 2001; Sugai *et al*., 2003; Keidar *et al*., 2008), laser ablation (Kokal *et al*., 2000; Scott *et al*., 2001) and chemical vapor deposition (Chhowalla *et al*., 2001; Hofmann *et al*., 2003; Reina *et al*., 2008; Kumar and Ando, 2010). For the first two methods, solid-state carbon precursors are used to synthesize nanotube structure, however, producing an excess of by-products. The chemical vapor deposition (CVD) methods employ hydrocarbon gases as carbon atoms sources to nucleate the growth of CNTs with

organized patterns of nanotube structure on surface, comprising both SWCNTs and MWCNTs (Terrones, 2004). The CNTs have been utilized in the construction of various detection devices, such as gas sensors (Li *et al*., 2003; Zhang *et al*., 2006; Du *et al*., 2007), electrochemical detectors (Wang and Musameh, 2003; Cui *et al*., 2007; Meng *et al*., 2009) and biosensors with immobilized biomolecules (Wohlstadter *et al*., 2003; Tripathi *et al*., 2006; Maehashi *et al*., 2007; Sanchez *et al*., 2008).

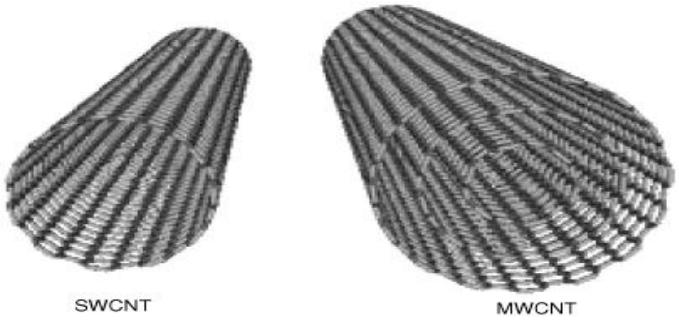

Figure 1.6. The structures of single-wall carbon nanotube (SWCNT) and multi-wall carbon nanotube (MWCNT).
(Scarselli *et al*., 2012)

1.2.1.2. Quantum dots

Quantum dots (QDs) are semiconductor nanocrystals with unique size-dependent optical properties (Hoshino *et al*., 2004), that can emit light in all colours of the spectrum depending on their size (Figure 1.7). Fluorescent QDs are able to be conjugated with bioactive antibodies (Goldman *et al*., 2002; Hoshino *et al*., 2005) or ligands (Gao *et al*., 2004; Sperling *et al*., 2008), to target specific cellular structures, such as peroxisomes (Fu *et al*., 2006), DNA (Fu *et al*., 2004; Raymond *et al*., 2005; Kim *et al*., 2007) and cell membrane receptors (Bannai *et al*., 2007; Smith *et al*., 2008; Yum *et al*., 2009). Bioconjugated QDs are employed as tools for site-specific gene and drug delivery (Suri *et al*., 2007; Mishra *et al*., 2010; Parveen *et al*., 2012) and also explored for the creation

of flat–panel light-emitting diode (LED) displays (Tan *et al*., 2007; Rizzo *et al*., 2007; Jang *et al*., 2010).

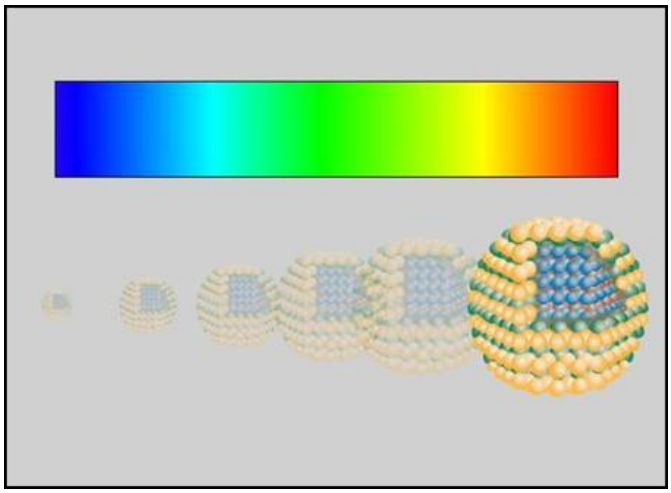

Figure 1.7. The size-dependent spectrum property of Quantum dots. Aerospace Concepts consultant.
(http://www.concepts.aero/system/files/quantum-dots.jpg)

1.2.1.3. Liposome

A liposome is an artificial spherical vesicle with a membrane composed of phospholipids bilayer (Figure 1.8). Liposomes are designed to deliver drug or genetic material into a cell (Shaheen *et al*., 2006; Wasankar *et al*., 2012), and are composed of naturally-derived phospholipids with mixed lipid chain (Kolusheva *et al*., 2000; Goldenbogen *et al*., 2011), or of pure components (Fox *et al*., 2011; Ranjan, 2012). Liposomes are commonly classified into multilamellar vesicles (MLV), large unilamellar vesicles (LUV), and small unilamellar vesicles (SUV), according to their lamellarity and size (Mujoriya *et al*., 2011; Tejera-Garcia *et al*., 2011; Akbarzadeh *et al*., 2013). It has been shown that liposomes can be utilized for plenty of therapeutic areas, such as drug/ protein delivery (Tan *et al*., 2010; Al-Jamal and Kostarelos, 2011; Vivero-Escoto, 2013); antimicrobial, antifungal

and antiviral therapy (Nakonechny *et al*., 2010; Malmsten, 2011; Xu and Burgess, 2012); tumour therapy (Zhang *et al*., 2010; Kueffer *et al*., 2013); gene delivery (Candiani *et al*., 2010; He *et al*., 2010) and immunology (Alving, 2006; Henriksen-Lacey *et al*., 2010; Altin, 2012).

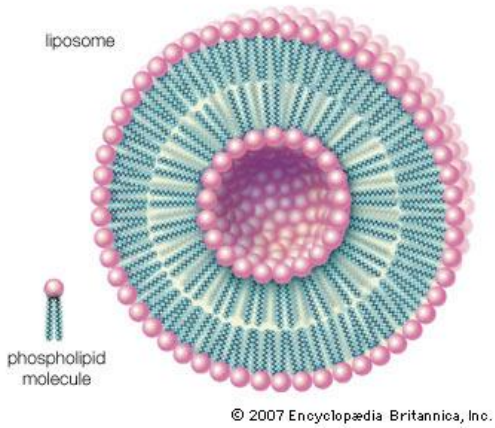

Figure 1.8. The structure of liposome. Encyclopædia Britannica. (http://www.britannica.com/EBchecked/media/92244/Phospholipids-can-be-used-to-form-artificial-structures-called-liposomes)

1.2.2. Metal nanoparticles

It has shown that the properties of metallic nanoparticles differ substantially from their constituent atoms or bulk counterparts, including electronic, physical, and also chemical properties (Rivera-Gil *et al*., 2010; Sau *et al*., 2010; Rivera-Gil *et al*., 2012). Because of their small size, metal nanoparticles have a very large surface area-to-volume ratio, which affects their individual as well as interaction properties (Mahmoudi *et al*., 2011). They also perform a high fraction of edge- and corner-like curved regions, which have more coordinatively unsaturated atoms than the flat surface, leading to higher surface energy and its affections of surface bonding properties and chemical reactivity (Pozun *et al*.,

2011; Zasada *et al*., 2011; Pacchioni and Freund, 2012). Furthermore, one of the motivations of the studies of metallic nanoparticles is their unique optical properties, especially from copper, gold and silver. Metallic nanoparticles can strongly couple with incident light through excitation of their surface plasmon resonances, leading to collective oscillations of the free conduction electrons near the interface between the metal nanoparticle and ambient (Banerjee *et al*., 2010; Paudel and Leuenberger, 2012; Losurdo *et al*., 2013). This coupling leads to unique optical properties, named as localized surface plasmon resonance (LSPR), particularly in gold and silver (Ringe *et al*., 2010; Larguinho and Baptista, 2012).

1.2.2.1. Application of metallic nanoparticles

The optical properties of metal nanoparticles and their arrays have been exploited for a great deal of applications such as controlling the growth of nanoparticles by enhancing optical forces (Messina *et al*., 2011; Ni *et al*., 2012); improving efficiency of photovoltaic devices by increasing light absorption (Atwater and Polman, 2010; Han and Chen, 2010); photothermal destruction of cancer cells (Huang and El-Sayed, 2010; Fan *et al*., 2012) and pathogenic bacteria (Alkilany *et al*., 2012; Rosenberg and Petrie, 2012); enhancement in the sensitivity of sensors and spectroscopies (Margueritat *et al*., 2011; Pryce *et al*., 2011); energy transport and storage (Liu and Lee, 2010; Ferier *et al*., 2012; Solis-Jr *et al*., 2012).

Metal nanoparticles have possible and potential applications in various areas. For example, nanoparticles can be induced to merge into a solid at relatively low temperatures, often without melting, leading to improved and easy-to-create coatings for electronic applications, which are the basic property for capacitors (Thakkar *et al*., 2010;

Sengar and Mehta, 2012). Furthermore, nanoparticles possess a wavelength below the critical light wavelength, that makes them more transparent and useful for applications in cosmetics (Julia and Li, 2011; Chen *et al*., 2012), coatings (Yu *et al*., 2010; Stojanovic *et al*., 2012), and packaging (Jeong *et al*., 2010). Metal nanoparticles can be attached, nondestructively, to single strands of DNA thus opening up avenues for medical diagnostic applications (Poon *et al*., 2010; Busson *et al*., Rosarin and Mirunalini, 2011). Nanoparticles can pass through the vasculature, the blood brain barrier and localize any target organ (Na *et al*., 2011; Krol *et al*., 2012; Wang *et al*., 2012) which can, potentially, lead to novel therapeutic, imaging and biomedical applications.

Table 1.2. Examples of metal nanoparticles potential applications.

Nanoparticles	Applications	References
Copper Metal NPs	Biosensor; drug delivery; Alzheimer's therapeutics	Bracey *et al*., 2009; Liu *et al.*, 2012; Zhang *et al.*, 2013
Gold Metal NPs	Biomarker; biosensors; colouration; drug delivery system; tumour therapeutics	Hong *et al*., 2010; Nash *et al*., 2010; Alhasan *et al*., 2012; Lee *et al*., 2012
Palladium Metal NPs	Biosensor; drug delivery system;	Lu *et al*., 2011; Das *et al*., 2013
Platinum Metal NPs	Biosensor; drug delivery system	Su *et al*., 2010; Mclamore *et al*., 2011
Ruthenium Metal NPs	Drug delivery	Kenezevic *et al*., 2012; Wang *et al*., 2012
Silver Metal NPs	Antibacterial and antifungal agent; biosensor; coating	Marambio-Jones and Hoek, 2010; Arnaout and Gunsch, 2012; Singh *et al*., 2012;

1.2.2.2. Synthesis of metallic nanoparticles

There are two alternative approaches for the synthesis of metal nanoparticles: the 'bottom-up' approach and the 'top-down' approach. The former means self assembly, or the construction of a structure atom-by-atom, molecule-by-molecule, or cluster-by-cluster (Strackarn *et al*., 2012). In this approach, initially the nanostructured building blocks are formed and, subsequently, assembled into the final material using chemical or biological procedures (Thakkar *et al*., 2010; Orbach *et al*., 2012). A typical advantage of the bottom-up approach is the enhanced possibility of obtaining metal nanoparticles with considerably less defects and more homogeneous chemical composition (Sau and Rogach, 2010). In the top-down approach, a suitable starting material is reduced in size using physical, mechanical or chemical methods (Singh *et al*., 2010; Ambrosi *et al*., 2012; Yadav *et al*., 2012). A major drawback of the top-down approach is the imperfection of the surface structure which could impact on physical properties and also surface chemistry due to the high aspect ratio (Shahbazi *et al*., 2012; Suresh, 2012; von Freymann *et al*., 2013).

Several methods and recipes for the preparation of metal nanoparticles have been reported so far, and only those that are common and well established will be mentioned.

1.2.2.2.1. Chemical reduction method

The traditional and most widely used method for synthesis of metal nanoparticles is using wet-chemical procedures. A typical procedure involves growing nanoparticles in a liquid medium containing various reactants, in particular reducing agents such as sodium borohydride or potassium bitartrate or methoxypolyethylene glycol (Polte *et al*., 2010; van Heusden *et al*., 2010; Abeylath and Amiji, 2011; Singh *et al*., 2011). To prevent the

aggregation of metal nanoparticles, a stabilizing agent such as sodium dodecyl/benzyl sulfate or polyvinyl pyrrolidone is also necessary in the reaction mixture (Badawy *et al*., 2010; Goldshleger *et al*., 2012). It was reported that ion exchange resins have been used to produce nickel nanoparticles varying in size 3-5 nm (Railsback *et al*., 2010). Generally, the chemical methods are low-cost and rapid for high volume (Rangappa *et al*., 2010; Lu *et al*., 2011; Kim *et al*., 2012); however, their drawbacks include contamination from chemicals, toxic solvents and the generation of hazardous by-products, and furthermore there is limited control on the shape and size of the nanoparticle (Malekzadeh and Halali, 2011; Virkutyte and Varma, 2011). Interestingly, several developed chemical approaches for controlled-size and shape nanoparticles have been reported recently. For example, stable Pt/Ru nanoparticles with 2.1-2.8 nm in diameter were synthesized by ethanol (Liu *et al*., 2011; Wang *et al*., 2011). Tannic acid was used as both reducing and stabilizing agent to synthesize spherical gold (Aromal and Philip, 2012), nickel (Dutta and Dolui, 2011) and silver nanoparticles (Yi *et al*., 2011). Green, effective chemical routes for the synthesis of nanoparticles are getting more and more attractive.

1.2.2.2.2. Biological synthesis

Biosynthetic methods employ the resources available in nature to prepare metal nanoparticles (Han *et al*., 2012). It was reported that a number of biological materials have been involved in biosynthetic pathways, including algae, bacteria, fungi, plant and yeast (Table 1.3). There are quite a few reports of algae being used as a biomaterial for the synthesis of metal nanoparticles. *Sargassum wightii* was the first marine algae reported to be used to synthesize stable extracellular gold particles under relatively simple conditions (Singaravelu *et al*., 2007). Prokaryotic bacteria are the most common

biological resources employed in metal nanoparticle synthesis because of their relative ease of manipulation (Mondal *et al*., 2011). It was reported that the crystalline Ag nanoparticles could be extracellularly produced when silver-resistant *Morganella sp.* RP-43 was exposed to silver nitrate ($AgNO_3$), and it was the first report that elucidates the molecular evidence of silver resistance in bacteria (Parik *et al*., 2008). The first intracellularly synthesized nanoparticles was cadmium sulfide (CdS), by incubating *E. coli* with cadmium chloride ($CdCl_2$) and sodium sulfide (Na_2S), and it showed that the formation of nanoparticles was markedly affected by physiologic parameters (Sweeney *et al*., 2004). Fungi have been reported as a kind of ideal biomaterial to synthesize metal nanoparticles. One of the distinct advantages is that fungi showed the ease in their scale-up, just using thin solid substrate fermentation for the synthesis of metal nanoparticles (Ahmad *et al*., 2002; Ahmad *et al*., 2005). Plant leaf extract has been exploited to synthesize gold, silver and platinum nanoparticles with different size depending on the pH (Sharma *et al*., 2007; Kumar and Yadav, 2009; Mubarak-Ali *et al*., 2011; Vinod *et al*., 2011).

Table 1.3. Some examples of microorganisms involving in metal nanoparticles synthesis.

Microorganism	Type of nanoparticles	References
Algae		
Sargassum wightii	Au	Oza *et al*., 2012
Bacteria		
Clodtridium thermoaceticum	CdS	Thakkar *et al*., 2010
Escherichia coli	Ag, Au	Aubin-Tam and Hamad-Schifferli, 2005; Shahverdi *et al*., 2007
Klebsiella pneumoniae	Ag, CdS	Krumov *et al*., 2009; Mokhtari *et al*., 2009
Lactobacillus strains	Ag, Au	Nair and Pradeep, 2002; Vaidyanathan *et al*., 2009

Fungi		
Trichoderma asperellum	Ag, Au	Mukherjee *et al*., 2008; Mukherjee *et al*., 2012
Verticillium	Ag, Au	Sharma *et al*., 2007
Plant		
Azadirachta indica	Ag, Au	Leela and Willner, 2004; Rajasekharreddy *et al*., 2010
Diopyros kaki	Pt	Song *et al.*, 2010
Eucalyptus hybrida	Ag	Dubey *et al*., 2009
Magnolia kobus	Au	Song *et al*., 2009
Terminalia catappa	Au	Ankamwar, 2010
Yeast		
MKY3	Ag	Katz and Wilner, 2004

.

It was reported that viruses have been investigated as a biomaterial to synthesize gold and silver nanoparticles (Kramer *et al*., 2004; Loo *et al*., 2006; Niikura *et al*., 2009). The viral capsids act as molecular containers for the encapsulation of genomic nucleic acid, and they can also be used as constrained reaction vessels for packaging and entrapment of synthetic nanoparticles (Liepoold *et al*., 2005). One of the distinct advantages is that a virus can provide an ideal protein cage structure. An excellent example is icosahedral cowpea chlorotic mottle virus (CCMV) (Figure 1.9). The CCMV capsids undergoes a pH and metal-ion dependent swelling, which results in a reversible structural transition of the capsid (open or closed), releasing the interior of the protein cage to the medium (Renggli *et al.*, 2011). The virus also presents a confined environment and unique protein surface topology, including polarity, residue charge and surface relief (Slocik *et al*., 2005). The metal nanoparticles synthesized in the virus protein cage are tiny enough to cross cell membranes and make them potential for medical applications. Generally, the biological methods are environmentally friendly, but high-cost and slow for high-volume due to the complicated preparation procedure and specific temperature and pH conditions.

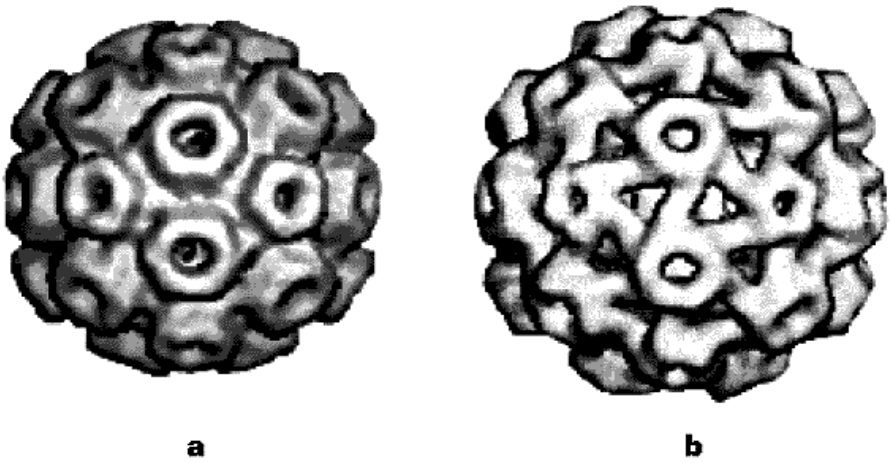

Figure 1.9. Cryo-electron microscopy and image reconstruction of the cowpea chlorotic mottle virus. a), in an unswollen condition induced by low pH; b), in a swollen condition induced by high pH.
(Douglas and Young, 1998)

1.2.3. Safety of nanotechnology

Nanotechnology is an emerging science, and the novel and unique properties of nanoparticles may pose a health risk to humans and the environment. It is estimated that the average person consumes 1012 submicron-sized particles per day, from the food additives consisting primarily of titanium dioxide (TiO_2) and aluminosilicates (Stem and McNeil, 2008). Correspondingly, the study of the hazardous effects of these particles, particulate toxicology, has been underway for many decades. Therefore due to the potential nanomaterial risks, there has been a dramatic increased concern to safety research. Potential routes of nanoparticle exposure include inhalation, dermal, oral and in the case of biomedical applications, the toxicity resulting from nanoparticle exposure could occur via the lungs and skin (Papp *et al.*, 2008).

The toxicology of nanoparticles should involve the study of the interactions of those ultrafine particles with biological systems and the environment, and also the investigation of their potential risk at a molecular level (Lai and Sayre, 2009; Yildirimer *et al*., 2011; Yah *et al.*, 2012). A number of studies on the effects of nanoparticles on biological cells, tissues, animals and environment system have been carried out (Braydich-Stolle *et al*., 2010; Shvedova *et al*., 2010; Celardo *et al.*, 2011). For example, the metallic nanoshells, as a drug delivery agent have been extensively studied for the controlled release in chemotherapy (Rosler *et al*., 2001; Xu *et al*., 2006; Gu *et al*., 2007; Haidar, 2010; Huschka *et al*., 2012). They are generally composed of inert metals such as gold or titanium, and each of these platforms is inert and biocompatible. It was reported that a significant fraction of the particles is retained in the body after administration, and this can lead to toxicity (Wang and Thanou, 2010; Werner *et al*., 2012). Therefore, most of the work on metal nanoparticle drug delivery has been in the preclinical stage.

1.3. Present research

1.3.1. Hypothesis

Silver nanoparticles of controlled size and shape can significantly interfere with the activity of methylhydroxyethylthiazolekinase enzyme from *Plasmodium falciparum* thereby introducing a new, promising and potential approach to control malaria.

1.3.2. Objectives

- Chemical synthesis of silver nanoparticles by reducing a silver salt with $NaBH_4$ or tannic acid.

- Cloning, expression, purification and characterization of the biomedical target: methylhydroxyethylthiazolekinase from *Plasmodium falciparum* (*Pf*ThzK).
- *In vitro* evaluation of these silver nanoparticles against methylhydroxyethylthiazolekinase from *Plasmodium falciparum* (*Pf*ThzK).

Chapter 2
Isolation of the genes encoding methylhydroxyethylthiazolekinase from *Plasmodium falciparum* (*Pf*ThzK)

2.1. Introduction

Vitamin B_1 (thiamine) is an essential cofactor for several key enzymes of carbohydrate metabolism, and it occurs ubiquitously in all organisms. Humans obtain it from their diet, and in the case of bacteria, fungi, plants and malaria parasite, it is synthesized *de novo.* And then thiamine has to be salvaged by thiamine pyrophosphokinase to be active cofactor thiamine pyrophosphate (Thi-PP) (Begley *et al.,* 1999; Wightman and Meacock, 2003).

2.1.1. Biosynthesis of thiamine phosphate in *P. falciparum*

The biosynthetic pathway of vitamin B_1 in *Escherichia coli* and *Saccharomyces cerevisiae* is well understood (Scott and Phillips, 1997; Taylor *et al.,* 1998; Begley *et al.*, 1999; Mizote *et al.,* 1999; Wightman and Meacock, 2003). In bacteria the thiazole can be converted to thiazole-phosphate (THZ-P) by ThiM (thiazole kinase of bacteria); thiamine or components of thiamine, can be salvaged (Figure 2.1). In bacteria, thiamine can be converted to thiamine-phosphate by thiamine kinase (ThiK), or be converted to thiamine-diphosphate by thiamine pyrophosphokinase (ThiN), the corresponding enzyme in higher organism such as yeast for example, is THI80 (Jurgenson *et al.*, 2009).

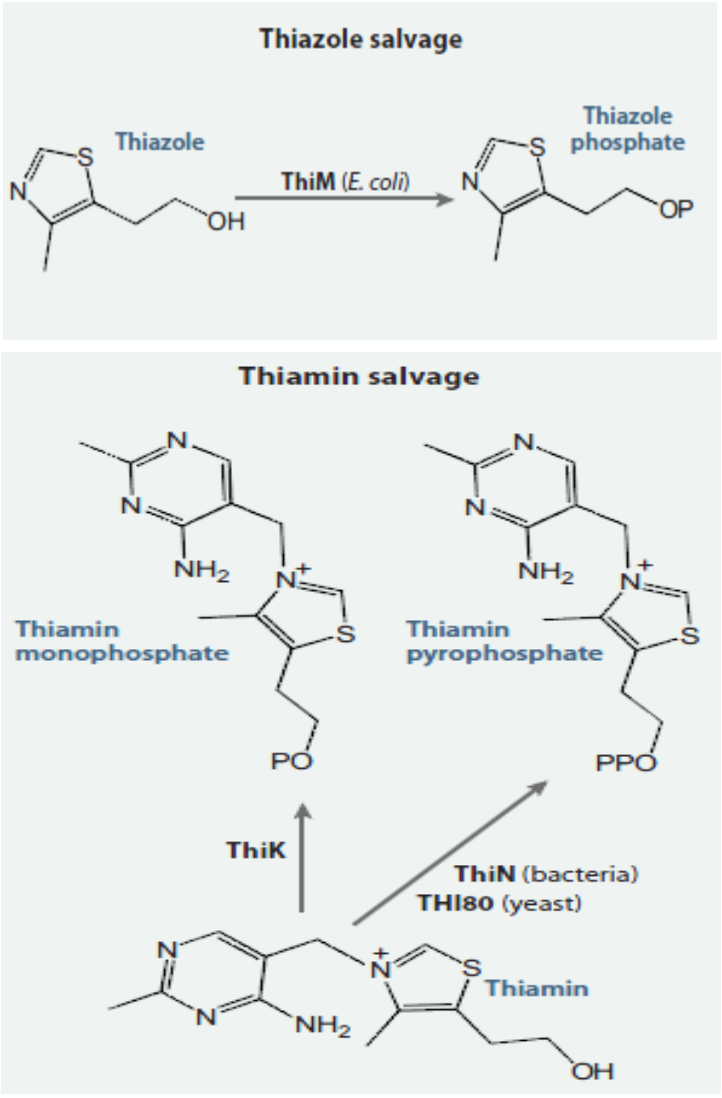

Figure 2.1. Salvage pathways for thiazole and thiamine in *E. coli.*

ThiM from *Bacillus subtilis* and *Salmonella typbimurium* have been biochemically characterized (Zhang *et al*., 1997; Petersen and Downs, 1997), and the structure of the *B. subtilis* ThiM was determined (Campobasso *et al.*, 2000). ThiM from *B. subtilis* is a trimer, and each protomer contains 9 β-strands and 12 α-helices (Figure 2.2). The corresponding enzyme in *P. falciparum, Pf*ThzK, hasn't been structurally characterized

by X-ray, but it was evaluated to be a monomer, with a molecular mass of 34 kDa (Wrenger, 2006).

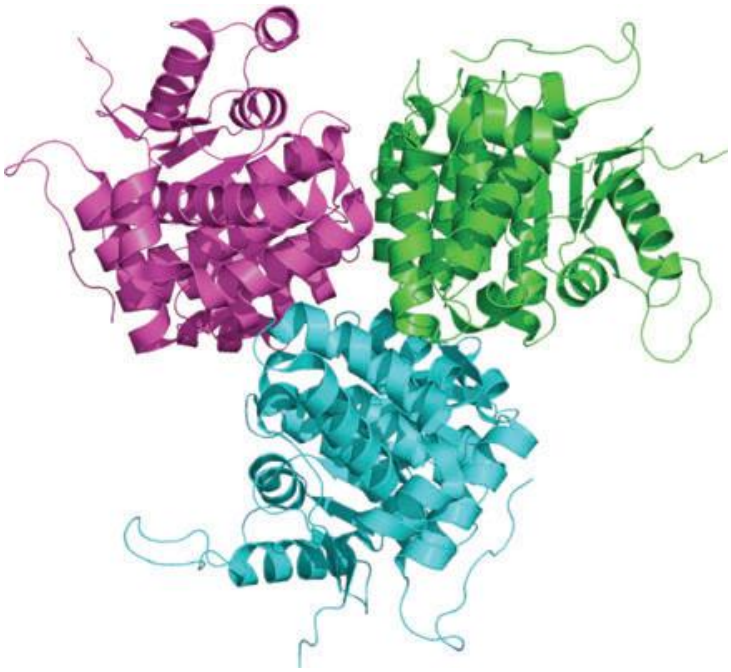

Figure 2.2. X-ray structure of thiazolekinase from *B. subtilis* (Jurgenson *et al*., 2009).

The plasmodial pathway identified three vitamin B_1 biosynthetic enzymes: a) 5-(2-hydroxy-ethyl)-4-methylthiazole (THZ) kinase (ThzK), b) 4-amino-5-hydroxymethyl-2-methylpyrimidine (HMP) HMP-P kinase (ThiD) and c) thiamine phosphate synthase (ThiE). The biosynthesis of thiamine phosphate is divided into two branches: the thiazole branch and the pyrimidine branch. The thiamine biosynthesis branch starts with 5-(2-hydroxyethyl)-4-methylthiazole (THZ), which is activated and converted by THZ kinase (ThzK) to 4-methyl-5-(2-phosphoethyl)-thiazole (THZ-P). The precursor of the pyrimidine branch is 4-amino-5-hydroxymethyl-2-methylpyrimidine (HMP), which has

to be phosphorylated in two steps to 4-amino-2-methyl-5-hydroxymethyl pyrimidine diphosphate (HMP-PP) by HMP/HMP-P kinase (ThiD). The first phosphorylation, however, can also be effected by pyridoxine kinase (PdxK), which is involved in the activation of vitamin B_6, as demonstrated for the parasites *Trypanosoma brucei* and *P. falciparum* (Morett *et al*., 2003; Wrenger *et al*., 2005). HMP itself is synthesized in bacteria by the HMP biosynthesis enzyme, whereas it has been suggested that in eukaryotes pyridoxine and histidine are possibly bound to HMP (Wrenger *et al*., 2006). Finally, the thiazole and pyrimidine moieties, HMP-PP and THZ-P, are merged to form thiamine phosphate (Thi-P) by thiamine phosphate synthase (ThiE) (Figure 2.3).

Arbitrary use of malarial chemotherapeutic agents increased drug resistance and a loss in efficiency. Therefore, new antimalarial drugs and novel drug targets are urgently required. These drugs should be developed to target only parasites and not be harmful to the human host. The three enzymes involved in the parasitic metabolic thiamine synthetic pathway, ThiD, THiE and ThzK are absent in the human host, especially, ThzK which is structurally and functionally different from the corresponding enzymes in bacteria and yeasts; this makes ThzK ideal as a potential drug target.

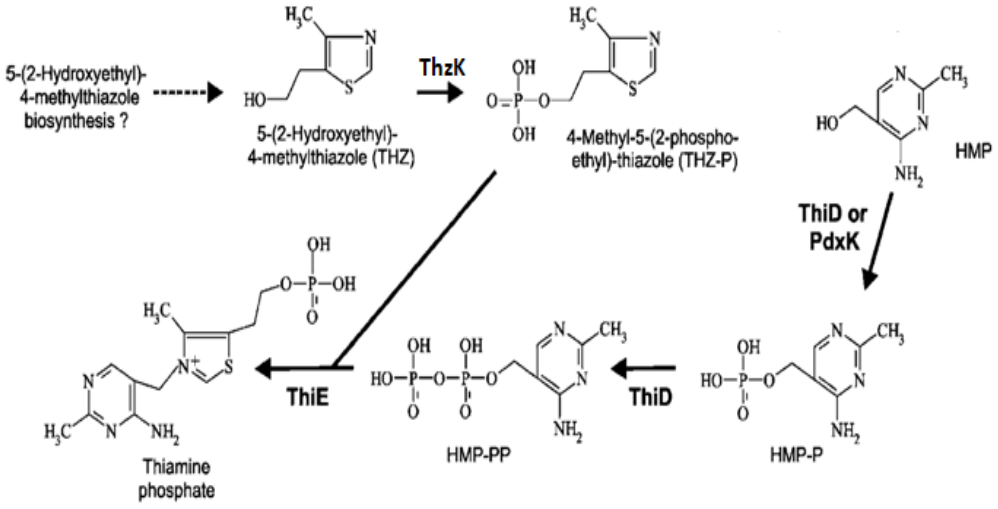

Figure 2.3. Thiamine phosphate biosynthesis in *P. falciparum* (Wrenger *et al*., 2006).

The 5-(2-hydroxyethyl)-4-methylthiazole (THZ) synthesized *de novo* will be phosphorylated to THZ-P by THZ-kinase (ThzK). In the pyrimidine branch, 4-amino-5-hydroxymethyl-2-methylpyrimidine (HMP) is phosphorylated to HMP-P by either the pyridoxinekinase (PdxK) or the HMP-(P)-kinase (ThiD). Subsequently, HMP-P is phosphorylated to HMP-PP by HMP-(P)-kinase. THZ-P and HMP-PP are merged to thiamine phosphate in a reaction catalysed by thiamine synthase (ThiE).

2.1.2. Gene sequence encoding *Pf*ThzK used in this study

Polymerase chain reaction (PCR) amplification of the genomic DNA using primers based on published sequence data is commonly used to isolate the gene encoding specific proteins of interest. However, the entire *P. falciparum* genome sequence was only published in 2002, and it is the most A-T rich genome sequenced to date. Very few studies on cloning of ThzK gene from *P. falciparum* were published so far (Gerdner *et al*., 2002; Wrenger *et al.*, 2006).

The opening reading frame (ORF) encoding for the methylhydroxyethylthiazolekinase comprises 909 base pairs (bp), the sequence data (NCBI Reference Sequence: AY166865) is shown in Appendix 1.

2.2. Materials and methods

2.2.1. Chemicals and reagents

All the chemicals and reagents utilized to prepare strain cultures and amplify *Pf*ThzK gene are described in Appendix 2 (Media and Buffers).

2.2.2. Genomic DNA, bacterial strains, plasmids and culture conditions

P. falciparum 3D7 genomic DNA (MRA-120G, MR4) was used as a template to amplify *Pf*ThzK gene sequence, which was purchased from American Type Culture Collection (ATCC). Oligonucleotides and restriction enzymes, *NdeI* and *EcoRI*, which were used for the design of primers and double digestion, were obtained from IDT® (South Africa). Recombinant plasmids were expressed in *E. coli* strains JM109 or *E. coli* BL21 (DE3) containing pRARE (Invitrogen), those strains were grown at 37℃ at 160 rpm under aeration in LB media or on LA plates (Appendix 2) supplemented with antibiotics to which the plasmids conferred resistance (30 µg/ml kanamycin or/and 34 µg/ml chloramphenicol).

The plasmids used in this chapter are pSmart and pET28b(+), where 30 µg/ml kanamycin was used as antibiotic marker. Plasmid pSmart was used as a cloning vector and pET28b(+) was used to generate target proteins fused with a N-terminal His-tag, and therefore these target proteins could be subsequently purified by Ni-affinity chromatography.

2.2.3. PCR amplification

The ORFs encoding for *Pf*ThzK were amplified by polymerase chain reaction from *P. falciparum* 3D7 genomic DNA (MRA-120G, MR4) using oligonucleotides: *PfThzK-NdeI*: 5'-CATATGAGAAAATATAATTTTTTTACAAAAAGTCGC-3'; *PfThzK-EcoRI:* 5'-GAATTCTTATGCTACTTTGTAAATATCTACGATTTGG-3' (Table 2.1). PCR of the plasmodial constructs was performed in a total reaction volume of 50 µl using Phusion®

Hot Start II polymerase (Finzymes, Thermo Scientific, Finland) by Thermal Cycler (MJ Mini™, Bio-RAD) and using the following thermal cycling program: initial denaturation for 2 min at 98 ℃, followed by 35 cycles of 20 sec at 95 ℃, 10 sec at 64 ℃, 10 sec at 59 ℃, 1 min at 60 ℃, and 8 min at 60 ℃ (Table 2.2).

Table 2.1 Oligonucleotide primers used for PCR amplification.

Primer	Sequence	Temperature
*Pf*ThzK-*NdeI*	5'-CATATGAGAAAATATAATTTTTTTACAAAAAGTCGC-3'	54.0 ℃
*Pf*ThzK-*EcoRI*	5'-GAATTCTTATGCTACTTTGTAAATATCTACGATTTGG-3'	56.4 ℃

The PCR amplification and DNA products were analyzed by electrophoresis (90V; 60 min) on 0.8% agarose gel in TAE buffer (0.04 M Tris-HCl, 1 mM EDTA pH 8.0, 0.021 mM glacial acetic acid) containing 0.6 μg/ml ethidium bromide. The products were visualized using Uviprochemi gel imaging system (UVitec) or VIBER LOURMAT (ECX-1.5L) with low radiation UV source, and the DNA products were then isolated from the gel using Biospin Gel Extraction Kit (BioFlux, Bioer Technology Co., Ltd) based on the manufacturer's instructions (Appendix 3). The nucleic acid concentrations were determined with a Nanodrop 2000 spectrophotometer (Thermo Scientific).

Table 2.2a. PCR reaction components.

Component	50 µl reaction	Final concentration
H_2O	16.5	
5xPhusion® HF Buffer	10	1x
dNTPs	1	0.8 mM
Forward primer (*Pf*ThzK-*NdeI*)	10	0.5 µM
Reverse primer (*Pf*ThzK-*EcoRI*)	10	0.5 µM
Template DNA	2	25 ng/µl
Phusion® Hot Start II DNA polymerase	0.5	0.02 U/µl

Table 2.2b. PCR thermal cycling program.

Cycle step	Temperature	Time	Cycles
Initial denaturation	98 ℃	2 min	1
Denaturation	98 ℃	20 sec	35
Annealing	64 ℃	10 sec	
Annealing	59 ℃	10 sec	
Extension	60 ℃	1 min	
Final extension	60 ℃	8 min	1
Cooling	4 ℃	∞	1

2.2.4. Ligation

The cleaned DNA products (approximately 900 bp) isolated from the gel were ligated into pSmart Vector system (Lucigen). Each ligation was carried out as per manufacturer's instructions, with a total volume of 10 µl, containing PEG4000 (1 µl), 10×ligation buffer,

T4 DNA ligase, pSmart vector and DNA product with 1:1 molar ratio of vector: insert DNA (see Table 2.3). Each ligation was performed at 4 ℃ overnight.

Table 2.3. Ligation components

Component	10 µl reaction	Final concentration
H_2O	0	
Insert DNA	6	4.2 ng/µl
PEG4000 (50%)	1	5%
10xLigation buffer	1	1x
T4 DNA ligase	1	0.3 U/µl
pSmart vector	1	25 ng/µl

2.2.5. Transformation and cloning

Competent *E. coli* strains JM109 and *E. coli* BL21 (DE3) cells (Invitrogen) were prepared according to the modified methods described before (Hanahan, 1983; Chung *et al.*, 1989), with the procedure as follows :

- A single colony of *E. coli* cells was inoculated into 5 ml LB medium, and incubated overnight at 37 ℃ with aeration.
- The overnight culture (1.0 ml) was inoculated into SOB media (20 g/L tryptone, 5 g/L yeast extract, 0.584 g/L NaCl, 0.186 g/L KCl, 2.034 g/L $MgCl_2$, 2.464 g/L $MgSO_4$), and grown at 37 ℃ with aeration at 160 rpm until OD_{600} reached 0.6.
- The culture was cooled (ice-water bath; 10 min), and centrifuged (3,000 × g; 10 min; 4 ℃).
- The pellets were resuspended in 80 ml pre-cooled TB buffer (2.6 g/L HEPES, 2.203 g/L $CaCl_2$, 18.638 g/L KCl, 10.886 g/L $MnCl_2$, pH 6.7) followed by a second centrifugation (3,000 × g; 10 min; 4 ℃) and resuspended in 20 ml pre-cooled TB buffer (Appendix 2).

- DMSO was added to the suspension to a final concentration of 7% (1.4 ml DMSO/20ml suspension), and the mixture was cooled (ice; 10 min), then divided into aliquots (100 µl) and stored at -80 ℃ until required.

Competent *E. coli* JM109 cells (100 µl aliquot) were thawed on ice and ligated product *Pf*ThzK-pSmart (10 µl) was added. The mixture was placed on ice (30 min), followed by heating (42 ℃; 40 sec), cooling (ice-water bath; 2 min) and then treated with 250 µl pre-warmed SOC media (20 g/L tryptone, 5 g/L yeast extract, 0.584 g/L NaCl, 0.186 g/L KCl, 2.034 g/L $MgCl_2$, 2.464 g/L $MgSO_4$), and then incubated (37 ℃, 60 min).

The *Pf*ThzK-pSmart-JM109 culture was plated onto LA plates (Appendix 2) containing 30 µg/ml of kanamycin, and incubated at 37 ℃ overnight. Single transformation colonies were selected and inoculated into a LB culture (5 ml; containing 30 µg/ml of kanamycin) and incubated (37 ℃; 16 h). The DNA of the gene with interest was isolated by BioSpin Plasmid Extraction Kit (BioFlux, Bioer Technology Co., Ltd) according to the manufacturer's instructions (Appendix 4).

2.2.6. Sequencing

Restriction fragment length polymorphism was used as a screening method in double digestion using *EcoRI* and *NdeI* restriction enzymes. The double digestion was performed (10 µl; 37 ℃; 12 h), the digested products sequenced (Inqaba Biotechnical Industries, Pty, Ltd; South Africa) and aligned with the reference sequence from NCBI database.

The pSmart plasmids containing the desired insert were double digested by *EcoRI* and *NdeI* and then ligated to pET28b(+) using the same method (Section 2.2.4). The pET28b(+) plasmid containing the desired insert were cleaned from the agarose gel by

BioSpin Gel Extraction Kit (BioFlux, Bioer Technology Co., Ltd) according to the same protocol describe before (Section 2.2.5). The cleaned *Pf*ThzK-pET28b(+) were ligated and the products transformed into competent *E. coli* BL21 [DE3 (with pRARE)] cells then inoculated onto LA plates containing 30 µg/ml kanamycin and 34 µg/ml chloramphenicol. Positive transformants selected (Section 2.2.5) were then ready for expression.

Table 2.4. Double digestion components.

Component	10 µl reaction
H_2O	6 µl
Isolated plasmid	2 µl
Buffer O	1 µl
NdeI	0.5 µl
EcoRI	0.5 µl

2.3. Results and discussion

2.3.1. PCR amplification

Two primers *PfThzK-NdeI* and *PfThzK-EcoRI* were designed to amplify and express the *Pf*ThzK gene as described in Section 2.2.3. Vector pET28b(+) were utilized for fusion proteins and hexa-Histidine tags (Figure 2.4).

The *Pf*ThzK gene was successfully amplified by PCR (Section 2.2.3), after agarose electrophoresis it contained a band of approximately 900 bp (Figure 2.5), which agrees with NCBI database (909 bp), and it was also confirmed by Bozdech (2005) and Wrenger (2006).

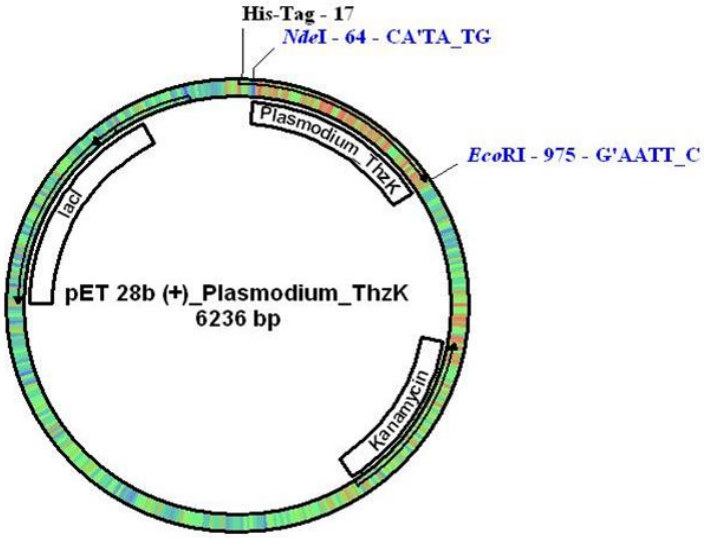

Figure 2.4. Vector map of pET28b(+) containing His-tag binding site, *NdeI* and *EcoRI* cloning sites, and the kanamycin resistance gene.

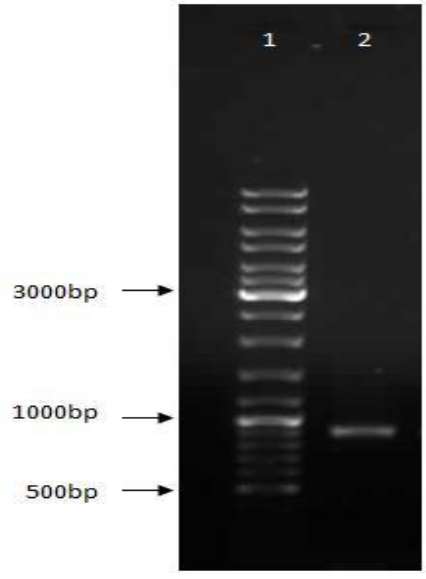

Figure 2.5. Agarose gel electrophoresis of the PCR amplified *Pf*ThzK gene. Lane 1 represents the DNA marker; lane 2 represents the amplified *Pf*ThzK gene (approximate 900 bp).

2.3.2. Transforming and cloning

The amplified *Pf*ThzK gene was cleaned by Biospin Gel Extraction Kit (Section 2.2.3), the concentration of isolated genomic DNA was 138.4 ng/µl, and it was pure of good quality (A260/A280 = 1.9), which could be used for subsequent experiments.

Double digestion with *EcoRI* and *NdeI* restriction enzymes was performed (Section 2.2.6) and the agarose electrophoretogram contained 2 bands: one of approximately 900 bp and another around 1.8 kb, which confirmed that the insert was the gene of interest (Figure 2.6).

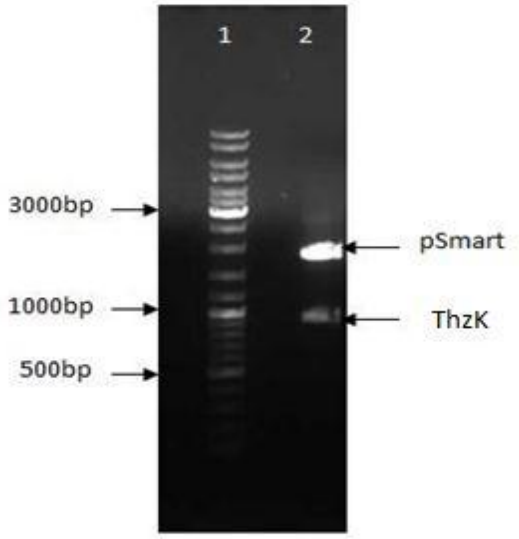

Figure 2.6. Agarose gel electrophoresis of the double digestion with *NdeI* and *EcoRI* restriction enzymes. Lane 1 represents the DNA marker; lane 2 represents the double digested products: *Pf*ThzK (909 bp), pSmart (1.8 kb).

The double digested products were sent to Inqaba Biotech Industries (South Africa) for sequencing (Section 2.2.6), and alignment of the insert showed 99.9% identity (908/909) to the reference gene (Figure 2.7). The ORF encoding for *Pf*ThzK was identified on

chromosome12 by BLAST analysis (http://blast.ncbi.nlm.nih.gov). The ORF comprises 909 bp and does not contain any introns. The *Pf*ThzK gene sequence shows moderate sequence identities of 99% and 99% to *P. falciparum* 3D7 chromosome12 (AE014188.3) and *P. falciparum* ThzK mRNA (AY166865.1) respectively.

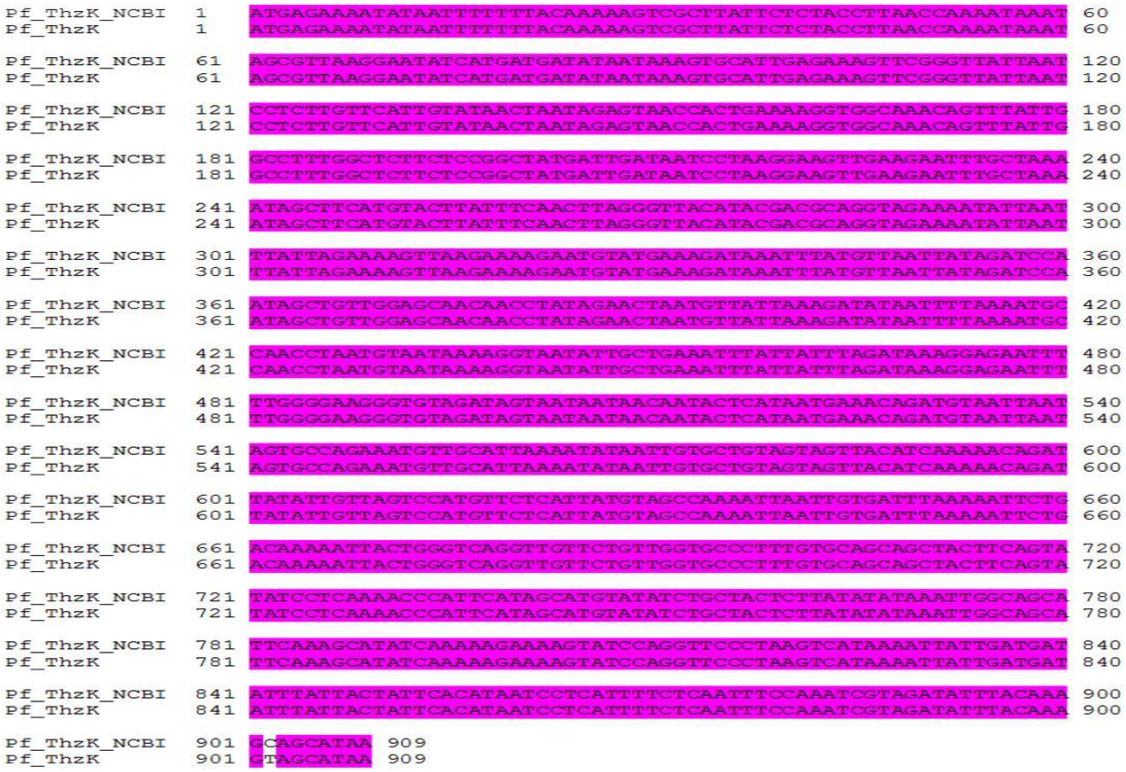

Figure 2.7. Sequence alignments of the reference ThzK from *P. falciparum* database and the cloned gene from *P. falciparum*. The cloned *Pf*ThzK gene showed 99.9% identity to the reference gene, mismatch: 1 bp.

The desired insert was separated from pSmart plasmid after double digestion with *EcoRI* and *NdeI*, and it was cleaned from the gel and ligated into pET28b(+) in *E. coli* BL21 cells (Section 2.2.6). These cells were inoculated onto LA plates (containing 30 µg/ml kanamycin and 34 µg/ml chloramphenicol) and incubated at 37 ℃ overnight.

Seven colonies were grown and selected for plasmid extraction (Section 2.2.5), agarose gel electrophoresis contained 2 bands (Figure 2.8), one of approximate 900 bp represented *Pf*ThzK (909 bp) and another of about 5 kb, represented pET28b(+) vector (5,368 bp), and the insert with correct size was selected after double digestion which was used for expression experiments.

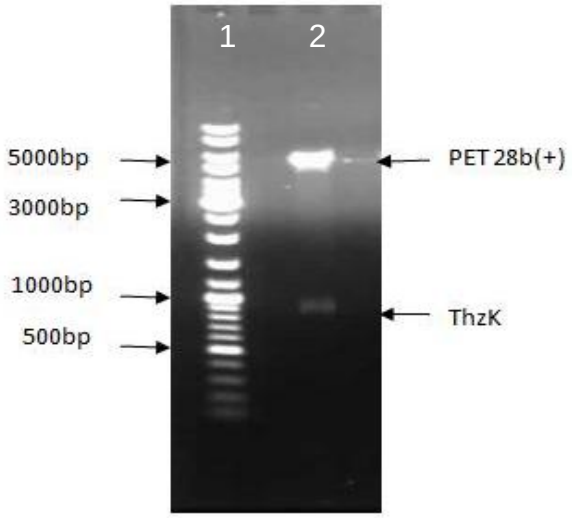

Figure 2.8. Agarose gel electrophoresis of the double digestion with *NdeI* and *EcoRI* restriction enzymes. Lane 1 represents the DNA marker; lane 2 represents the double digested products: *Pf*ThzK (909 6p), pET28b(+) (5,368 bp).

The *Pf*ThzK gene was amplified and identified in the present study through cloning of its genomic DNA by PCR with Phusion® Hot Start II polymerase. This was the second approach to amplify ThzK gene from *P. falciparum* by PCR method. In the present study, *NdeI* and *EcoRI* restriction enzymes were utilized to design shorter primers compared to previous studies (Wrenger, 2006). The Phusion polymerase employed in this study offered accurate and progressive performance. The PCR program was modified and different from the one commonly used: Higher denature temperature. This is because the

Phusion® Hot Start II polymerase combines the DNA polymerase and is reversibly bound, which inhibits the 3'-5' exonuclease activity of the polymerase, preventing degradation of the primers and DNA polymerase. Due to the high thermostability of Phusion polymerase, a temperature of 98℃ or even higher can be used. A longer extension process was employed in this study because of the complexity of *Pf*ThzK gene.

In conclusion, methylhydroxyethylthiazolekinase gene was successfully amplified and pure *Pf*ThzK gDNA was transformed into pET28(+) vectors, which were ready for protein expression. The deduced protein sequence of ORF encoding for the *P. falciparum* methylhydroxyethylthiazolekinase consists of 302 amino acids and has a molecular mass of 34 kDa. The amino acid sequence shows moderate sequence identities 39%, 35% and 33% to *Clostridum sporogenes* (accession no. ZP 02994013.1), *Spirosoma linguale* (accession no. YP003388301.1) and *Arthrobacter arilaitensis* (accession no. YP003915272.1), respectively. The *Pf*ThzK protein shows homology to the C-terminus and is only approximately half of the size of its fungal counterparts, whereas its bacterial homologues are of the same size (Wrenger, 2006).

Chapter3
Expression, purification and characterization of methylhydroxyethylthiazolekinase (*Pf*ThzK)

3.1. Introduction

High concentration of pure protein is necessary for laboratorial analysis *in vitro*, however, the 'traditional' or 'conventional' purification methods, which extract protein from its source, can't meet these requirements, because the products are potentially pathogenic and the yields are really low, making it more expensive.

The Gram-negative bacteria *E. coli* is the most frequently used prokaryotic expression system available and it has evolved as a standard organism for the production of enzymes for analytical and diagnostic use. The gene encoding the target protein is introduced to the cell as part of an expression vector (Neidhardt *et al*., 1996; Hottenrott *et al*., 1997; Banyex, 1999).

Promoters are DNA sequences which direct RNA polymerase binding and transcription initiation. *E. coli* has seven different types of promoter, and some are commonly used, such as *lac, T7* and *trp* (Oehler *et al.*, 1994; Hasan and Szybalski, 1995).

3.1.1. *T7* RNA polymerase heterologous expression system

The *T7* polymerase system is highly processive and recognizes conserved sequences covering a region between -17 and +6 bp relative to the mRNA starting site (Ramos *et al*.,

2004). It is the strongest promoter described for microorganisms so far and it is quite efficient, leading to an accumulation of the desired protein of about 40-50% of total cell protein (Dubendorff and Studier, 1991; Savalia *et al*., 2010). One of the most useful systems for expression of recombinant proteins in *E. coli* is the pET vector series, which is based on the *T7* phage RNA polymerase promoter (Ramos *et al*., 2004). The expression of the recombinant protein using these plasmids is tightly regulated and, when induced, produces high levels of transcripts and recombinant proteins (Oliveria *et al*., 2001).

However, it has several drawbacks. One problem of using the *T7* expression system may result in plasmid or expression instability due to the leaky expression (Sagawa *et al*., 1996). If the desired recombinant protein is toxic to host cells, this leads to low or negligible expression (Miroux and Walker, 1996).

3.1.2. The Histidine-tags to improve heterologous expression

A DNA sequence containing six histidine residues is frequently used in vectors for production of recombinant proteins, leading to the expression of a recombinant protein with 6xHis-tag fused to its N- or C-terminus. Several pET vectors have a 6xHis-tag which permits the purification of recombinant protein on metal charged columns (Crowe *et al*., 1994). Expressed His-tag recombinant proteins can be purified and detected easily because the histidine residues bind to several types of immobilized metal ions, such as nickel, cobalt and copper (Hoffman and Roeder, 1991; Franken *et al*., 2000). Nickel is the most frequently used metal ion for purification of His-tagged proteins, because nickel provides good binding efficiency. The problem of using nickel affinity chromatography,

however, is that nickel also tends to bind unspecific proteins that contain any histidine clusters (Muller *et al*., 1998).

For nickel affinity chromatography, His-tags are likely to bind to resins in near-neutral buffer conditions. Moreover, in a typical binding buffer, low-concentration imidazole helps wash out any unspecific proteins that contain histidine clusters. Elution of His-tagged protein from the resin is then carried out with a subsequent elution using a high concentration of imidazole (Schmitt *et al*., 1993; Arnau *et al*., 2006; Ganesana *et al*., 2011).

3.1.3. Size exclusion chromatography

Size exclusion chromatography (SEC) is a chromatographic procedure in which particles are separated based on their size. It is commonly used for separating large molecules or macromolecular complexes such as proteins and industrial polymers. Separation is achieved by the different exclusion from the pores of the packing material. The principle feature of SEC is its gentle non-adsorptive interaction with the sample, enabling high retention of biomolecular activity (Wen *et al*., 1996; De Nobili and Chen, 1999; Al-Bokari *et al*., 2002). A protein mixture is poured into a column, which contains a suspension of tiny beads with different-sized macroscopic pores (Figure 3.1). As the proteins pass through the column, the larger proteins can only fit into fewer pores and thus have a more direct and faster path through the beads. In contrast, the smaller proteins can fit through more pores and take a meandering and longer path as they get caught in various holes and thus, take a longer time to flow through the column. As time passes, the eluates containing the larger proteins pass through quickly, while smaller proteins will

elute later. For the separation of biomolecules in aqueous or aqueous/organic mobile phases, SEC is referred to as gel filtration chromatography. The main application of gel filtration chromatography is the fractionation of proteins and other water-soluble polymers (Kieft, 1991; Bollag, 1995).

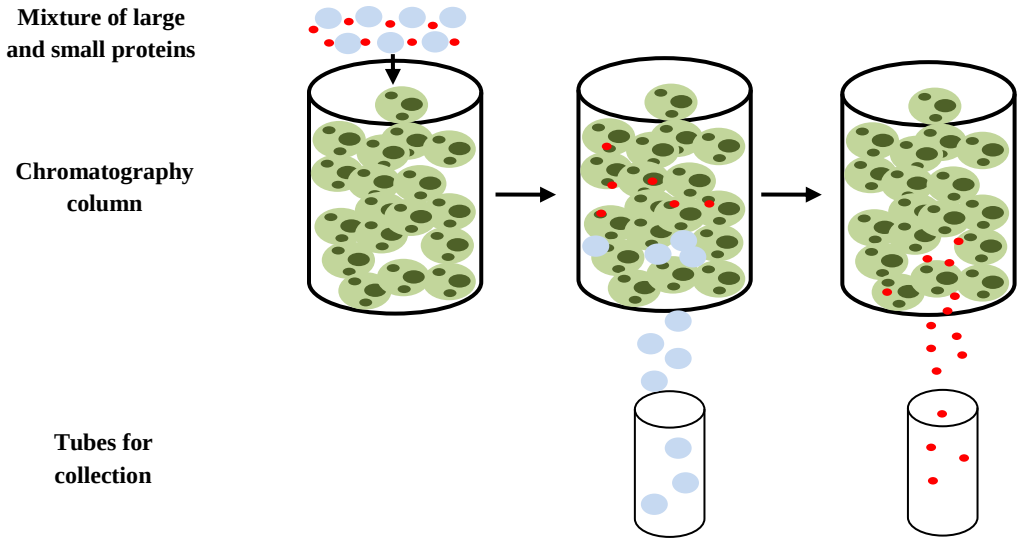

Figure 3.1 Size exclusion chromatography columns contain beads with various pores. The larger proteins, which fit in fewer pores, take a more direct path through the column and elute first. The smaller proteins are slower to elute as they meander in and out of pores.

3.2. Materials and methods

3.2.1. Reagents and chemicals

All reagents used in purification and characterization of the *Pf*ThzK in this chapter are detailed in Appendix 2.

3.2.2. Plasmids and culture conditions

The *Pf*ThzK-pET28(+) constructs from the previous study (Section 2.3.2) were stored at -20 ℃. LA plates and LB media (Appendix 2) with two antibiotics were used for colony selection (30 μg/ml kanamycin and 34 μg/ml chloramphenicol in ethanol). Auto-induction media (Table 3.1) were used to over-express *Pf*ThzK proteins.

Table 3.1. *Auto-induction components.*

Auto-induction media	Component	Final concentration	Sterilization
20×NPS	0.5 M $(NH_4)_2SO_4$ 1 M KH_2PO_4 1 M Na_2HPO_4	50 ml/ L	Filter sterilize
50×5052	250 g/L Glycerol 25 g/L Glucose 100 g/L α-Lactose	20 ml/L	Filter sterilize
$MgSO_4$	1M $MgSO_4$	2 ml/L	Filter sterilize
ZY	10 g/L Tryptone 5 g/L yeast extract	928 ml	Autoclave
Antibiotics	30 μg/ml kanamycin 34 μg/ml chloramphenicol	1 ml/L	

3.2.3. Expression of *Pf*ThzK protein

The *Pf*ThzK-pET28(+) constructs were transformed into *E. coli* BL21 competent cells and plated out on LA with 30 μg/ml kanamycin and 34 μg/ml chloramphenicol. Positive colonies were selected and inoculated to LB broth with the same antibiotic pressure, and incubated in a rotary shaker (160 rpm; 37 ℃; 14 h). The culture was inoculated into the auto-induction media (10 ml culture/1 L auto-induction media) and dispensed into ten 500 ml sterile flasks (100 ml per flask), incubated in a rotary shaker (160 rpm; 20 ℃; 36 h). One flask was randomly chosen and used for induction study: 1 ml of culture from this flask was taken every 2 hours for 36 h, washed with Tris-HCl buffer (50 mM; pH

7.0), pelleted by centrifugation (1,500 × g; 5 min), frozen (-80 ℃) and retained as "Induction sample1-18 (IS1-IS18)".

The cultures in other flasks were centrifuged (5, 000 × g; 20 min; 4 ℃) in an Avanti® J-E centrifuge and a JA-14 rotor (Beckman Coulter) after 36 h incubation period. The cell pellet was resuspended in Tris-HCl buffer (50 ml; 50 mM; pH 7.0), centrifuged at 5,000 × g; 20 min; 4 ℃), and the cell pellet weighed, then resuspended in the same buffer (20 ml buffer/1 g cells). The cells suspensions were lyzed using lysozyme (1 mg lysozyme/1 ml suspension), incubated in a rotary shaker (160 rpm; 37 ℃; 1 h), and finally stored at -80 ℃.

3.2.4. Purification of *Pf*ThzK protein

The frozen cell lysate was thawed at 4 ℃ overnight, the unbroken cells and debris were removed by centrifugation (2, 700 × g; 30 min; 4 ℃), an aliquot of supernatant (1.0 ml) was retained for "total protein (T)", and the remaining supernatant clarified by ultra-centrifugation (28,000 × g, 4°C, 90 min) with an Optima™ L-90K centrifuge (Beckman Coulter). An aliquot of this supernatant (1.0 ml) was saved as "clarified protein (C)".

The recombinant protein *Pf*ThzK was then purified by nickel affinity and size exclusion chromatography. The "clarified protein" (150 ml) mixed with 50 ml binding buffer (50 mM NaCl, 50 mM Tris-HCl, pH 7.5) was loaded onto a His-trap FF column (5 ml, Amersham Biosciences) at 5 ml/min, which was pre-washed by binding buffer, and the bound protein eluted with elution buffer (0.5 M NaCl, 0.5 M imidazole, 20 mM Tris-HCl, pH 7.5) in a linear 0-0.5 M imidazole gradient. An aliquot of the active fractions (1.0 ml) was retained for "His-trap fractions (H)", and the remaining active fractions pooled and

concentrated to 2 ml by Vivaspin2 centrifugal concentrators MWCO 10,000 (Sartorius Stedim Biotech, Germany). The concentrated sample was loaded onto Sephacryl S100HR gel filtration column, equilibrated and eluted using gel filtration buffer (50 mM NaCl, 50 mM Tris-HCl, pH 7.5) at 1 ml/min. An aliquot of the active fractions (1.0 ml) was retained for "gel filtration fractions (G)", and the remainder pooled and dialyzed (50 mM Tris-HCl, pH 7.0, 16 h, 4℃). The dialyzed protein (D) was then ready for subsequent analysis.

3.2.5. Characterization of recombinant *Pf*ThzK protein

3.2.5.1. SDS-PAGE analysis

Sodium dodecyl sulphate polyacrylamide gel electrophoresis (SDS-PAGE) is the most widely used method for analyzing protein mixtures qualitatively and also for evaluation of purity of protein during protein purification steps. The protein sample is boiled in loading buffer containing β-mercaptoethanol, which disrupts the secondary, tertiary and quaternary structure of the protein by destroying the disulphide bridges. This leads to the opening up of the protein into a linear rod-shaped structure coating with a series of negatively charged SDS molecules of constant charge density per unit mass, thus facilitating electrophoretic mobility (Wilson and Walker, 1994).

Polyacrylamide gels were prepared by the free radical polymerization of acrylamide and the cross linking agent tetramethylethylenediamine (TEMED) bisacrylamide (Figure 3.2), the procedure is detailed in Appendix 5.

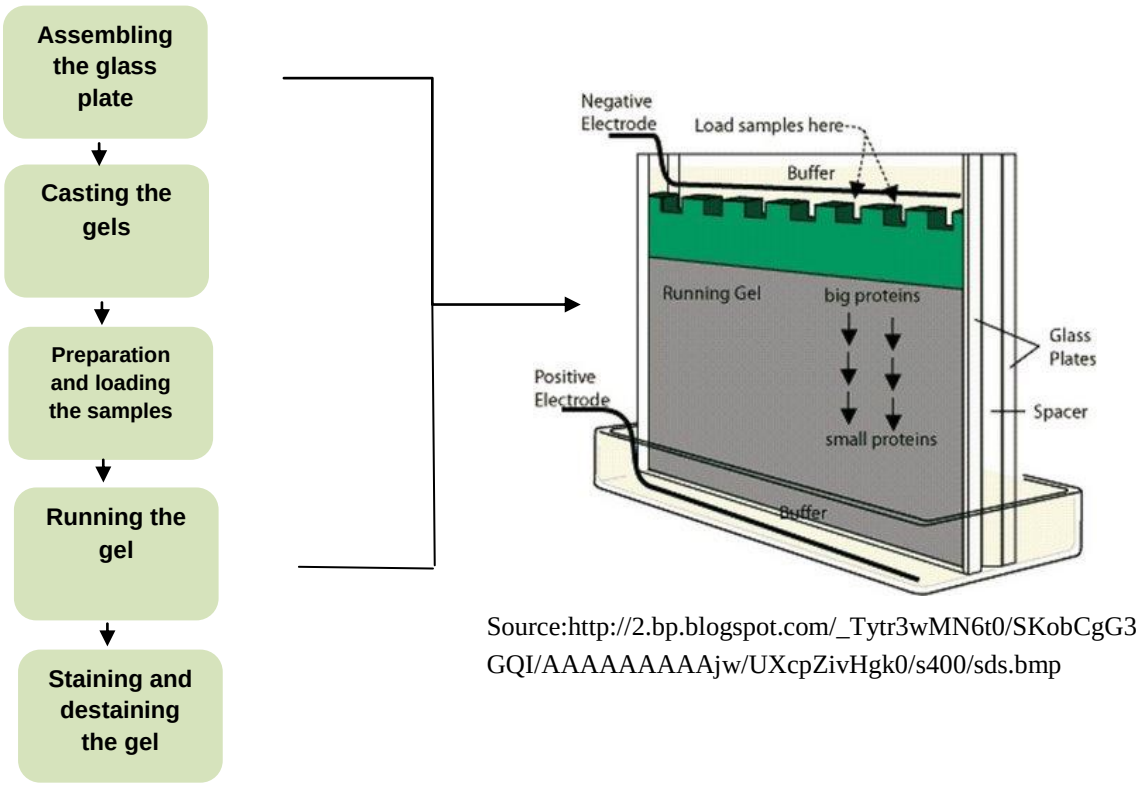

Source:http://2.bp.blogspot.com/_Tytr3wMN6t0/SKobCgG3GQI/AAAAAAAAAjw/UXcpZivHgk0/s400/sds.bmp

Figure 3.2. The flow chat of SDS-PAGE and the setting of electrophoresis gel.

The proteins present in each fraction from the previous step were determined by SDS-PAGE electrophoresis using 10% resolving gel and 4% stacking gel (Laemmli, 1970). PageRuler™ Prestained Protein Ladder (Fermentas) was used as molecular weight markers and an estimation of the molecular weights of protein bands visualized on the gels. Electrophoresis was carried out using the Mini-PROTEAN3 Electrophoresis System (Bio-Rad) with SDS running buffer (Appendix 2) at 100 V until the desired separation had been achieved. Bands of protein were visualized on the SDS-PAGE gels by staining with Coomassie Blue (Fairbanks *et al*., 1971). Three staining solutions, each containing 10% acetic acid and progressively lower concentrations of Coomassie Brilliant Blue R-

250 were used, and the staining and destaining protocol is shown in Appendix 6. All solutions used for SDS-PAGE analysis of proteins are listed in Appendix 2.

3.2.5.2. Protein concentration

Protein concentrations were evaluated using the Pierce® BCA Protein Assay Kit (Thermo SCIENTIFIC), which is based on bicinchoninic acid (BCA) for the colorimetric detection and quantification of total protein. This method is highly sensitive to the colorimetric detection of the cuprous cation. The purple-coloured reaction product of the assay is water-soluble and exhibits a strong absorbance at 562 nm that is linear with an increased protein concentration over a broad working range (20-2,000 µg/ml). Protein concentrations in this study were determined with reference to standards of bovine serum albumin (Appendix 7). A series of dilutions of known concentration was prepared, and 50 µl of each sample was added to 1 ml of the working reagent, vortexed, and then incubated (60 ℃; 30 min). The absorbance was read at 562 nm with a Spectroquant® Pharo300 spectrophotometer (Merck Pty Ltd).

3.2.5.3. *Pf*ThzK activity determination

Purified *Pf*ThzK activities were determined by an improved molybdate method, which is based on the colorimetric determination of inorganic phosphate (Fiske and Subbarow, 1925). In the enzyme assay reaction, *Pf*ThzK converts 5-(2-hydroxyethyl)-4-methylthiazole to 4-methyl-5-(2-phosphoethyl)-thiazole (THZ-P) and inorganic phosphate “Pi”, which reacts with ammonium molybdate to produce a coloured complex (Chifflet *et al*., 1988). This activity assay should be carried out in an acidic solution containing excess ascorbic acid to prevent the complex from slowly oxidizing. The “Pi”

concentrations in the samples were determined by extrapolation from the inorganic phosphate standard curve, which was prepared by serial dilutions of a standard phosphate solution. The enzyme assay was in a standard condition with a total volume of 97 µl consisting of Tris-HCl buffer (29 mM, pH 7.5), $MgSO_4$ (6 mM), ATP (3 mM) and THZ (3 mM). The reaction mixture was incubated at a certain temperature for 10 min and stopped by heating (100 ℃, 2 min).

Sample (80 µl) was placed in a 96-well microtitre plate, followed by 160 µl of Reagent C [0.65% $(NH_4)_2MoO_4$; 9% Ascorbic acid]. The mixture was allowed to stand (10 min; room temperature) for colour development, and the absorbance of each solution read at 700 nm by microtitre plate reader (Biotek Epoch). All the reagents used and the standard curve are shown in Appendix 8.

3.2.5.4. The temperature profile of *Pf*ThzK

The optimum temperature for the purified *Pf*ThzK was determined under the same enzyme assay conditions (Section 3.2.5.3). The purified *Pf*ThzK was incubated at varying temperatures ranging from 10-80 ℃, and then 6 µl of each sample was added to enzyme assay reactions.

3.2.5.5. The pH profile of *Pf*ThzK

The optimum pH condition for purified *Pf*ThzK was determined under the same enzyme assay conditions (Section 3.2.5.3). The purified *Pf*ThzK was incubated with a 0.1 M buffer cocktail (0.1 M sodium acetate pH 3.5-5, MES pH 5.5-6.5 and Tris-HCl pH 7-9), and then 6 µl of each sample was added to enzyme assay reactions.

3.2.5.6. The thermal stability of purified *Pf*ThzK

The optimal temperature and pH were used to determine the thermal stability of purified *Pf*ThzK. Pre-activated *Pf*ThzK activity at time zero was considered to be 100% relative activity, and the activity was measured at 30 min interval for 5 h. A half-life ($t_{1/2}$), which is the time required for the enzyme to lose 50% of its initial activity, was also measured.

3.2.5.7. Kinetic study

For analysis of the substrate THZ specificity of *Pf*ThzK, the standard assay was executed with varying concentrations of THZ between 0 and 0.3 mM. The reaction products were treated as per the standard and measurement was carried out at 700 nm (Appendix 7) as described in section 3.2.5.3.

Enzyme-catalyzed reactions are characterized by the formation of a complex between the enzyme and its substrate (the ES complex). The Michaelis-Menten equation is the rate equation for a one-substrate enzyme catalyzed reaction. It quantitatively relates the initial rate, the maximum rate, and the initial substrate concentration to the Michaelis constant K_m.

$$v_0 = \frac{V_{max}[S]}{K_m + [S]}$$

Hanes-Woolf Plot is one of the linear plots of the Michaelis-Menten Equation:

$$\frac{[S]}{v} = \frac{1}{V_{\max}}[S] + \frac{K_m}{V_{\max}}$$

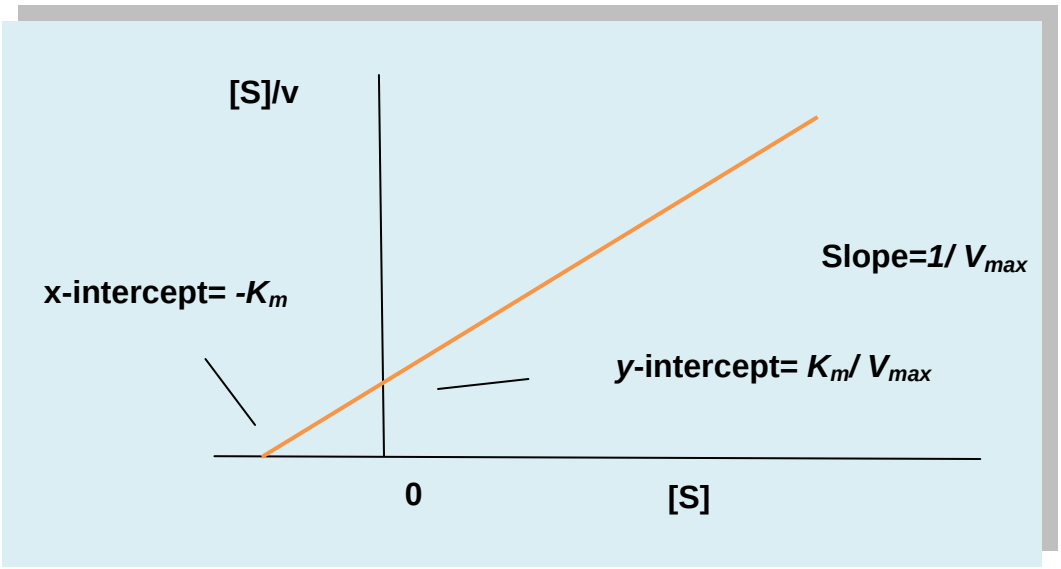

Figure 3.3. Hanes-Woolf Plot.

Where V_{max} is the activity of the enzyme approached at saturating concentrations of substrate, K_m is the concentration of substrate required to produce a velocity that 50% of V_{max} (Gilbert, 2000).

3.3. Results and discussions

3.3.1. Expression of recombinant *Pf*ThzK

SDS-PAGE was carried out with each sample (Figure 3.4). The bands represent *Pf*ThzK (around 34 kDa) were visible from sample IS5-IS18, indicating that after 10-hour induction period, certain amount of proteins was expressed by the cells. Low concentration of protein was noticed after 10-hour induction (IS5) while the most protein was expressed after 32 h induction (IS16).

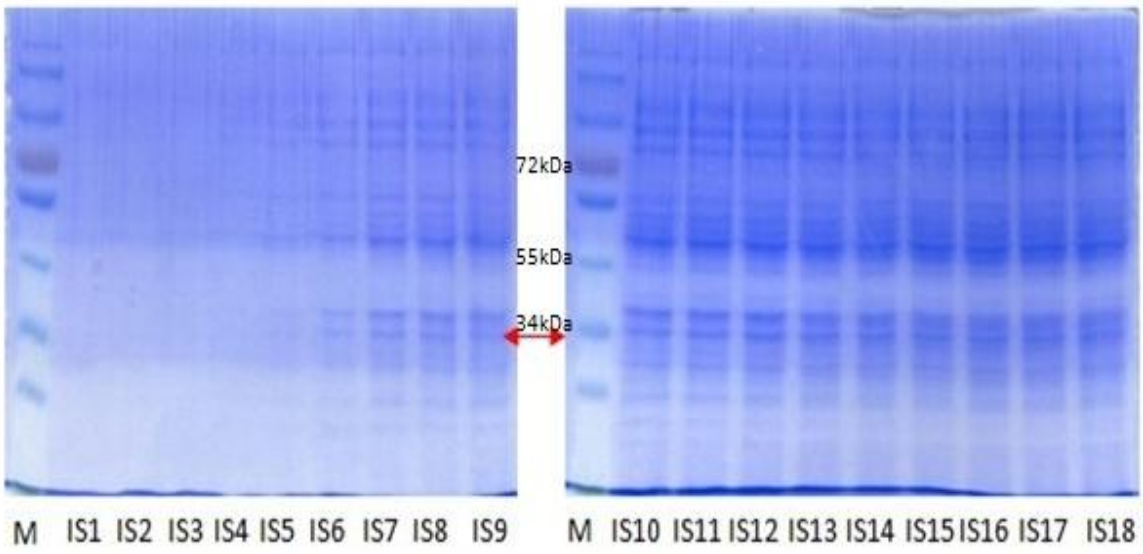

Figure 3.4. SDS-PAGE analysis of the auto-induction study. (M): marker, (IS1-IS18): samples of auto-induction culture from time 2 h to time 36 h with 2 h intervals.

3.3.2. Purification of recombinant *Pf*ThzK

The expressed protein was applied to a Ni-affinity column and all of the collected fractions (Figure 3.5) were analyzed by SDS-PAGE electrophoresis to detect which fractions contained *Pf*ThzK. The fractions of interest were then concentrated and loaded onto a gel filtration column, and eluted by 50 mM Tris-HCl with 50 mM NaCl, the elution profile is shown in Figure 3.6. One main protein peak was observed between elution volumes 60-100 ml, indicating that *Pf*ThzK was monomer.

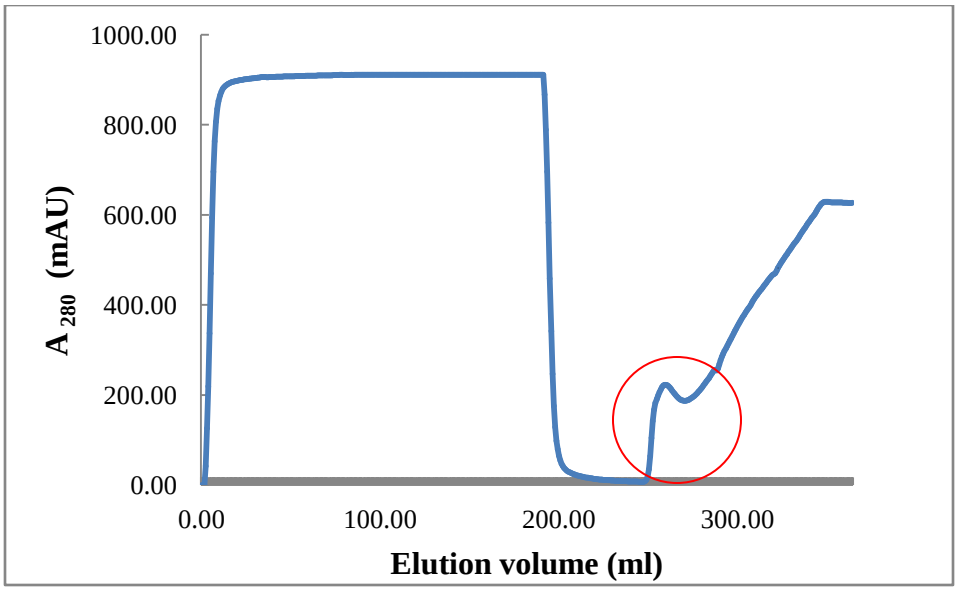

Figure 3.5. Elution profile obtained from nickel affinity resin. Flow rate: 5 ml/min, elution fraction size: 5ml. The bound proteins shown in red were the fractions collected.

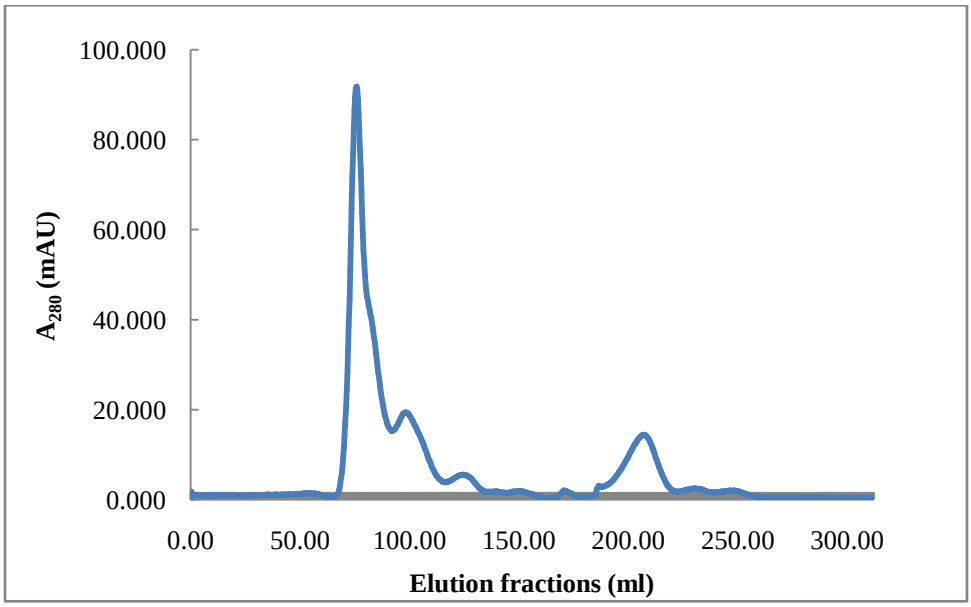

Figure 3.6. Protein elution profile obtained from size exclusion chromatography (Sephacryl S100HR gel filtration column).

After each purification step, SDS-PAGE was employed to determine the molecular weight of the protein(s) as shown in Figure 3.7. Several bands were observed from the first two samples, reflecting various soluble proteins in the "Total protein" sample. After nickel-affinity chromatography, from the third band, only a few intensive bands were observed, indicating that the majority of those soluble proteins were unbound proteins, and had been washed out through His-trap column. After size exclusion chromatography, only one intensive band of 34 kDa was observed, corresponding to *Pf*ThzK. Dialysis, as the final purification step, removed some of the contaminating bands and also the salts from gel filtration buffer. Samples from each purification step were collected:

- The supernatant of post-centrifuged frozen cell lysate (Total protein "T")
- The supernatant of post-ultracentrifugation (Clarified protein "C")
- His-trap nickel affinity chromatography ("H")
- Gel filtration chromatography ("G")
- Dialysis ("D")

A summary of the purification procedure after centrifugation, ultracentrifugation, His-trap nickel affinity chromatography, gel filtration chromatography and dialysis is shown in Table 3.2. After His-trap Ni-affinity, the amount of total protein decreased from166.44 mg to 4.89 mg, indicating that most of the expressed proteins were unbound, and washed out, which can be also observed form SDS-PAGE analysis (Figure 3.7). It also resulted in the loss of total activity from 21.30 µmol/min/ml of the starting material to 0.22 µmol/min/ml after final dialysis. The specific activity, however, increased accordingly at every step.

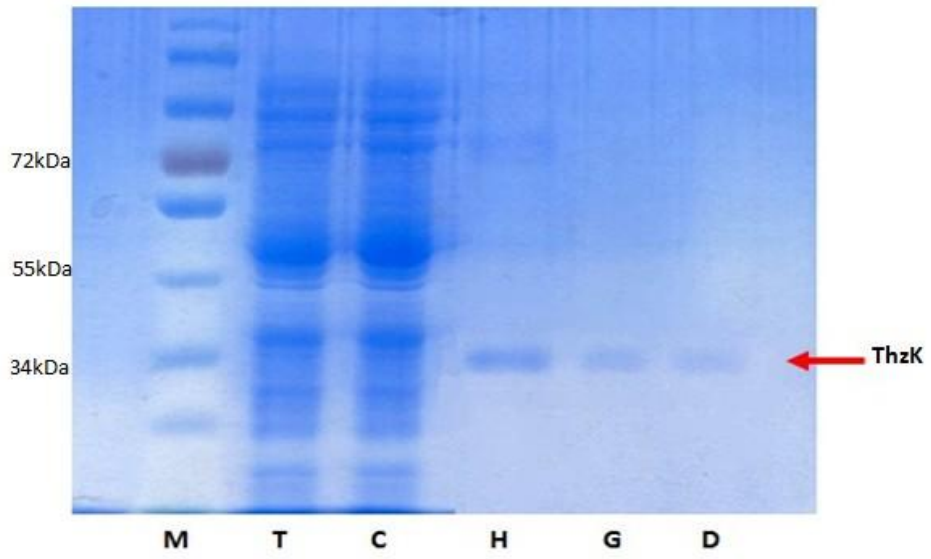

Figure 3.7. 10% SDS-PAGE analysis of each purification step. (M): marker, (T), (C), (H), (G) and (D) indicates each step during purification. Total protein "T": The supernatant of post-centrifuged frozen cell lysate; Clarified protein "C": The supernatant of post-ultracentrifugation; "H": His-trap nickel affinity chromatography; "G": Gel filtration chromatography; "D": Dialysis.

Table 3.2. Purification table of *Pf*ThzK. The enzyme activity was calculated in U, which means the amount of the enzyme catalyzing the conversion of 1 µmol of substrate per minute (U= µmol/min/ml).

Purification step	Volume (ml)	Total protein (mg)	Total activity (U)	Specific activity (U/mg)	Purification fold	Yield (%)
Post centrifuge	170	174.62	21.30	0.12	1	100
Post ultracentrifuge	167	166.44	19.46	0.11	0.92	91.4
His-trap	25	4.89	0.62	0.13	1.04	2.9
Gel filtration	25	0.95	0.26	0.27	2.26	1.23
Dialysis	24.8	0.80	0.22	0.28	2.33	1.03

3.3.3. Characterization of recombinant *Pf*ThzK

3.3.3.1. SDS-PAGE analysis and protein concentration

SDS-PAGE analysis and protein concentration determination were carried out after each purification step and after dialysis, only one single band of 34 kDa was observed (Figure 3.7).

The final concentration of purified *Pf*ThzK was 32.26 µg/ml. It was also noticed that after dialysis, protein concentration was quite low for characterization, thus pure *Pf*ThzK was concentrated by Vivaspin2 centrifugal concentrators MWCO 10,000 (Sartorius Stedim Biotech, Germany) for subsequent analysis.

3.3.3.2. Temperature optimum profile

The activities were determined over a range of temperatures, from 10 ℃ to 80 ℃, and the temperature curve follows a typical bell shape (Figure 3.8). The rate of enzymatic reaction increases as the temperature increases from 10 ℃ to 30 ℃ with a maximum *Pf*ThzK activity seen at 37 ℃.

Previous studies on ThzK characterized from *Bacillus subtilis* and *E. coli* had also found an optimal temperature of 35-37 ℃ range (Zhang *et al.*, 1997; Begley *et al.*, 1999). The downside to this reaction, was noted at 50 ℃ and higher temperatures, because protein structures could be disrupted, leading to inactivation and denaturation (Hohmannand Meacok, 1998). At 60 ℃ and higher temperatures, the bigger error bars represent the lager variability of data, and also reflect that *Pf*ThzK were denatured at those temperatures and the measurements were not really accurate according to the low activities.

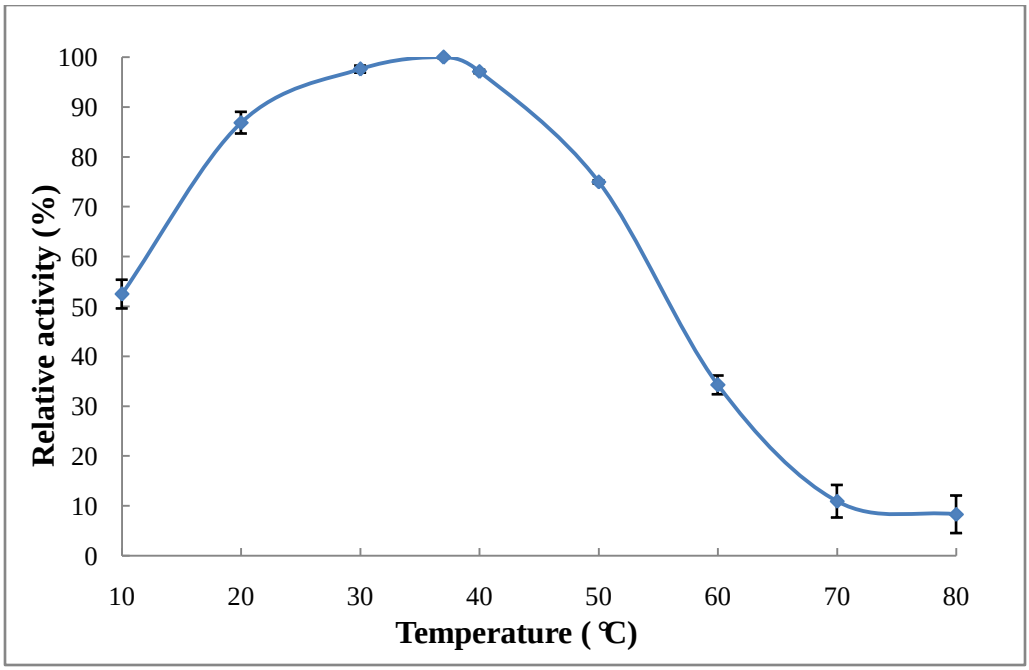

Figure 3.8. Temperature profile of purified *Pf*ThzK enzyme. Hundred percent activity (0.027 U/ml) was observed at 37 ℃.

3.3.3.3. pH optimum profile

The rate of enzyme activity is commonly influenced by the structure of enzyme. The change in pH results in breaking of the ionic bonds which hold the tertiary structure of the enzyme together and the enzyme loses its functional shape, particularly the shape of the active site. Most enzymes normally present a strong dependence of activity on the pH conditions, so it is important to optimize the pH of purified *Pf*ThzK (Dixon, 1952; Wikinson, 1960; Dyson and Noltmann, 1967). The purified *Pf*ThzK in this study had an optimal pH at 7.5 (Figure 3.9). Previous studies on ThzK from *B. subtilis* had an optimal pH to be pH 7-7.5 (Zhang *et al*., 1997).

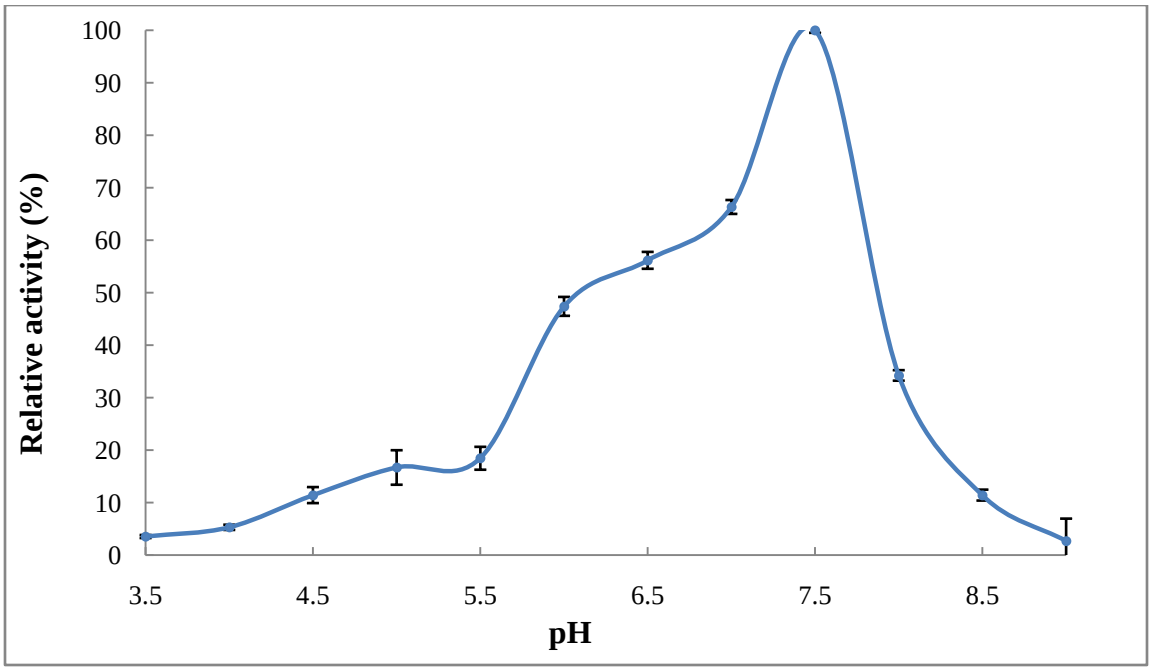

Figure 3.9. pH profile of the purified *Pf*ThzK enzyme. Hundred percent activity (0.028 U/ml) was observed at pH 7.5.

3.3.3.4. Thermal stability of purified *Pf*ThzK

The purified *Pf*ThzK was incubated with thiazole at the optimum conditions (37 ℃; pH 7.5) and the enzyme activities were determined at 30 min intervals for 5 hours. The slight activity loss was observed during the first 1 hour, and then enzyme activity decreased rapidly with the increased incubation time (Figure 3.10). The evident activity loss from 0.027 U/ml to 0.0051 U/ml during 1.5 h-3.5 h incubation periods, and after 3.5 hour incubation, 80% of the activity had been lost, thereafter slight decrease was observed. The purified *Pf*ThzK in this study had a half life of 2.66 hours ($t_{½}$=2.66).

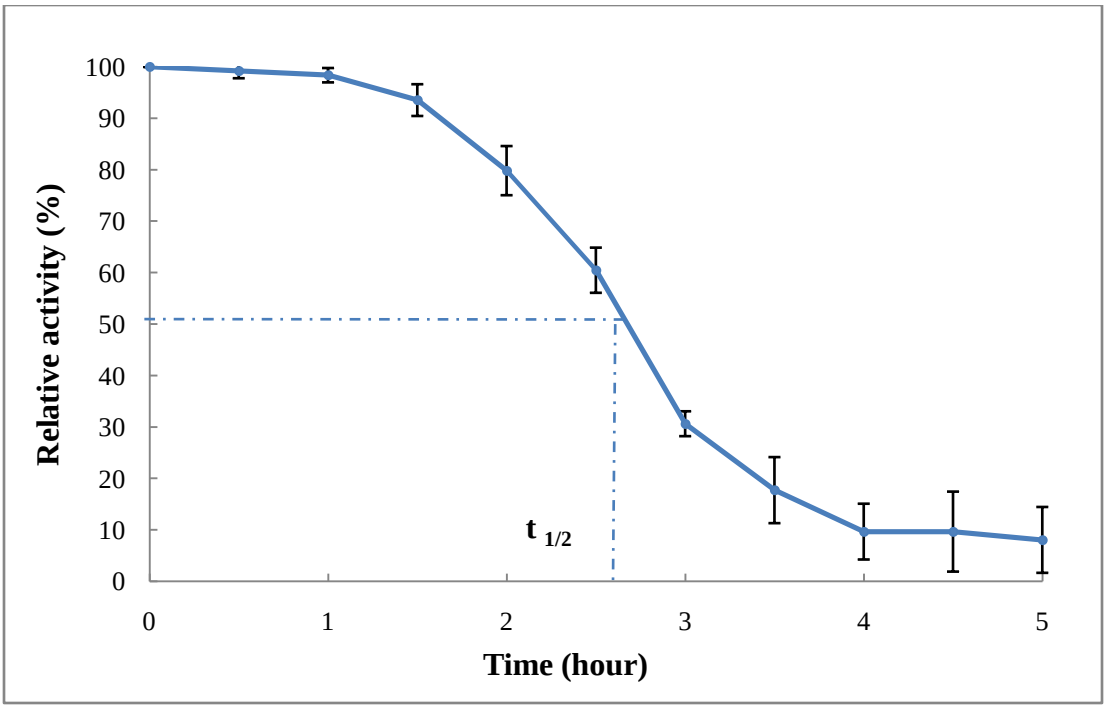

Figure 3.10. Thermal stability of purified *Pf*ThzK. The 100% activity was 0.029 U/ml, the initial enzyme activity at time zero.

3.3.3.5. Kinetic study

The effect of substrate concentration on the purified *Pf*ThzK was evaluated by measuring the *Pf*ThzK activity with a range of THZ concentration of (0-0.3 mM). The activities curve followed Michaelis-Menten, the *Pf*ThzK activity increased hyperbolically with the increased THZ concentration from 0-0.06 mM, and the activity remained relatively constant according to the substrate saturation (Figure 3.11).

The initial velocity of the reaction at different substrate concentrations was measured, and kinetic parameters K_m and V_{max} values were calculated by using Hanes–Woof ([S]/v-[S] plot) analysis (Figure 3.12). The Michaelis constant (K_m) value of *Pf*ThzK was found to be 0.065 mM while the specific activity was 295.04 nmol/mg which is a little higher

than previous study of 249±14 nmol/mg (Wrenger *et al.*, 2006). V_{max} calculated from the inverse of the slope (Figure 3.12) is 0.037 µmol/min/ml.

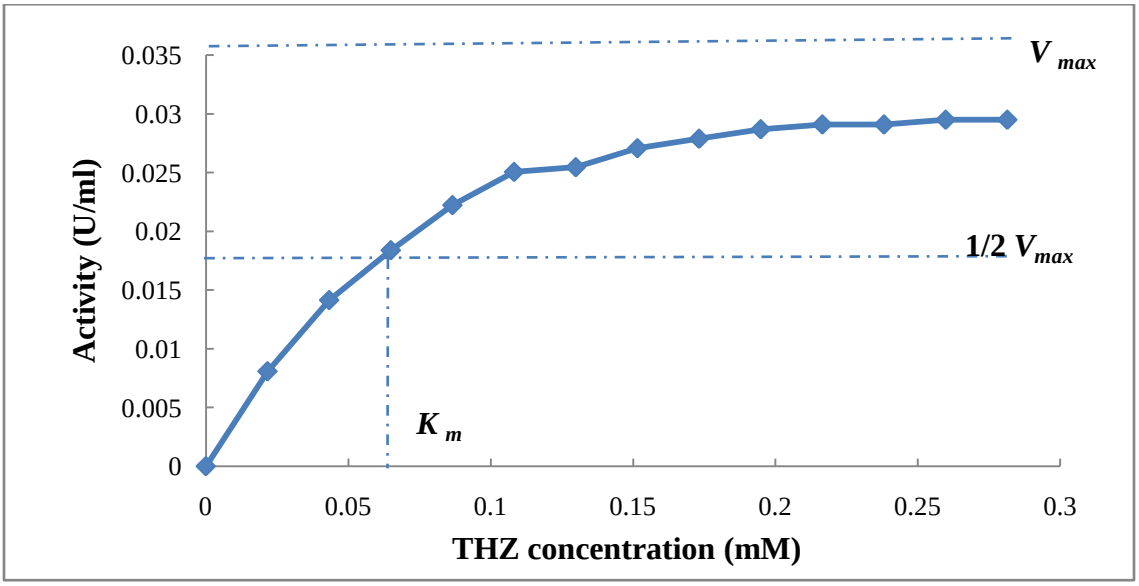

Figure 3.11. Michaelis-Menten plot of purified *Pf*ThzK enzyme activity versus THZ concentration.

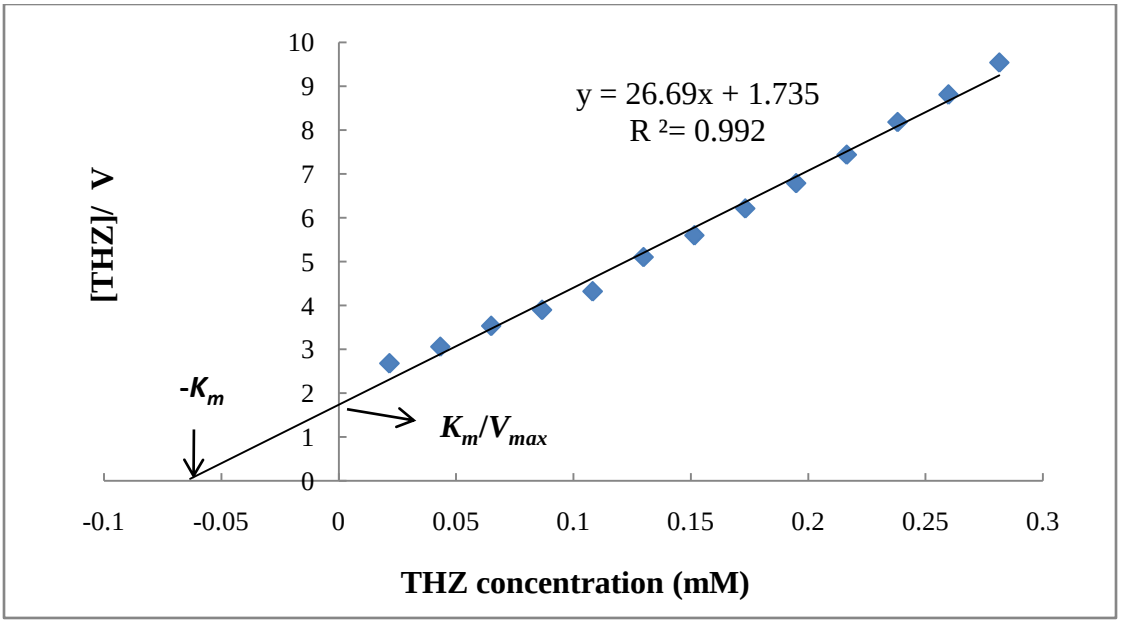

Figure 3.12. Hanes-Woolf plot of purified *Pf*ThzK enzyme activity versus THZ concentration.

3.4 Conclusions

To summarize, the ORF encoding methylhydroxyethylthiazolekinase form *P. falciparum* (*Pf*ThzK) was cloned into the expression vector pET28b(+) and recombinantly expressed in *E. coli* BL21 (DE3) in auto-induction medium with a yield of 0.8 mg/L of bacteria culture. The expressed protein was purified by nickel affinity chromatography and the purity of the recombinant enzyme was assessed by SDS-PAGE analysis. *Pf*ThzK eluted as a single peak corresponding to a molecular mass of 34 kDa, suggesting a monomeric structure. The optimal temperature and pH were 37 ℃ and 7.5 respectively, and the specific activity was found to be 295.04 nmol/mg, with a k_{cat} value of 0.149 s^{-1}. The kinetic parameters of the *Pf*ThzK were also analyzed with a V_{max} value of 0.037 μmol/min/ml and K_m value of 0.065 mM, which was 2-fold higher than the counterpart from *B. subtilis* (Zhang *et al.*, 1997). Furthermore, the specific activity of *Pf*ThzK is a little higher than that in previous study (Wrenger, 2006), but 10-fold higher comparing to *B. subtilis* value (Campobasso *et al*., 2000). In addition, the catalytic efficiency was calculated to be $2.3 \times 10^3\ M^{-1}s^{-1}$, which is slightly higher than that from a previous study of $2 \times 10^3\ M^{-1}s^{-1}$ (Wrenger, 2006).

Chapter4
Synthesis of Ag Nanoparticles and Interaction with methylhydroxyethylthiazolekinase

4.1. Introduction

Nanotechnology and nanoparticles have been increasingly recognized for their potential applications in aerospace engineering, nano-electronics, environmental remediation, medical healthcare and consumer products in the past decade (Gerber and Lang, 2006; Sing *et al*., 2009). It is estimated that of all the metal nanoparticles in consumer products, silver nanoparticles (Ag NPs) have the highest degree of applications of commercialization (Maynard and Michelson, 2007). Various Ag NPs applications have been reported recently, ranging from disinfection medical devices and home appliances to water treatment (Vigneshwaran *et al*., 2007; Tolaymat *et al*., 2010). Moreover, the unique plasmon–resonance optical scattering properties of Ag NPs allow them to be used in bio-sensing and imaging applications (Dubas and Pimpan, 2008; Schrand *et al*., 2008). Furthermore, Ag NPs have also shown the important potential applications in the treatment of disease (Moghimi *et al*., 2001; Panyam and Labhasetwar, 2003), for example, Ag NPs have been shown to interact with the HIV-1 virus and inhibit the virus to bind host cells *in vitro* (Elechiguerra *et al*., 2005).

The metallic nanoparticles have shown significant mechanical, electronic, magnetic, optical and catalytic properties, which are highly influenced by their size, shape and

composition (Buzea *et al.,* 2007; Das and Marsili, 2011; Burda *et al*., 2005). Therefore, the specific synthetic route should be improved upon according to the properties of metal nanoparticles (Perez-Juste *et al.*, 2005; Cuenya, 2010; Chen and Liu, 2011). Numerous approaches to synthesize Ag NPs have been published recently, such as microwave treatment (Salkar *et al.*, 1999); phase transfer processes (Li *et al.*, 2002); laser ablation (Dolgaev *et al*., 2002); photochemical synthesis (Mallick *et al*., 2004); micro-emulsion (Huseln *et al.,* 2004) and ɣ-irradiatation (Shin *et al*., 2004). Chemical synthetic routes (Kheybari *et al*., 2010; Sadeghi *et al.*, 2010; Prabhu *et al.*, 2010; Khan *et al.*, 2011; Hussain *et al.,* 2011; Dawy*et al.,* 2012) and biological routes (Shahverdi *et al*., 2007; Masurkar *et al.,* 2011; Chaudhari *et al*., 2012; Chan and Mashitah, 2012) for Ag NPs have been extensively used to improve the methods with the latter having been designed to be more environmental and eco-friendly. The chemical reduction methods, however, involve the synthesis of Ag NPs with well-controlled size in which silver ions are reduced by reductants and stabilizer or protective agents to prevent these NPs from aggregation (van Dong *et al*., 2012).

4.1.1. Characterization of nanoparticles

Nanoparticles must be characterized to understand their unique properties, such as size, shape, surface charge, and adsorption, in terms of application of these nanoparticles (Rivera-Gil *et al*., 2012). A number of methods are currently used to characterize nanoparticles, and the most commonly used are introduced as followed.

4.1.1.1. Ultraviolet-visible spectroscopy

Ultraviolet and visible spectrometers (Uv-vis spectrometers) have been generally employed in the laboratory for many years and have become the most important analytical instrument in the modern day research (Milone, 2012). For a liquid sample, a standard spectroscopy measures direct transmittance as a percentage, which represents the percentage of the incident beam of light transmitted by the sample. The value is then used to calculate absorbance, which is widely used to measure concentration in liquid solutions (Smith, 2011; Tripathi *et al*., 2012). Gold and silver nanoparticles have been extensively characterized by this technique due to their unique plasmon nature and optical properties, such as concentration and aggregation state (Chandra *et al*., 2010; Cheng *et al*., 2011; Prathna *et al*., 2011; Lombardi *et al*., 2012).

4.1.1.2. Transmission electron microscopy

Nanoparticles always present different shapes and sizes, which can be usually detected by transmission electron microscopy (TEM) (Figure 4.1). TEM is a microscopy technique, which transmit a beam of electrons through an ultra-thin specimen, and interact with the specimen (Kruse, 2009; Gahlaut, 2012). The denser parts of specimen absorb more electrons, and make them look darker on the resulting image (Briggman and Bock, 2012; Staniewicz *et al*., 2012). The remarkable advantage of TEM is that they give images with high resolutions. The drawback, however, is that they can be used only on thin specimens, artefacts such as folds, bubbles, can be found on the image (Findlay *et al.*, 2009; Ong *et al*., 2011; Akhtar, 2012; Fultz and Howe, 2012). Furthermore, the slicing and staining process is complex and expensive (Dudkiewicz *et al*., 2011).

4.1.1.3. Scanning electron microscopy

The scanning electron microscopy (SEM) is an electron microscope (Figure 4.2) which produces an image of a sample by scanning it with a focused beam of electrons, and the electrons interact with sample electrons, producing various signals which can be detected as the information of the sample surface topography and composition (Ayache *et al*., 2010; Vermeij *et al*., 2012; Maco *et al*., 2013). The specimens can be observed in high vacuum, low vacuum and the environmental SEM specimens can be observed in wet conditions (Gandolfi *et al*., 2010).

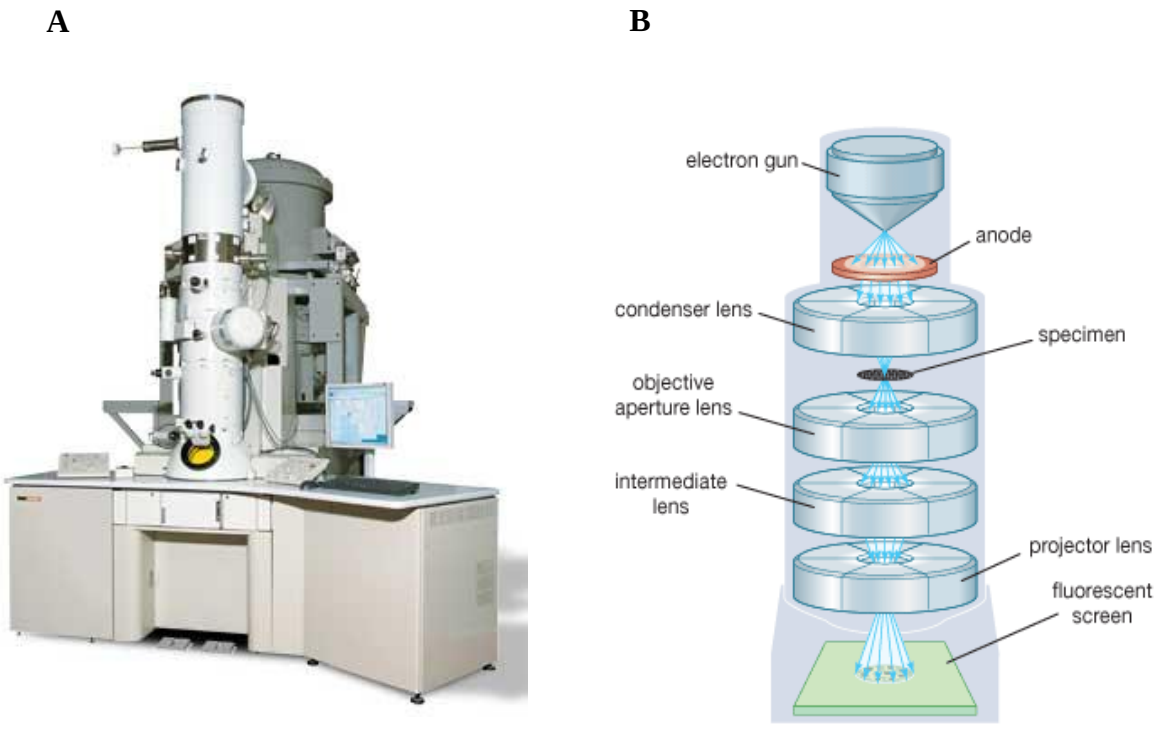

Figure 4.1. Transmission electron microscope (TEM). A) A conventional TEM instrument (JEM-2100F, JEOL); B) Schematic representation of the TEM.
(JEOL global solutions provider for advanced technology; A pocket merlin, 2008).

For a standard SEM, an electron is thermionically emitted from an electron gun which is fitted with a tungsten or lathan hexaboride cathode filament. The tungsten filament is the most commonly used because of its higher melting temperature (Li *et al.*, 2012). The electron beam generally has an energy ranging from 0.2 keV to 50 keV, which is much lower than TEM with voltage of 300 keV. It is focused by two condenser lenses to a spot about 0.4 nm to 5 nm in diameter (Guan, 2010; Dellby, 2012; Zhou, 2013). The 1 ° electrons lose energy by repeated random scattering and absorption within the specimen, which extend from less than 0.1-5 μm into the surface. The energy exchange between the electron beam and the sample leads to the reflection of high-energy electrons by elastic scattering, emission of 2 ° electrons can be picked up by specialized detectors depending on the type of different instrumentations. SEM is a valuable tool to determine the purity of nanoparticles, and also quite important to determine the level of dispersion and uniformity of metal nanoparticles.

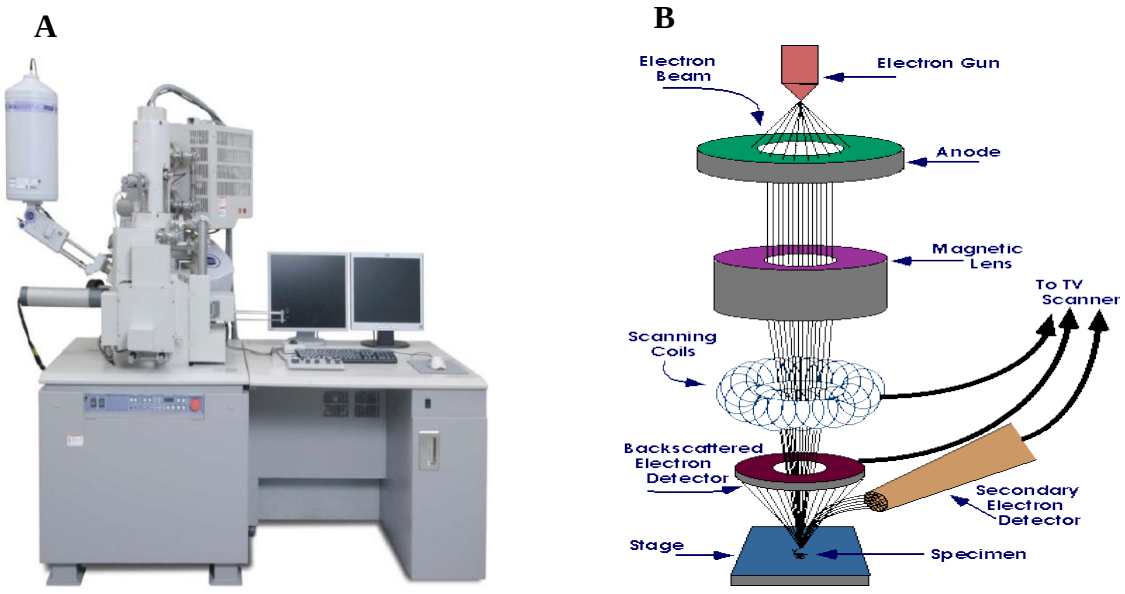

Figure 4.2. Scanning electron microscope (SEM). A) A conventional SEM instrument (Hitachi SU6600, Direct Industry); B) Schematic representation of the SEM. (Direct Industry-The Virtual Industrial Exhibition; Schweitzer, Radiological and Environmental Management, 2013).

4.1.2. The objectives of this chapter

The objectives of this chapter are:

i. Synthesis of Ag NPs by both sodium borohydride and tannic acid.
ii. Characterization of Ag NPs by UV-vis spectrophotometer and transmission electron microscopy (TEM).
iii. Evaluate the effect of Ag NPs on the methylhydroxyethylthiazolekinase activity ex *P. falciparum*.

4.2. Materials and methods

4.2.1. Materials

Silver nitrate ($AgNO_3$) and sodium borohyride ($NaBH_4$) were obtained from Merck (South Africa). Tannic acid ($C_{76}H_{52}O_{46}$) was purchased from Sigma-Aldrich (South Africa). All the reagents and buffers were prepared using deionized water obtained from Milli-Q system.

4.2.2. Methods

4.2.2.1. Nanoparticles synthesis

4.2.2.1.1. Synthesis of Ag nanoparticles with $NaBH_4$

Ag nanoparticles were synthesized in the presence of ice-cold $NaBH_4$ as described by Solomon (2007) with some modifications. $AgNO_3$ (1.0 mM) was added dropwise (about 1 drop per second) to ice-cold $NaBH_4$ (2.0 mM) in an ice-bath. The reaction mixture was

stirred vigorously on a magnetic stir plate until full reaction was achieved as determined by visual change in colour.

4.2.2.1.2. Synthesis of Ag nanoparticles with tannic acid

Ag nanoparticles were synthesized in the presence of tannic acid as described by Sivaraman (2009) with some modifications. $AgNO_3$ (2.95 mM) was added as one portion to tannic acid solution (0.15 mM), while stirring at room temperature. The stirring was continued till there was no further change in colour.

4.2.2.2. Characterization

4.2.2.2.1. UV-visible spectroscopy

Samples were 10-fold diluted with deionized water and a spectral scan between 250-900 nm was carried out using a UV-visible spectrophotometer (Spectroquant Pharo 300, Merck) to evaluate plasmon resonance associated with the synthesized Ag nanoparticles.

4.2.2.2.2. Transmission electron microscopy (TEM)

Samples were 10-fold diluted with deionized water, and one drop of sample was applied on a carbon-coated copper grid, excess sample was removed using blotting paper after one minute, the grid was air-dried at room temperature. The electron photographs of nanoparticles were taken by JEOL JEM-1210 TEM operating at 80 keV. The Ag nanoparticle sizes were determined by analysis of 200 particles from 5-10 photographs of each sample using ‘Scandium’ computer software.

4.2.2.3. Effect of Ag nanoparticles on *Pf*ThzK activity

Constant concentrations of Ag nanoparticles (5, 10, 15, 20, 25, 30 µM) were prepared by diluting the synthesized sample with deionized water. Ag nanoparticles were incubated with purified *Pf*ThzK under standard condition (29 mM Tris-HCl, pH 7.5; 6 mM $MgSO_4$, 3 mM ATP, 3 mM THZ) for up to 5 hours, varying periods of incubation at intervals of 10, 20, 30, 60, 90, 120, 150, 180, 300 minutes were applied. The thiazolekinase activity was determined colorimetrically at 700 nm as described in Chapter 3 (3.2.5.3). To determine the inhibitor constant value K_i, purified *Pf*ThzK was treated with Ag NPs (5, 10, 15, 20, 25, 30 µM) in the presence of varying amounts of the substrate THZ (0.05-0.3 mM), the inhibition was monitored by determining the kinetic properties of the enzyme by Hanes-Woolf plot. K_i was calculated using equation: $Ki = \frac{[NPs\}.Vmax*}{Vmax - Vmax*}$. Where [NPs] = concentration of Ag nanoparticles; V_{max} and V_{max}*= maximum enzyme catalyzed reaction in absence and presence of nanoparticles respectively.

4.3. Results and discussion

4.3.1. Synthesis of Ag nanoparticles.

A fixed concentration of $AgNO_3$ was added dropwise to chilled $NaBH_4$ solution in an ice-bath with stirring, the concentration of Ag salt to $NaBH_4$ ratios of 1:6-1:30. A rapid colour change was observed from colourless to yellow and brownish with increased colour intensity depending on the amount of Ag metal present in the solution (Figure 4.3). The change of colour was the first indication of nanoparticles formation. Aggregation and precipitation was noticed from the molar ratio of $AgNO_3$ to $NaBH_4$ less than 1: 7.5

[sample (D) and (E)]. A large excess of $NaBH_4$ was needed both to reduce the ionic silver and to stabilize the silver nanoparticles that form, which was also reported in literature (Khan and Talib, 2010; Eising *et al*., 2011).

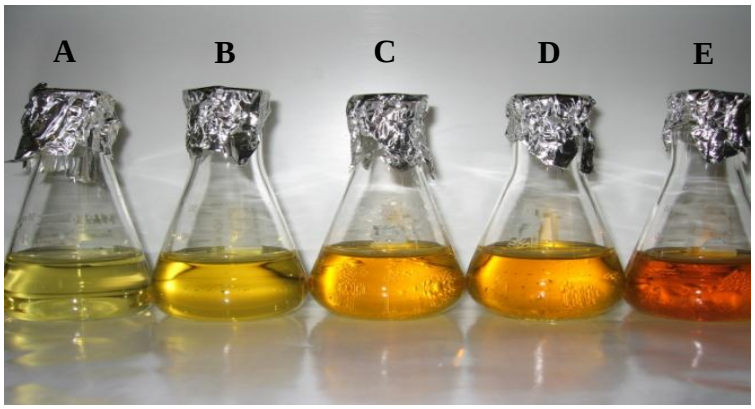

Figure 4.3. *The Ag nanoparticles synthesized with $NaBH_4$ at different molar ratios of metal salt to $NaBH_4$: A) 1:30; B) 1:15; C) 1:10; D) 1:7.5; E) 1:6.*

Tannic acid as a reducing agent and stabilizer was also employed to synthesize Ag nanoparticles. When $AgNO_3$ (2.95 mM) was added to tannic acid solution with stirring, a rapid colour change was observed from yellow to brown (Figure 4.4). Furthermore, no aggregation was noticed even after several months (Sivaraman *et al*., 2009). Tannic acid has been studied for its anti oxidant properties, and also as a chelating agent for several inorganic cations (Gonzalez *et al*., 2010; Yi *et al*., 2011).

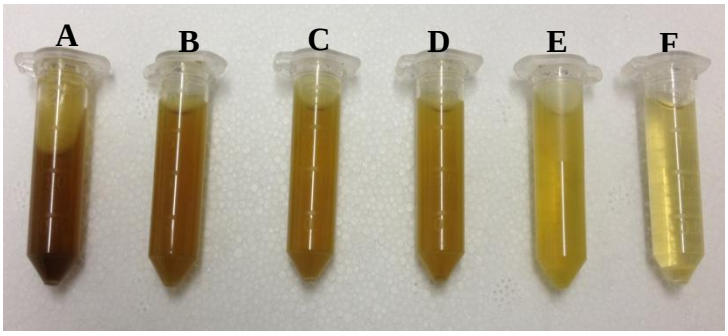

Figure 4.4. The Ag nanoparticles synthesized with different concentrations of tannic acid: A) 60 µM; B) 50 µM; C) 40 M; D) 30 µM; E) 20 µM; F) 10 µM.

4.3.2. Characterization of Ag nanoparticles

4.3.2.1. UV-visible spectroscopy

Synthesized Ag nanoparticles were characterized by UV-visible spectroscopy and the absorption maximum was analyzed by a spectral scan between 200-900 nm. The UV-vis absorption spectrum of silver nanoparticles synthesized using $NaBH_4$ and tannic acid as reducing agent are shown in Figure 4.5. The UV-vis absorption spectrum reveals the formation of silver nanoparticles by showing surface plasmon absorption maxima at 403 nm and 410 nm respectively. The position and shape of the plasmon absorption depends on the particles size, shape and the dielectric constant of the surrounding medium (Amendola *et al*., 2010; Khan *et al*., 2012; Mahmoud *et al*., 2012). It was also reported that the increased particles size or particle aggregation may lead to the shift of SPR maximum shift (Jain and El-Sayed, 2010; Ringe *et al*., 2010).

4.3.2.2. Transmission electron microscopy analysis

Nanoparticles samples were characterized by TEM in order to confirm the synthesis of Ag and also to determine the shape and size of Ag nanoparticles (Figure 4.6). In general, the silver particles are spherical. Analysis of 200 particles in each set of experimental sample, the average size of Ag nanoparticles synthesized with $NaBH_4$ is 12.9 ± 4.21 nm, which was in good agreement to that reported in literature (Dong *et al*., 2010; Yu *et al*., 2011). For those Ag nanoparticles synthesized with tannic acid, the mean size is 7.06 ± 2.41 nm, which was also mentioned before (Sivaraman *et al*., 2009). It was reported that the size of synthesized Ag nanoparticles depends on the initial molar ratio (MR) of tannic acid to $AgNO_3$, and the smaller size could be achieved when MR=0.05. It was also

reported that the small Ag nanoparticles with more surface area and more active site were potential for higher antimicrobial activity and inhibitory effects (Jin *et al*., 2010; Kin *et al*., 2010; Das *et al*., 2012). Considering the size and stability of Ag nanoparticles synthesized by these two methods, the nanoparticles synthesized by tannic acid were used for subsequent experiment.

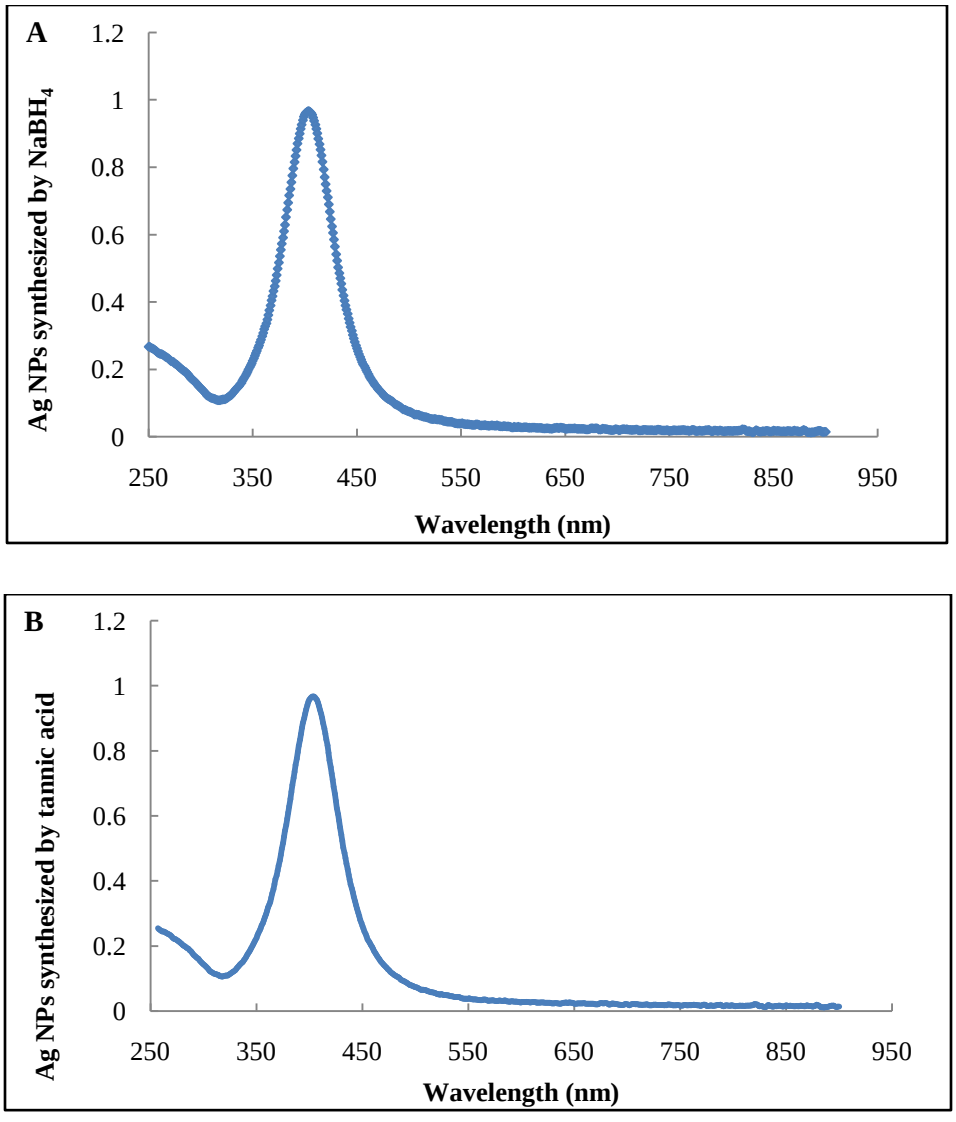

Figure 4.5. UV-visible absorbance spectra of Ag nanoparticles showing the typical surface plasmon resonance. A) Ag nanoparticles synthesized by $NaBH_4$; B) Ag nanoparticles synthesized by tannic acid.

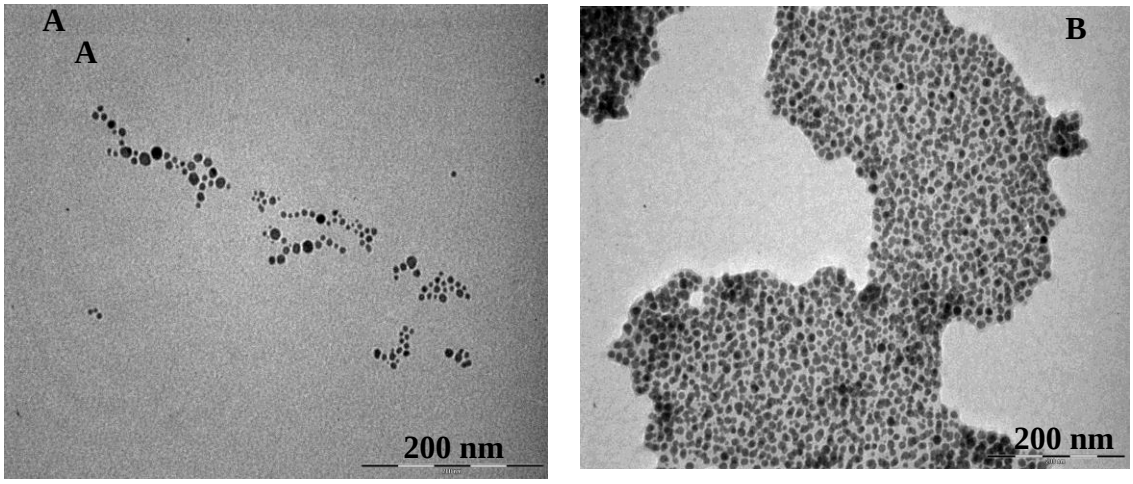

Figure 4.6. TEM images of Ag nanoparticles synthesized by A) $NaNH_4$; B) tannic acid.

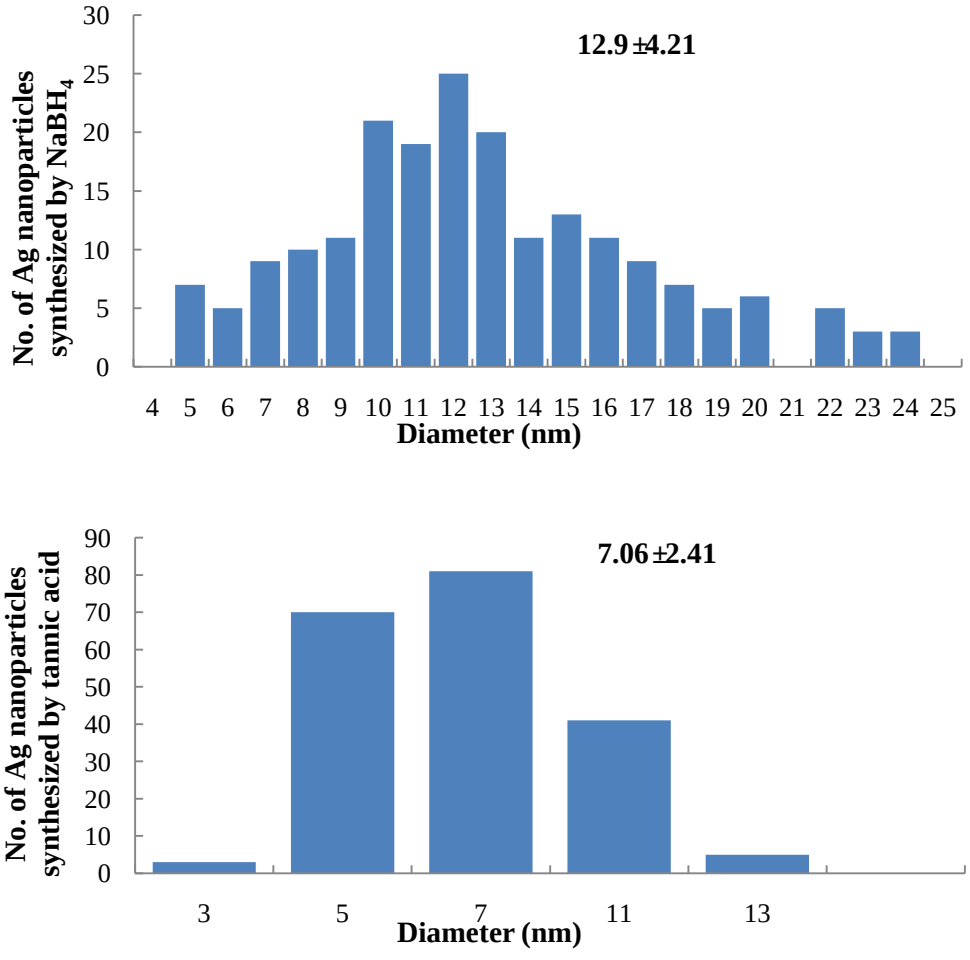

Figure 4.7. Size distribution of Ag nanoparticles synthesized by $NaBH_4$: 12.9 ±4.21 nm; tannic acid: 7.06 ±2.41 nm.

4.3.3. Effect of Ag nanoparticles on *Pf*ThzK activity

The effect of Ag nanoparticles on methylhydroxyethylthiazolekinase was investigated by the method described in 4.2.2.3 with thiazole as substrate. The activity of control (*Pf*ThzK without Ag nanoparticles) was assayed together at the same experimental conditions. For time dependence it was noticed that there was an increase inhibition during the first 60 min, the strongest inhibition (89% inhibition) was obtained when *Pf*ThzK was incubated with 10 µM Ag NPs for 30 min. Furthermore, higher inhibition was observed with lower concentration of Ag NPs (10-20 µM). Interestingly, enzyme activity was restored to the value of control after *Pf*ThzK was incubated with Ag NPs for longer than 2 hours. It is probably because with the time, the nanoparticles aggregated and dissociated from *Pf*ThzK and restored its activity.

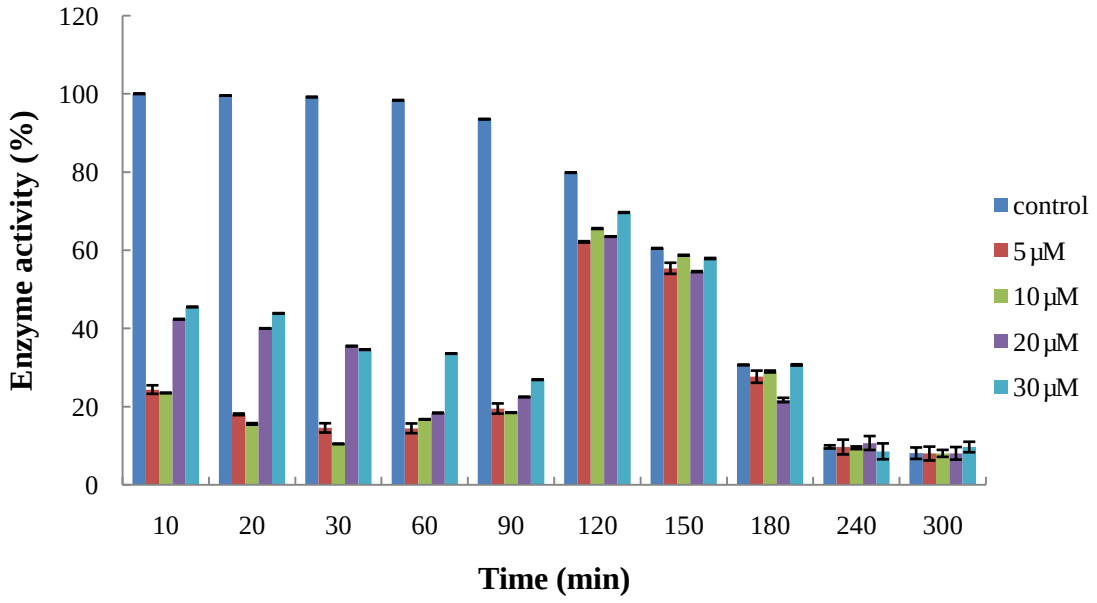

Figure 4.8. The *Pf*ThzK inhibitory effects of AgNPs

For substrate dependence (Figure 4.9), *Pf*ThzK was competitively inhibited at all the concentrations of Ag NPs (5-30 µM). The V_{max} decreased in the presence of Ag NPs (see Table 4.1), with the inhibitory constant value K_i of 6.54 µM.

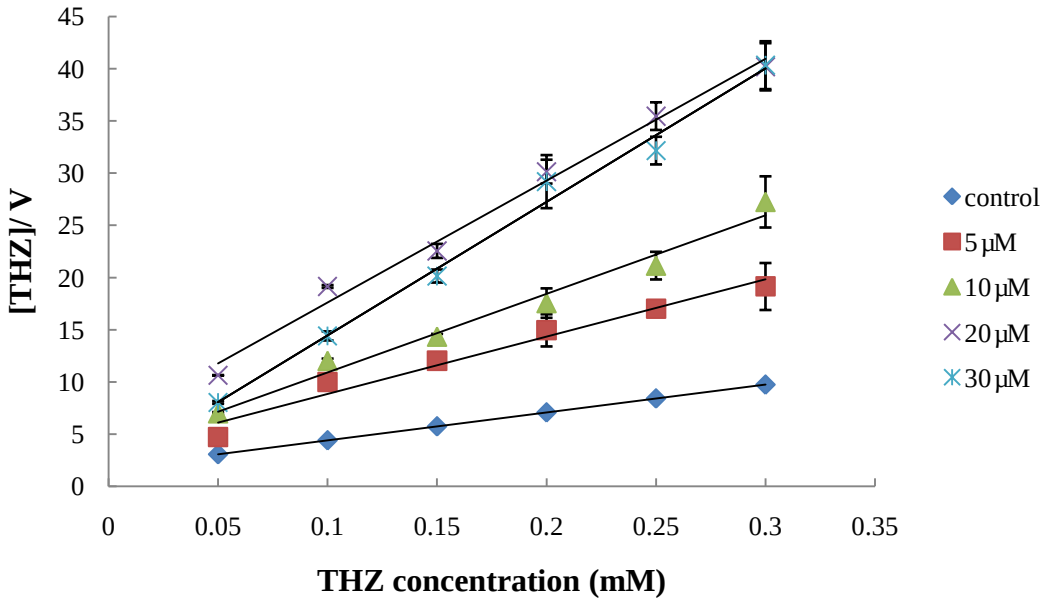

Figure 4.9. Hanes-Woolf plot showing influence of Ag NPs on purified *Pf*ThzK.

Table 4.1. Kinetic parameters determined from the interaction of Ag NPs on *Pf*ThzK using different substrate concentrations.

Ag NPs concentration	0 (control)	5 µM	10 µM	20 µM	30 µM
K_m (mM)	0.065	0.064	0.05	0.0507	0.013
V_{max} (µmol.min^{-1}.ml^{-1})	0.037	0.0203	0.0139	0.00858	0.0078
k_{cat} (s^{-1})	0.15	0.082	0.056	0.034	0.032

Ag Nanoparticles were successfully synthesized by $NaBH_4$ and tannic acid, and the comparison of these two chemical processes concluded that the tannic acid route was milder and more eco-friendly. Relatively uniform sized and shaped Ag nanoparticles synthesized by tannic acid were utilized to determine the influences of Ag NPs on *Pf*ThzK, and it was shown that *Pf*ThzK was competitively inhibited with the inhibitory constant value K_i of 6.54 μM, 89% inhibition was observed when *Pf*ThzK was incubated with 10 μM Ag NPs for 30 min. The present work is the first study that evaluated the effects of Ag nanoparticles on the activities of methylhydroxyethylthiazolekinase from *Plasmodium falciparum*, and the inhibition effects of Ag nanoparticles on *Pf*ThzK could be utilized to disrupt the metabolism of vitamin B_1 in the parasite, which could be potential used to control malaria disease.

Chapter 5
Conclusions

5.1. General conclusions

5.1.1. Isolation, expression, purification and characterization of *PfThzK*

*Pf*ThzK is a very important enzyme in plasmodial vitamin B_1 biosynthesis and was recombinantly produced as 6×His fusion protein in *E. coli* BL21, with a yield of 0.8 mg per lire of bacteria culture. The enzyme was then successfully over-produced and purified by Ni-affinity chromatography and size exclusion chromatography. Purified *Pf*ThzK activity was analyzed by an improved molybdate method, and the optimal conditions determined as 37℃, pH 7.5, and the specific activity was found to be 295.04 nmol/mg, with V_{max} value of 0.037 μmol/min/ml and K_m value of 65 μM. ThzK enzyme activity in *B. subtilis* had been found, and the apparent K_m value for thiazole was reported to be 34 μM (Campobasso *et al*., 2000), which is comparable to the plasmodial counterpart in this study.

5.1.2. Synthesis of Ag nanoparticles

Metallic nanoparticles are becoming more attractive in various fields of science because of their high surface energy and high surface-to-volume properties (Chaudhari *et al*., 2012). Ag nanoparticles are the most applicable of all the metal nanoparticles in

consumer products (Maynard and Michelson, 2007); and Ag nanoparticles have been one of the most interesting metallic nanoparticles in research due to their exceptional properties (Perez-Juste *et al.*, 2005). The metallic nanoparticles have shown significant mechanical, electronic, magnetic, optical and catalytic properties, which are highly influenced by their size, shape and composition (Buzea *et al*, 2007; Das and Marsili, 2011; Burda *et al*., 2005). Therefore, the specific synthesized route should be selected according to the properties of metal nanoparticles (Perez-Juste *et al.*, 2005; Cuenya, 2010; Chen and Liu, 2011). Recently biological synthetic routes have been designed to be environmentally friendly, however, the improved chemical synthetic pathways for silver nanoparticles have been shown to be more versatile, and more environmentally friendly (Khan *et al.,* 2011; Dawy *et al.,* 2012). In the present study, Ag nanoparticles were synthesized by two chemical methods, the Ag ions were reduced by $NaBH_4$ and tannic acid and possessed optical properties similar to those reported in the literature. Moreover, the tannic acid synthetic method is more ideal, as the conditions of synthesis were generally mild and simple. The morphologies of these Ag nanoparticles (in terms of size) appeared to be more controlled with the size of 7.06 ± 2.41 nm, compared with those synthesized by $NaBH_4$, with the size of 12.9 ± 4.21 nm. Furthermore, no extra stabilizer was needed for this method since tannic acid acted as a reducing agent and stabilizer thereby preventing aggregation and precipitation of the Ag nanoparticles.

5.1.3. Interaction of Ag nanoparticles with *Pf*ThzK

The potential neurotoxicity of Ag nanoparticles was determined by an *in vitro* study of their effects on the enzymatic activity of *Pf*ThzK, a very important enzyme in plasmodial vitamin B_1 biosynthesis pathway. It was noticed that the enzymatic activity was inhibited

with the inhibitory constant value K_i of 6.54 μM. Heavy metals, especially Ag nanoparticles have been reported to be toxic as they bind to functional groups of proteins leading to protein deactivation and denaturation (Valodkar *et al*., 2011; Elzoghby *et al*., 2012).

The inhibition of Ag nanoparticels on *Pf*ThzK produces a new potential approach to control malaria disease. Conversely, the present study also demonstrated that *Pf*ThzK may still be novel biomedical targets in the combat against malaria. As introduced in Chapter 1, *Pf*ThzK are only found in *Plasmodium* parasite and not in humans, because they are responsible for the metabolism of vitamin B_1. The inhibition effects of Ag nanoparticles on methylhydroxyethylthiazolekinase have possible clinical applications in the treatment of malaria disease.

5.2. Future work

The present work is the first study that evaluated the effects of Ag nanoparticles on the activities of *Pf*ThzK, and it can be considered as the beginning of future work relevant to vitamin B_1 biosynthetic enzymes. The results of this research also cause other research questions, which may increase the knowledge and understanding of the therapy of malaria disease. From this study, it would be more interesting to carry out many relevant researches as following:

As introduced in Chapter 1, there are three key enzymes involved in plasmodial vitamin B_1 biosynthetic pathways: 1) 5-(2-hydroxy-ethyl)-4-methylthiazole (THZ) kinase (*Pf*ThzK); 2) 4-amino-5-hydroxymethyl-2-methylpyrimidine (HMP) HMP-P kinase (*Pf*ThiD) and 3) thiamine phosphate synthase (*Pf*ThiE). In the present study, only

*Pf*ThzK was purified and evaluated, and it would be of interest to see the effect of Ag nanoparticles on the other two enzymes.

It is reported that it is possible to synthesize Ag nanoparticles by biological methods, such as cowpea chlorotic mosaic virus (CCMV). The virus cage is small enough to enter the blood brain barrier which must be important and specific for cerebral malaria. It is important to evaluate the activation/inhibition of the NPs synthesized by virus protein on *Pf*ThzK and other plasmodial vitamin B_1 biosynthetic enzymes.

Recently, various nanoparticles have been studied at laboratory level, such as copper, gold, platinum and silver. From the present study, it's becoming more interesting to determine the activation/inhibition of different nanoparticles on *Pf*ThzK, and contribute more knowledge and understanding to nanotechnology and malaria therapy.

References

Abeylath, S. C., and Amiji, M. M. (2011) 'Click' synthesis of dextran macrostructures for combinatorial-designed self-assembled nanoparticles encapsulating diverse anticancer therapeutics. *Bioorganic and Medicinal Chemistry*. Volume 19(21): 6167-6173.

Ahmad, A., Mukherjee, P., Mandal, D., Senapati, S., Khan, M. I., Kumar, R., and Sastry, M. (2002) Enzyme mediated extracellular synthesis of CdS nanoparticles by the fungus, *Fusarium oxysporum*. *Journal of the American Chemical Society*. Volume 124(41): 12108-12109.

Ahmad, A., Senapati, S., Khan, M. I., Kumar, R., and Sastry, M. (2005) Extra-/Intracellular Biosynthesis of Gold Nanoparticles by an Alkalotolerant Fungus, *Trichothecium sp*. *Journal of Biomedical Nanotechnology*. Volume 1(1): 47-53.

Akbarzadeh, A., Rezaei-Sadabady, R., Davaran, S., Joo, S. W., Zarghami, N., Hanifehpour, Y., Samiei, M., Kouhi, M., and Nejati-Koshki, K. (2013) Liposome: classification, preparation, and applications. *Nanoscale Research Letters*. Volume 8(1): 102.

Akhtar, S. (2012) *Transmission Electron Microscopy of Graphene and Hydrated Biomaterial Nanostructures: Novel Techniques and Analysis* (Doctoral dissertation, Uppsala University).

Al-Bokari, M., Cherrak, D. and Guiochon, G. (2002) Determination of the porosities of monolithic columns by inverse size exclusion chromatography. *Journal of Chromatography A*. Volume 975: 275-284.

Alhasan, A. H., Kim, D. Y., Daniel, W. L., Watson, E., Meeks, J. J., Thaxton, C. S., and Mirkin, C. A. (2012) Scanometric MicroRNA Array Profiling of Prostate Cancer Markers Using Spherical Nucleic Acid–Gold Nanoparticle Conjugates. *Analytical chemistry*. Volume 84(9): 4153-4160.

Al-Jamal, W. T., and Kostarelos, K. (2011) Liposomes: from a clinically established drug delivery system to a nanoparticle platform for theranostic nanomedicine. *Accounts of chemical research*. Volume 44(10): 1094-1104.

Alkilany, A. M., Thompson, L. B., Boulos, S. P., Sisco, P. N., and Murphy, C. J. (2012) Gold nanorods: their potential for photothermal therapeutics and drug delivery, tempered by the complexity of their biological interactions. *Advanced Drug Delivery Reviews*. Volume 64(2): 190-199.

Altin, J. G. (2012) Liposomes and Other Nanoparticles as Cancer Vaccines and Immunotherapeutics. In *Innovation in Vaccinology* (Page 135-178). Springer Netherlands.

Alving, C. R. (2006) Antibodies to lipids and liposomes: immunology and safety. *Journal of Liposome Research*. Volume 16(3): 157-166.

Ambrosi, A., Chua, C. K., Khezri, B., Sofer, Z., Webster, R. D., and Pumera, M. (2012) Chemically reduced graphene contains inherent metallic impurities present in parent natural and synthetic graphite. *Proceedings of the National Academy of Sciences*. Volume 109(32): 12899-12904.

Amendola, V., Bakr, O. M., and Stellacci, F. (2010) A study of the surface plasmon resonance of silver nanoparticles by the discrete dipole approximation method: effect of shape, size, structure, and assembly. *Plasmonics*. Volume 5(1): 85-97.

Ankamwar, B. (2010) Biosynthesis of gold nanoparticles (green-gold) using leaf extract of *Terminalia catappa*. *Journal of Chemistry*. Volume 7(4): 1334-1339.

Arnaout, C. L., and Gunsch, C. K. (2012) Impacts of silver nanoparticle coating on the nitrification potential of Nitrosomonas europaea. *Environmental Science and Technology*. Volume 46(10): 5387-5395.

Arnau, J. Lauritzen, C. Petersen, C. L. and Pedersen, J. (2006) Current strategies for the use of affinity tags and tag removal for the purification of recombinant proteins. *Protein Expression and Purification*. Volume 48: 1-13.

Atwater, H. A., and Polman, A. (2010) Plasmonics for improved photovoltaic devices. *Nature Materials*. Volume 9(3): 205-213.

Aubin-Tam, M. E., and Hamad-Schifferli, K. (2005) Gold nanoparticle-cytochrome c complexes: the effect of nanoparticle ligand charge on protein structure. *Langmuir*. Volume 21(26): 12080-12084.

Ayache, J., Beaunier, L., Boumendil, J., Ehret, G., and Laub, D. (2010) The Different Observation Modes in Electron Microscopy (SEM, TEM, STEM). In *Sample Preparation Handbook for Transmission Electron Microscopy* (Page 33-55). Springer New York.

Badawy, A. M. E., Luxton, T. P., Silva, R. G., Scheckel, K. G., Suidan, M. T., and Tolaymat, T. M. (2010) Impact of environmental conditions (pH, ionic strength, and electrolyte type) on the surface charge and aggregation of silver nanoparticles suspensions. *Environmental Science and Technology*. Volume 44(4): 1260-1266.

Badireddy, A. R., Budarz, J. F., Chellam, S., and Wiesner, M. R. (2012) Bacteriophage inactivation by UV-A illuminated fullerenes: Role of nanoparticle-virus association and biological targets. *Environmental Science and Technology*. Volume 46(11): 5963-5970.

Bakry, R., Vallant, R. M., Najam-ul-Haq, M., Rainer, M., Szabo, Z., Huck, C. W., and Bonn, G. K. (2007). Medicinal applications of fullerenes. *International Journal of Nanomedicine*. Volume 2(4), 639.

Banerjee, P., Conklin, D., Nanayakkara, S., Park, T. H., Therien, M. J., and Bonnell, D. A. (2010) Plasmon-induced electrical conduction in molecular devices. *ACS nano*. Volume 4(2): 1019-1025.

Bannai, H., Lévi, S., Schweizer, C., Dahan, M., and Triller, A. (2007) Imaging the lateral diffusion of membrane molecules with quantum dots. *Nature Protocols*. Volume 1(6): 2628-2634.

Banyex, F. (1999) Recombinant protein expression in *Escherichia coli*. *Current opinions in Biotechnology*. Volume 10: 411-421.

Barth, J. V., Costantini, G., and Kern, K. (2005) Engineering atomic and molecular nanostructures at surfaces. *Nature*. Volume 437(7059): 671-679.

Begley, T. P., Downs, D. M., Ealick, S. E., Mc Lafferty, F. W., Van Loon, A. P., Talyor, S., Campobasso, N., Chiu, H. J., Kinsland, C., Reddick, J. J. and Xi, J. (1999) Thiamine biosynthesis in prokaryotes. *Archives of Microbiology.* Volume 171: 193-300.

Behrens, R. H., Carroll, B., Smith, V., and Alexander, N. (2008) Declining incidence of malaria imported into the UK from West Africa. *Malaria Journal*. Volume 7(1): 235.

Berube, K., Balharry, D., Sexton, K., Koshy, L., and Jones, T. (2007) Combustion- derived Nanoparticles: Mechanisms of Pulmonary Toxicity. *Clinical and Experimental Pharmacology and Physiology*. Volume 34(10): 1044-1050.

Besteiro, S., Biran, M., Biteau, N., Coustou, V., Baltz, T., Canioni, P., and Bringaud, F. (2002) Succinate secreted by *Trypanosoma brucei* is produced by a novel and unique glycosomal enzyme, NADH-dependent fumarate reductase. *Journal of Biological Chemistry*. Volume 277(41): 38001-38012.

Bollag, D. M. (1995) Gel-filtration chromatography. *Methods in Molecular Biology.* Volume 36: 1-9.

Bosi, S., Da Ros, T., Spalluto, G., and Prato, M. (2003) Fullerene derivatives: an attractive tool for biological applications. *European Journal of Medicinal Chemistry*. Volume 38(11): 913-923.

Bozdech, Z., and Ginsburg, H. (2005) Data mining of the transcriptome of *Plasmodium falciparum*: the pentose phosphate pathway and ancillary processes. *Malaria Journal*. Volume 4(1): 17.

Bracey, C. L., Ellis, P. R., and Hutchings, G. J. (2009) Application of copper–gold alloys in catalysis: current status and future perspectives. *Chemical Society Reviews*. Volume 38(8): 2231-2243.

Braydich-Stolle, L. K., Lucas, B., Schrand, A., Murdock, R. C., Lee, T., Schlager, J. J., hussain, S. M., and Hofmann, M. C. (2010) Silver nanoparticles disrupt GDNF/Fyn kinase signaling in spermatogonial stem cells. *Toxicological Sciences.* Volume 116(2): 577-589.

Briggman, K. L., and Bock, D. D. (2012) Volume electron microscopy for neuronal circuit reconstruction. *Current Opinion in Neurobiology*. Volume 22(1): 154-161.

Burda, C., Chen, X.B., Narayanan, R., and El-Sayed, M. A. (2005) Chemistry and Properties of Nanocrystals of Different Shapes. *Chemical Reviews*. Volume 105: 1025-1102.

Burgess, R. (2012) *Understanding Nanomedicine: An Introductory Textbook*. Pan Stanford Pub.

Busson, M. P., Rolly, B., Stout, B., Bonod, N., Larquet, E., Polman, A., and Bidault, S. (2011) Optical and topological characterization of gold nanoparticle dimers linked by a single DNA double strand. *Nano Letters*. Volume 11(11): 5060-5065.

Bulte, J. W. (2007) Nanoparticles in biomedical imaging: emerging technologies and applications (Fundamental biomedical technologies. Volume 3.

Buzea, C., Blandino, I. I. P., and Robbie, K. (2007) Nanomaterials and nanoparticles: Sources and toxicity. *Biointerphases.* Volume 2: MR17- MR172.

Campobasso, N., Mathews, II., Begley, T. P. and Ealick, S. E. (2000) Crystal structure of 4-methyl-5-β-hydroxyethylthiazole kinase from *Bacillus subtilis* at 1.5 ˚A resolution. *Biochemistry*. Volume 39:7868–7877.

Candiani, G., Pezzoli, D., Ciani, L., Chiesa, R., and Ristori, S. (2010) Bioreducible liposomes for gene delivery: from the formulation to the mechanism of action. *PloS one*. Volume 5(10): e13430.

Cassera, M. B., Gozzo, F. C., Fabio, L. D., Merino, E. F., Del Portillo, H. A., Peres, V. J., Igor, C and Katzin, A. M. (2004) The methylerythritol phosphate pathway is functionally active in all intraerythrocytic stages of *Plasmodium falciparum*. *Journal of Biological Chemistry*. Volume 279(50): 51749-51759.

Celardo, I., Pedersen, J. Z., Traversa, E., and Ghibelli, L. (2011) Pharmacological potential of cerium oxide nanoparticles. *Nanoscale*. Volume 3(4): 1411-1420.

Chan, Y. S., and Mashitah, M. D. (2012) Instantaneous biosynthesis of silver nanoparticles by selected macro fungi. *Australian Journal of Basic and Applied Sciences.* Volume 6: 86-88.

Chandra, M., Dowgiallo, A. M., and Knappenberger Jr, K. L. (2010) Controlled plasmon resonance properties of hollow gold nanosphere aggregates. *Journal of the American Chemical Society*. Volume 132(44): 15782-15789.

Chaudhari, P. R., masurkar, S. A., Shidore, V. B., and Kamble, S. P. (2012) Antimicrobial activity of extracellularly synthesized silver nanoparticles using lactobacillus species obtained from VIZYLAC capsule. *Journal of Applied Pharmaceutical Science.* Volume 2: 25-29.

Chen, H., and Li, J. (2007) Nanotechnology. *Microarrays* (Page 411-436). Humana Press.

Chen, H. M., and Liu, R. S. (2011) Architecture of Metallic Nanostructures: Synthesis Strategy and Specific Applications. *The Journal of Physical Chemistry*. Volume 115: 3513-3527.

Chen, J., Zhang, P., Fang, G., Weng, C., Hu, J., Yi, P., .YU, X., and Li, X. (2012) One-pot synthesis of amphiphilic reversible photoswitchable fluorescent nanoparticles and their fluorescence modulation properties. *Polymer Chemistry*. Volume 3(3): 685-693.

Chen, Y. W., Hwang, K. C., Yen, C. C., and Lai, Y. L. (2004) Fullerene derivatives protect against oxidative stress in RAW 264.7 cells and ischemia-reperfused lungs. *American Journal of Physiology-Regulatory, Integrative and Comparative Physiology*. Volume 287(1): R21-R26.

Chen, Z., Ma, L., Liu, Y., and Chen, C. (2012) Applications of functionalized fullerenes in tumor theranostics. *Theranostics*. Volume 2(3): 238.

Cheng, Y., Yin, L., Lin, S., Wiesner, M., Bernhardt, E., and Liu, J. (2011) Toxicity reduction of polymer-stabilized silver nanoparticles by sunlight. *The Journal of Physical Chemistry C*. Volume 115(11): 4425-4432.

Chhowalla, M., Teo, K. B. K., Ducati, C., Rupesinghe, N. L., Amaratunga, G. A. J., Ferrari, A. C., Roy, D., Robertson, J., and Milne, W. I. (2001) Growth process conditions of vertically aligned carbon nanotubes using plasma enhanced chemical vapor deposition. *Journal of Applied Physics*. Volume 90(10): 5308-5317.

Chifflet, S., Torriglia, A., Chiesa, R. and Tolosa, S. (1988) A method for the determination of inorganic phosphate in the presence of labile organic phosphate and high concentration of protein: Application to lens ATPases. *Analytical Biochemistry*. Volume 168: 1-4.

Chung, C. T., Niemela, S. L. and Miller, R. H. (1989) One-step preparation of competent *Escherichia coli*: Transformation and storage of bacterial cells in the same solution. *Proceedings of the National Academy of Sciences.* Volume 86: 2172-2175.

Croft, A. M., and Geary, K. G. (2001) Drugs used in malaria Chemoprophylaxis. *Travelers' malari:* 163.

Crowe, J., Dobeli, H., Gentz, R., Hochuli, E., Stuber, D. and Henco, K. (1994) 6xHis-Ni-NTA chromatography as a superior technique in recombinant protein expression/purification. *Methods in Enzymolog*y.Volume 31: 271-387.

Cuenya, B. R. (2010) Synthesis and catalytic properties of metal nanoparticles: size, shape, support, composition, and oxidation state effects. *Thin Solid Films.* Volume 518: 3127-3150.

Cui, H. F., Ye, J. S., Zhang, W. D., Li, C. M., Luong, J. H., and Sheu, F. S. (2007) Selective and sensitive electrochemical detection of glucose in neutral solution using platinum–lead alloy nanoparticle/carbon nanotube nanocomposites. *Analytica Chimica Acta*. Volume 594(2): 175-183.

Das, P., Xenopoulos, M. A., Williams, C. J., Hoque, M. E., and Metcalfe, C. D. (2012) Effects of silver nanoparticles on bacterial activity in natural waters. *Environmental Toxicology and Chemistry*. Volume 31(1): 122-130.

Das, S., Bhattacharya, A., Debnath, N., Datta, A., and Goswami, A. (2013) Nanoparticle-induced morphological transition of Bombyx mori nucleopolyhedrovirus: a

novel method to treat silkworm grasserie disease. *Applied Microbiology and Biotechnology*. Volume 2013: 1-12.

Das, S. K., and Marsili, E. (2011) Bioinspired Metal Nanoparticle: Synthesis, Properties and Application. *Nanomaterials.* ISBN: 978-953-307-913-4, InTech. Available from: www.intechopen.com/books/nanomaterials/bioinspired-metal-nanoparticle-synthesis-properties-andapplication.

Dawy, M., Rifaat, H. M., Moustafa, S. A., and Mousa, H. A. (2012) Physicochemical studies on nano silver particles preparated by different techniques. *Australian Journal of Basic and Applied Sciences.* Volume 6: 257-262.

De nobili, M. and Chen, Y. (1999) Size exclusion chromatography of humic substances: Limits, perspectives and prospective. *Soil Science.* Volume 164: 825-833.

Deen, J. L., Von Seidlein, L., and Dondorp, A. (2008) Therapy of uncomplicated malaria in children: a review of treatment principles, essential drugs and current recommendations. *Tropical Medicine & International Health*. Volume 13(9): 1111-1130.

Dellby, N. (2012) Gentle STEM of Single Atoms: Low keV Imaging and Analysis at Ultimate Detection Limits. *Low Voltage Electron Microscopy: Principles and Applications*, 119.

Dharia, N. V., Bright, A. T., Westenberger, S. J., Barnes, S. W., Batalov, S., Kuhen, K., Borboa, R., and Winzeler, E. A. (2010) Whole-genome sequencing and microarray analysis of ex vivo *Plasmodium vivax* reveal selective pressure on putative drug resistance genes. *Proceedings of the National Academy of Sciences*. Volume 107(46): 20045-20050.

Dixon, M. (1952) The effect of pH on the affinities of enzymes for substrates and inhibitors. *Biochemistry Journal*. Volume 55: 161-170.

Dolgaev, S. L., Simakin, A. V., Voronov, V. V., Shafeev, G. A., and Bozon Verduraz, F. (2002) Nanoparticles produced by laser ablation of solids in liquid environment. *Applied Surface Science.* Volume 186: 546-551.

Dong, X., Ji, X., Jing, J., Li, M., Li, J., and Yang, W. (2010) Synthesis of triangular silver nanoprisms by stepwise reduction of sodium borohydride and trisodium citrate. *The Journal of Physical Chemistry C*. Volume 114(5): 2070-2074.

Du, N., Zhang, H., Chen, B. D., Ma, X. Y., Liu, Z. H., Wu, J. B., and Yang, D. R. (2007) Porous Indium Oxide Nanotubes: Layer-by-Layer Assembly on Carbon-Nanotube Templates and Application for Room-Temperature NH_3 Gas Sensors. *Advanced Materials*. Volume 19(12): 1641-1645.

Du Mont, J. J. (2008) Trademarking Nanotechnology: Nano-Lies and Federal Trademark Registration. *AIPLA Quarterly Journal* Volume 36: 147.

Du Toit, L. C., Pillay, V., and Choonara, Y. E. (2010) Nano-microbicides: Challenges in drug delivery, patient ethics and intellectual property in the war against HIV/AIDS. *Advanced Drug Delivery Reviews*. Volume 62(4): 532-546.

Dubas, S. T., and Pimpan, V. (2008) Humic acid assisted synthesis of silver nanoparticles and its application to herbicide detection. *Materials Letters.* Volume 62: 2261-3.

Dubey, M., Bhadauria, S., and Kushwah, B. S. (2009) Green synthesis of nanosilver particles from extract of Eucalyptus hybrida (safeda) leaf. *Digest Journal of Nanomaterials and Biostructures*. Volume 4(3): 537-543.

Dudkiewicz, A., Tiede, K., Loschner, K., Jensen, L. H. S., Jensen, E., Wierzbicki, R., Boxall, A., and Molhave, K. (2011) Characterization of nanomaterials in food by electron microscopy. *Trends in Analytical Chemistry*. Volume 30(1): 28-43.

Dutta, A., and Dolui, S. K. (2011) Tannic acid assisted one step synthesis route for stable colloidal dispersion of nickel nanostructures. *Applied Surface Science.* Volume 257(15): 6889-6896.

Dyson, J. E. D. and Noltmann, E. A. (1967) The effect of pH and temperature on the kinetic parameters of phosphoglucose isomerise. *The Journal of Biological Chemistry.* Volume 248: 1401-1414.

Ehrhardt, S., and Meyer, C. G. (2009) Artemether–lumefantrine in the treatment of uncomplicated *Plasmodium falciparum* malaria. *Therapeutics and Clinical Risk Management*. Volume 5: 805.

Eising, R., Signori, A. M., Fort, S., and Domingos, J. B. (2011) Development of Catalytically Active Silver Colloid Nanoparticles Stabilized by Dextran. *Langmuir*. Volume 27(19): 11860-11866.

Elechiguerra, J. L., Burt, J., Morones. J. R., Camacho-Bragado, A., Gao, X. X., Humberto, H. L., and Yacaman, M. J. (2005) Interaction of silver nanoparticles with HIV-1. *Journal of Nanotechnology.* Volume 3: 6.

Elzoghby, A. O., Samy, W. M., and Elgindy, N. A. (2012) Albumin-based nanoparticles as potential controlled release drug delivery systems. *Journal of Controlled Release*. Volume 157(2): 168-182.

Fairbanks, G., Steak, T.L. and Wallach, D. F. H. (1971) Electrophoretic analysis of the major polypeptides of the human erythrocyte membrane. *Biochemistry*. Volume 10: 2606-2671.

Fan, Z., Senapati, D., Singh, A. K., and Ray, P. C. (2012) Theranostic Magnetic Core–Plasmonic Shell Star Shape Nanoparticle for the Isolation of Targeted Rare Tumor Cells from Whole Blood, Fluorescence Imaging, and Photothermal Destruction of Cancer. *Molecular pharmaceutics*.

Ferreira, P. (2010) *Molecular basis for the mechanism of action and resistance to artemisinin combination therapy in Plasmodium falciparum*. Inst for medicin, Solna/Deptment of Medicine, Solna.

Fevrier, M., Gogol, P., Aassime, A., Megy, R., Delacour, C., Chelnokov, A., Apuzzo, A., Blaize, S., Lourtioz, J. M., and Dagens, B. (2012) Giant coupling effect between metal nanoparticle chain and optical waveguide. *Nano Letters*. Volume 12(2): 1032-1037.

Findlay, S. D., Shibata, N., Sawada, H., Okunishi, E., Kondo, Y., Yamamoto, T., and Ikuhara, Y. (2009) Robust atomic resolution imaging of light elements using scanning transmission electron microscopy. *Applied Physics Letters*. Volume 95(19): 191913-191913.

Franken, K. L. M. C., Hiemstra, H. S., van Meijgaarden, K. E., Subronto, Y., den Hartigh, J., Ottenhoff, T. H. M. and Drijfhout, J. W. (2000) Purification of his-tagged protein by immobized chelate affinity chromatography: The benefits from the use of organic solvent. *Protein Expression and Purification*. Volume 18: 95-99.

Fox, C. B., Lin, S., Sivananthan, S. J., Dutill, T. S., Forseth, K. T., Reed, S. G., and Vedvick, T. S. (2011) Effects of emulsifier concentration, composition, and order of addition in squalene-phosphatidylcholine oil-in-water emulsions. *Pharmaceutical Development and Technology*. Volume 16(5): 511-519.

Fu, A., Micheel, C. M., Cha, J., Chang, H., Yang, H., and Alivisatos, A. P. (2004) Discrete nanostructures of quantum dots/Au with DNA. *Journal of the American Chemical Society*. Volume 126(35): 10832-10833.

Fu, S., Lim, C. S., Kwek, L. C., Chia, T. C., and Tang, C. L. (2006) ZnO/TiO/sub 2/Core-Shell Quantum Dots Application for Colorectal Cancer Fluorescence Image. In *Biomedical and Pharmaceutical Engineering. ICBPE 2006. International Conference on Biomedical and Pharmaceutical Engineering* (Page 377-380).

Fultz, B., and Howe, J. (2012) *Transmission electron microscopy and diffractometry of materials*. Springer Verlag.

Gahlaut, N. (2012) *Improving contrast in biological imaging: Time-resolved microscopy and protein-targeted dendrimers* (Doctoral dissertation, University of Illinois).

Gandolfi, M. G., Van Landuyt, K., Taddei, P., Modena, E., Van Meerbeek, B., and Prati, C. (2010) Environmental scanning electron microscopy connected with energy dispersive x-ray analysis and Raman techniques to study ProRoot mineral trioxide aggregate and calcium silicate cements in wet conditions and in real time. *Journal of Endodontics*. Volume 36(5): 851-857.

Ganesana, M., Istarnboulie, G., Marty, J. L. and Noguer, T. (2011) Site- specific immobilization of a (His)6-tagged acetylcholinesterase on nickel nanoparticles for highly sensitive toxicity biosensors. *Biosensors and Bioelectronics*. Volume 30: 43-48.

Gao, X., Cui, Y., Levenson, R. M., Chung, L. W., and Nie, S. (2004) In vivo cancer targeting and imaging with semiconductor quantum dots. *Nature Biotechnology*. Volume 22(8): 969-976.

Gardella, F., Assi, S., Simon, F., Bogreau, H., Eggelte, T., Ba, F., Foumane, V., Henry, M. C., Kientega, P. T., Basco, L., Trape, J. F., Lalou, R., Martelloni, M., Desbordes, M., Baragatti, M., Briolant, S., Almeras, L., Pradines, B., Fusai, T. and Rogier, C. (2008) Antimalarial drug use in general populations of tropical Africa. *Malaria Journal*. Volume 7: 124.

Garden, M. J., Hall, N., Fung, E., White, O., Berriman, M., Hyman, R. W., Calton, J. M., Pain, Nelson, K. E., Bowman, S., Paulsen, I. T., James, K., Eisen, J. A., Rutherford, K., Salzberg, S. L., Craig, A., Kyes, S., Chan, M. S., Nene, V., Shallom, S. J., Suh, B., Peterson, J., Angiuoli, S., Pertea, M., Allem, J., Selemgut, J., Haft, D., Mather, M. W., Vaidya, A. B., Martin, D. M., Fairlamb, A. H., Fraunholz, M. J., Ross, D. S., Ralph, S. A., Mcfadden, G. I., Cummings, L. M., Subramanian, G. M., Mungall, C., Venter, J. C., Carucci, D. J., Hoffman, S. L., Newbold, C., Davis, R. W., Fraser, C. M. and Barrell, B. (2002) Genome sequence of the human malaria parasite *Plasmodium falciparum*. *Nature.* Volume 419: 498-511.

Gerber, C., and Lang H. P. (2006) How the doors to the nano- world were opened. *Nanotechnology*. Volume 1: 3-5.

Goldenbogen, B., Brodersen, N., Gramatica, A., Loew, M., Liebscher, J., Herrmann, A., Egger, H., Budde, B., and Arbuzova, A. (2011) Reduction-sensitive liposomes from a multifunctional lipid conjugate and natural phospholipids: reduction and release kinetics and cellular uptake. *Langmuir*. Volume 27(17): 10820-10829.

Goldman, E. R., Anderson, G. P., Tran, P. T., Mattoussi, H., Charles, P. T., and Mauro, J. M. (2002) Conjugation of luminescent quantum dots with antibodies using an engineered adaptor protein to provide new reagents for fluoroimmunoassays. *Analytical Chemistry*. Volume 74(4): 841-847.

Goldshleger, N. F., Chernyak, A. V., Kalashnikova, I. P., Baulin, V. E., and Tsivadze, A. Y. (2012) Magnesium octa (benzo-15-crown-5) phthalocyaninate in the sodium dodecyl sulfate solutions: A study using electron and 1H NMR spectroscopy. *Russian Journal of General Chemistry*. Volume 82(5): 927-935.

Gonzalez, E., Vaillant, F., Rojas, G., and Perez, A. (2010) Novel semiautomated method for assessing in vitro cellular antioxidant activity using the light-scattering properties of human erythrocytes. *Journal of Agricultural and Food Chemistry*. Volume 58(3): 1455-1461.

Gregson, A., and Plowe, C. V. (2005) Mechanisms of resistance of malaria parasites to antifolates. *Pharmacological Reviews*. Volume 57(1): 117-145.

Gu, F. X., Karnik, R., Wang, A. Z., Alexis, F., Levy-Nissenbaum, E., Hong, S., Langer, R. S., and Farokhzad, O. C. (2007) Targeted nanoparticles for cancer therapy. *Nano Today*. Volume 2(3): 14-21.

Guan, Y. (2010) *Characterization of alginate scaffolds using X-ray imaging techniques* (Doctoral dissertation, University of Saskatchewan).

Gyang, K. O. (2009). *A Killer Called Malari: The Disease That Kills Two People Every Minute*. AuthorHouse.

Haidar, Z. S. (2010) Bio-inspired/-functional colloidal core-shell polymeric-based nanosystems: Technology promise in tissue engineering, bioimaging and nanomedicine. *Polymers*. Volume 2(3): 323-352.

Han, C., Pelaez, M., Nadagouda, M. N., Obare, S. O., Falaras, P., Dunlop, P. S., Byrne, J. A., Choi, H., and Dionysiou, D. D. (2012) The Green Synthesis and Environmental Applications of Nanomaterials. *Sustainable Preparation of Metal Nanoparticles: Methods and Applications*. Volume 19: 106.

Han, S. E., and Chen, G. (2010) Optical absorption enhancement in silicon nanohole arrays for solar photovoltaics. *Nano Letters*. Volume 10(3): 1012-1015.

Hanahan, D. (1983) Studies on transformation of *E. coli* with plasmid. *Journal of Molecular Biology*. Volume 166: 557-580.

Hatz, C. (2001) Clinical treatment of malaria in returned travelers. *Travelers' Malaria (Schlagenhauf, P. ed.), BC Decker*, 431-445.

Hasan, N. and Szybalski, W. (1995) Construction of *lac*I^{ts} and *lac*I^{qts} expreesion plasmids and evaluation of the thermosensitive lac repressor. *Gene.* Volume 163: 35-40.

Hayashi, A., Yamamoto, S., Suzuki, K., and Matsuoka, T. (2004) The first application of fullerene polymer-like materials, C60Pdn, as gas adsorbents. *Journal of Materials Chemistry*. Volume 14(17), 2633-2637.

He, Z. Y., Zheng, X., Wu, X. H., Song, X. R., He, G., Wu, W. F., Yu, S., Mao, S. J., and Wei, Y. Q. (2010) Development of glycyrrhetinic acid-modified stealth cationic liposomes for gene delivery. *International Journal of Pharmaceutics*. Volume 397(1): 147-154.

Hegde, N. R., Chevalier, M. S., Wisner, T. W., Denton, M. C., Shire, K., Frappier, L., and Johnson, D. C. (2006) The role of BiP in endoplasmic reticulum-associated degradation of major histocompatibility complex class I heavy chain induced by cytomegalovirus proteins. *Journal of Biological Chemistry*. Volume 281(30): 20910-20919.

Henriksen-Lacey, M., Christensen, D., Bramwell, V. W., Lindenstrøm, T., Agger, E. M., Andersen, P., and Perrie, Y. (2010) Comparison of the Depot Effect and Immunogenicity of Liposomes Based on Dimethyldioctadecylammonium (DDA), 3β-[N-(N′, N′-Dimethylaminoethane) carbomyl] Cholesterol (DC-Chol), and 1, 2-Dioleoyl-3-trimethylammonium Propane (DOTAP): Prolonged Liposome Retention Mediates Stronger Th1 Responses. *Molecular pharmaceutics*. Volume 8(1): 153-161.

Himmeldirk, K., Sayer, B. G., and Spenser, I. D. (1998). Comparative Biogenetic Anatomy of Vitamin B1: A 13C NMR Investigation of the Biosynthesis of Thiamin in *Escherichia coli* and in *Saccharomyces cerevisiae*. *Journal of the American Chemical Society*. Volume 120(15): 3581-3589.

Hodak, M., and Girifalco, L. A. (2001) Quasi-one-dimensional system of molecules inside carbon nanotubes: Exact solution for the lattice gas model and its application to fullerene-filled nanotubes. *Physical Review. Volume* B, 64(3): 035407.

Hoffmann, A. and Roeder, R. G. (1991) Purification of his-tagged proteins in non-denaturing conditions suggests a convenient method for protein interaction studies. *Nucleic Acids Research*. Volume 19: 6337-6338.

Hofmann, S., Ducati, C., Robertson, J., and Kleinsorge, B. (2003) Low-temperature growth of carbon nanotubes by plasma-enhanced chemical vapor deposition. *Applied Physics Letters*. Volume 83(1): 135-137.

Hohmann, S. and Meacock, P. A. (1998) Thiamin metabolism and thiamine diphosphate-dependent enzymes in the yeast *Saccharomyces cerevisiae*: genetic regulation. *Biochimica et BIophysica Acta.* Volume1385: 201-219.

Hong, W., Bai, H., Xu, Y., Yao, Z., Gu, Z., and Shi, G. (2010) Preparation of gold nanoparticle/graphene composites with controlled weight contents and their application in biosensors. *The Journal of Physical Chemistry C*. Volume 114(4): 1822-1826.

Hoshino, A., Fujioka, K., Oku, T., Suga, M., Sasaki, Y. F., Ohta, T., Yasuhara, M., Suzuku, K., and Yamamoto, K. (2004) Physicochemical properties and cellular toxicity of nanocrystal quantum dots depend on their surface modification. *Nano Letters*. Volume 4(11): 2163-2169.

Hoshino, A., Fujioka, K., Yamamoto, M., Manabe, N., Yasuhara, M., Suzuki, K., and Yamamoto, K. (2005) Simultaneous multicolor detection system of the single-molecular microbial antigen by total internal reflection fluorescence microscopy with fluorescent nanocrystal quantum dots. In *Optics East 2005* (Page 60090). International Society for Optics and Photonics.

Hossu, M., Ma, L., Zou, X., and Chen, W. (2013) Enhancement of biophoton emission of prostate cancer cells by Ag nanoparticles. *Cancer Nanotechnology*: 1-6.

Hottenrott, S., Schumann, T., Pluckthun, A., Fischer, G., Rahfeld, J. U. (1997) *The Escherichia* coli SlyD is a metal ion-regulated peptidyl-prolyl cis/trans-isomerase. *Journal of Biological Chemistry*. Volume 272:15697-15701.

Hu, W., Yu, Q., Hu, N., Byrd, D., Amet, T., Shikuma, C., Shiramizu, B., Halperin, J. A., and Qin, X. (2010) A high-affinity inhibitor of human CD59 enhances complement-mediated virolysis of HIV-1: implications for treatment of HIV-1/AIDS. *The Journal of Immunology*. Volume 184(1): 359-368.

Hu, Z., Guan, W., Wang, W., Huang, L., Xing, H., and Zhu, Z. (2007) Protective effect of a novel cystine C_{60} derivative on hydrogen peroxide-induced apoptosis in rat pheochromocytoma PC12 cells. *Chemico-biological interactions*. Volume 167(2): 135-144.

Huang, X., and El-Sayed, M. A. (2010) Gold nanoparticles: optical properties and implementations in cancer diagnosis and photothermal therapy. *Journal of Advanced Research*. Volume 1(1): 13-28.

Huschka, R., Barhoumi, A., Liu, Q., Roth, J. A., Ji, L., and Halas, N. J. (2012) Gene silencing by gold nanoshell-mediated delivery and laser-triggered release of antisense oligonucleotide and siRNA. *ACS nano*. Volume 6(9): 7681-7691.

Husein, M., Rodil, E., and Vera, J. H. (2004) Formation of silver bromide precipitate of nanoparticles in a single microemulsion utilizing the surfactant counterion. *Journal of Colloid and Interface Science.* Volume 273: 426-434.

Hussain, J. L., Kumar, S., Hashmi, A. A., and Khan, Z. (2011) Silver nanoparticles: preparation, characterization, and kinetics. *Advanced Materials Letters.* Volume 2: 188-194.

Hutchison, J. L., Kiselev, N. A., Krinichnaya, E. P., Krestinin, A. V., Loutfy, R. O., Morawsky, A. P., Muradyan, V. E., and Zakharov, D. N. (2001) Double-walled carbon nanotubes fabricated by a hydrogen arc discharge method. *Carbon*. Volume 39(5), 761-770.

Huthmacher, C., Hoppe, A., Bulik, S., and Holzhütter, H. G. (2010) Antimalarial drug targets in *Plasmodium falciparum* predicted by stage-specific metabolic network analysis. *BMC Systems Biology*. Volume 4(1): 120.

Inoue, H., Nojima, H. and Okayama, H. (1990) High efficiency transformation of *E. coli* with plamids. *Journal of Gene*. Volume 95: 23-28.

Isakovic, A., Markovic, Z., Todorovic-Markovic, B., Nikolic, N., Vranjes-Djuric, S., Mirkovic, M., Dramicanin, M., and Trajkovic, V. (2006) Distinct cytotoxic mechanisms of pristine versus hydroxylated fullerene. *Toxicological Sciences*. Volume 91(1): 173-183

Jain, P. K., and El-Sayed, M. A. (2010) Plasmonic coupling in noble metal nanostructures. *Chemical Physics Letters*. Volume 487(4): 153-164.

Jang, E., Jun, S., Jang, H., Lim, J., Kim, B., and Kim, Y. (2010) White-Light-Emitting Diodes with Quantum Dot Color Converters for Display Backlights. *Advanced Materials*. Volume 22(28): 3076-3080.

Jeong, S., Hu, L., Lee, H. R., Garnett, E., Choi, J. W., and Cui, Y. (2010) Fast and scalable printing of large area monolayer nanoparticles for nanotexturing applications. *Nano Letters*. Volume 10(8): 2989-2994.

Jin, X., Li, M., Wang, J., Marambio-Jones, C., Peng, F., Huang, X., Damoiseaux, R., and Hoek, E. M. (2010) High-throughput screening of silver nanoparticle stability and bacterial inactivation in aquatic media: influence of specific ions. *Environmental Science and Technology*. Volume 44(19): 7321-7328.

Judd, D. A., Nettles, J. H., Nevins, N., Snyder, J. P., Liotta, D. C., Tang, J., Ermolieff, J., Schinazi, R. F., and Hill, C. L. (2001) Polyoxometalate HIV-1 protease inhibitors. A new mode of protease inhibition. *Journal of the American Chemical Society*. Volume *123*(5): 886-897.

Julia, X. Y., and Li, T. H. (2011) Distinct biological effects of different nanoparticles commonly used in cosmetics and medicine coatings. *Cell and Bioscience*. Volume 1(1): 1-9.

Ju-Nam, Y., and Lead, J. R. (2008) Manufactured nanoparticles: an overview of their chemistry, interactions and potential environmental implications. *Science of the Total Environment*. Volume 400(1): 396-414.

Jurgenson, C. T., Begley, T. P., and Ealick, S. E. (2009) The Structural and Biochemical Foundations of Thiamin Biosynthesis. *Annual Review of Biochemistry*. Volume 78: 569-603.

Kar, P., and Knecht, V. (2012) Origin of decrease in potency of darunavir and two related antiviral inhibitors against HIV-2 compared to HIV-1 protease. *The Journal of Physical Chemistry.*Volume B116(8): 2605-2614.

Kawasaki, T., Iwashima, A., and Nose, Y. (1969) Regulation of thiamin biosynthesis in *Escherichia coli*. *Journal of Biochemistry.* Volume 65: 407-416.

Katz, E., and Willner, I. (2004) Integrated nanoparticle–biomolecule hybrid systems: synthesis, properties, and applications. *Angewandte Chemie International Edition*. Volume 43(45): 6042-6108.

Keidar, M., Levchenko, I., Arbel, T., Alexander, M., Waas, A. M., and Ostrikov, K. K. (2008) Increasing the length of single-wall carbon nanotubes in a magnetically enhanced arc discharge. *Applied Physics Letters*. Volume 92(4): 043129-043129.

Keiper, A. (2003) The nanotechnology revolution. *The New Atlantis*. Volume *2*: 17-34.

Khan, Z., AL-Thabaiti, S. A., Obaid, A. Y., Khan, Z. A., and Al-Youbi, A. A. (2012) Shape-directing role of cetyltrimethylammonium bromide in the preparation of silver nanoparticles. *Journal of Colloid and Interface Science*. Volume: 367(1), 101-108.

Khan, Z., Al-Thabaiti, S. A., Obaid, A. Y., and Al-Youbi, A. O. (2011) Preparation and characterization of silver nanoparticles by chemical reduction method. *Colloids and Surfaces.* Volume 82: 513-517.

Khan, Z., and Talib, A. (2010) Growth of different morphologies (quantum dots to nanorod) of Ag-nanoparticles: Role of cysteine concentrations. *Colloids and Surfaces B: Biointerfaces*. Volume 76(1): 164-169.

Kieft, K. A., Bocan, T. M. and Krause, B. R. (1991) Rapid on-line determination of cholesterol distribution among plasma lipoproteins after high- performance gel filtration chromatography. *The Journal of Lipid Research*. Volume 32: 859-866.

Kim, B., Park, C. S., Murayama, M., and Hochella Jr, M. F. (2010) Discovery and characterization of silver sulfide nanoparticles in final sewage sludge products. *Environmental Science and Technology*. Volume 44(19): 7509-7514.

Kim, J. H., Chaudhary, S., and Ozkan, M. (2007) Multicolour hybrid nanoprobes of molecular beacon conjugated quantum dots: FRET and gel electrophoresis assisted target DNA detection. *Nanotechnology*. Volume 18(19): 195105.

Kim, P., Adorno-Martinez, W. E., Khan, M., and Aizenberg, J. (2012) Enriching libraries of high-aspect-ratio micro-or nanostructures by rapid, low-cost, benchtop nanofabrication. *Nature Protocols*. Volume 7(2): 311-327.

Knezevic, N. Z., Trewyn, B. G., and Lin, V. S. Y. (2011).Functionalized mesoporous silica nanoparticle-based visible light responsive controlled release delivery system. *Chemical Communications*. Volume 47(10): 2817-2819.

Knockel, J., Bergmann, B., Muller, I. B., Rathaur, S., Walter, R. D., and Wrenger, C. (2008).Filling the gap of intracellular dephosphorylation in the *Plasmodium falciparum* vitamin B_1 biosynthesis. *Molecular and Biochemical Parasitology*. Volume 157(2): 241-243.

Kueffer, P. J., Maitz, C. A., Khan, A. A., Schuster, S. A., Shlyakhtina, N. I., Jalisatgi, S. S., Brockman, J. D., Nigg, D. W., and Hawthorne, M. F. (2013) Boron neutron capture therapy demonstrated in mice bearing EMT6 tumors following selective delivery of boron by rationally designed liposomes. *Proceedings of the National Academy of Sciences*. Volume 110(16): 6512-6517.

Kumar, M., and Ando, Y. (2010) Chemical vapor deposition of carbon nanotubes: a review on growth mechanism and mass production. *Journal of nanoscience and nanotechnology*. Volume 10(6): 3739-3758.

Kumar, V., and Yadav, S. K. (2009) Plant-mediated synthesis of silver and gold nanoparticles and their applications. *Journal of chemical Technology and Biotechnology*. Volume 84(2): 151-157.

Kumari, A., Yadav, S. K., and Yadav, S. C. (2010) Biodegradable polymeric nanoparticles based drug delivery systems. *Colloids and Surfaces B: Biointerfaces*. Volume 75(1): 1-18.

Kokai, F., Takahashi, K., Yudasaka, M., and Iijima, S. (2000) Laser ablation of graphite-Co/Ni and growth of single-wall carbon nanotubes in vortexes formed in an Ar atmosphere. *The Journal of Physical Chemistry B*. Volume 104(29): 6777-6784.

Kolusheva, S., Shahal, T., and Jelinek, R. (2000) Cation-selective color sensors composed of ionophore-phospholipid-polydiacetylene mixed vesicles. *Journal of the American Chemical Society*. Volume 122(5): 776-780.

Kramer, R. M., Li, C., Carter, D. C., Stone, M. O., and Naik, R. R. (2004) Engineered protein cages for nanomaterial synthesis. *Journal of the American Chemical Society*. Volume 126(41): 13282-13286.

Krol, S., Macrez, R., Docagne, F., Defer, G., Laurent, S., Rahman, M., Hajipour, M. J., Kehoe, P. G., and Mahmoudi, M. (2012) Therapeutic Benefits from Nanoparticles: The Potential Significance of Nanoscience in Diseases with Compromise to the Blood Brain Barrier. *Chemical Reviews*.

Krumov, N., Perner- Nochta, I., Oder, S., Gotcheva, V., Angelov, A., and Posten, C. (2009) Production of inorganic nanoparticles by microorganisms. *Chemical Engineering and Technology*. Volume 32(7): 1026-1035.

Kruse, P. (2009) Chemical Characterization of Biological and Technological Surfaces. *Functional Properties of Bio-Inspired Surfaces: Characterization and Technological Applications*, 233.

Laemmli, U. K. (1970) Cleavage of structural proteins during the assembly of the head of bacteriophage T4. *Nature*. Volume 227: 680-685.

Lai, D. Y., and Sayre, P. G. (2009) Toxicity testing and evaluation of nanoparticles: challenges in risk assessment. *Nanotoxicology from In Vivo and In Vitro Models to Health Risks*: 427-457.

Lai, H. S., Chen, W. J., and Chiang, L. Y. (2000) Free radical scavenging activity of fullerenol on the ischemia-reperfusion intestine in dogs. *World Journal of Surgery*. Volume 24(4): 450-454.

Lara, H. H., Ayala-Nunez, N. V., Ixtepan-Turrent, L., and Rodriguez-Padilla, C. (2010) Mode of antiviral action of silver nanoparticles against HIV-1. *Journal of Nanobiotechnology*. Volume 8(1): 1-8.

Larguinho, M., and Baptista, P. V. (2012) Gold and silver nanoparticles for clinical diagnostics—From genomics to proteomics. *Journal of Proteomics*. Volume 75(10): 2811-2823.

Lee, J., Cho, S., Hwang, Y., Cho, H. J., Lee, C., Choi, Y., Ku, B. C., and Kim, S. H. (2009) Application of fullerene-added nano-oil for lubrication enhancement in friction surfaces. *Tribology International*. Volume 42(3): 440-447.

Lee, S. Y., Forestiere, C., Pasquale, A. J., Walsh, G. F., Trevino, J., Romagnoli, M., and Dal Negro, L. (2012) Plasmon-enhanced isotropic structural coloration of metal films with homogenized Pinwheel nanoparticle arrays. In *Lasers and Electro-Optics (CLEO), 2012 Conference on.* (Page 1-2). IEEE.

Leela, A., and Vivekanandan, M. (2008) Tapping the unexploited plant resources for the synthesis of silver nanoparticles. *African Journal of Biotechnology*. Volume 7(17).

Li, C., Zhang, Y., Cole, M. T., Shivareddy, S. G., Barnard, J. S., Lei, W., Wang, B., Pribat, D., Amaratunga, G. A. J., and Milne, W. I. (2012) Hot electron field emission via individually transistor-ballasted carbon nanotube arrays. *ACS nano*. Volume 6(4): 3236-3242.

Li, D. Chen, S., Zhao, S., Hou, X., Ma, H., and Yang, X. (2002) A study of phase transfer processes of Ag nanoparticles. *Applied Surface Science.* Volume200: 62-67.

Li, J., Lu, Y., Ye, Q., Cinke, M., Han, J., and Meyyappan, M. (2003) Carbon nanotube sensors for gas and organic vapor detection. *Nano Letters*. Volume 3(7): 929-933.

Liepold, L. O., Revis, J., Allen, M., Oltrogge, L., Young, M., and Douglas, T. (2005) Structural transitions in *Cowpea chlorotic mottle virus* (CCMV). *Physical Biology*. Volume 2(4): S166.

Lindner, S. E., Miller, J. L., and Kappe, S. H. (2012) Malaria parasite pre-erythrocytic infection: preparation meets opportunity. *Cellular Microbiology*. Volume 14(3): 316-324.

Liu, G., Men, P., Zhu, X., and Perry, G. (2012) Iron chelation and nanoparticle target delivery in the development of new multifunctional disease-modifying drugs for Alzheimer's disease. *Therapeutic Delivery*. Volume 3(5): 571-574.

Liu, M., Zhang, J., Liu, J., and Yu, W. W. (2011) Synthesis of PVP-stabilized Pt/Ru colloidal nanoparticles by ethanol reduction and their catalytic properties for selective hydrogenation of *ortho*-chloronitrobenzene. *Journal of Catalysis.* Volume 278(1): 1-7.

Liu, R., Duay, J., and Lee, S. B. (2010) Redox exchange induced MnO2 nanoparticle enrichment in poly (3, 4-ethylenedioxythiophene) nanowires for electrochemical energy storage. *ACS nano*. Volume 4(7): 4299-4307.

liposome. Art. *Encyclopædia Britannica Online*. Retrieved 25 April 2013 from http://www.britannica.com/EBchecked/media/92244/Phospholipids-can-be-used-to-form-artificial-structures-called-liposomes.

Lombardi, A., Loumaigne, M., Crut, A., Maioli, P., Del Fatti, N., Vallee, F., Spuch-Calvar, M., Burgin, J., Majimel, J., and Treguer-Delapierre, M. (2012) Surface Plasmon Resonance Properties of Single Elongated Nano-objects: Gold Nanobipyramids and Nanorods. *Langmuir*. Volume 28(24): 9027-9033.

Loo, L., Guenther, R. H., Basnayake, V. R., Lommel, S. A., and Franzen, S. (2006) Controlled encapsidation of gold nanoparticles by a viral protein shell. *Journal of the American Chemical Society*. Volume 128(14): 4502-4503.

Losurdo, M., Brown, A. S., and Bruno, G. (2013) Real-Time Ellipsometry for Probing Charge-Transfer Processes at the Nanoscale. In *Ellipsometry at the Nanoscale* (Page 453-491). Springer Berlin Heidelberg.

Lu, L. M., Li, H. B., Qu, F., Zhang, X. B., Shen, G. L., and Yu, R. Q. (2011) In situ synthesis of palladium nanoparticle–graphene nanohybrids and their application in nonenzymatic glucose biosensors. *Biosensors and Bioelectronics*. Volume 26(8): 3500-3504.

Lu, X., Wu, J., Lin, T., Wan, D., Huang, F., Xie, X., and Jiang, M. (2011) Low-temperature rapid synthesis of high-quality pristine or boron-doped graphene via Wurtz-type reductive coupling reaction. *Journal of Materials Chemistry*. Volume 21(29): 10685-10689.

Maco, B., Holtmaat, A., Cantoni, M., Kreshuk, A., Straehle, C. N., Hamprecht, F. A., and Knott, G. W. (2013) Correlative In Vivo 2 Photon and Focused Ion Beam Scanning Electron Microscopy of Cortical Neurons. *PloS one*. Volume *8*(2): e57405.

Maehashi, K., Katsura, T., Kerman, K., Takamura, Y., Matsumoto, K., and Tamiya, E. (2007) Label-free protein biosensor based on aptamer-modified carbon nanotube field-effect transistors. *Analytical Chemistry*. Volume 79(2): 782-787.

Mahmoud, M. A., Chamanzar, M., Adibi, A., and El-Sayed, M. A. (2012) Effect of the Dielectric Constant of the Surrounding Medium and the Substrate on the Surface Plasmon Resonance Spectrum and Sensitivity Factors of Highly Symmetric Systems: Silver Nanocubes. *Journal of the American Chemical Society*. Volume 134(14): 6434-6442.

Mahmoudi, M., Sant, S., Wang, B., Laurent, S., and Sen, T. (2011) Superparamagnetic iron oxide nanoparticles (SPIONs): development, surface modification and applications in chemotherapy. *Advanced Drug Delivery Reviews*. Volume 63(1), 24-46.

Malekzadeh, M., and Halali, M. (2011) Production of silver nanoparticles by electromagnetic levitation gas condensation. *Chemical Engineering Journal*. Volume 168(1): 441-445.

Mallick, K. Witcomb, M J., and Scurrell, M. S. (2004) Polymer stabilized silver nanoparticles: a photochemical synthesis route. *Journal of Materials Science*. Volume39: 4459-4463.

Malmsten, M. (2011) Antimicrobial and antiviral hydrogels. *Soft Matter*. Volume 7(19): 8725-8736.

Marambio-Jones, C., and Hoek, E. M. (2010) A review of the antibacterial effects of silver nanomaterials and potential implications for human health and the environment. *Journal of Nanoparticle Research*. Volume 12(5): 1531-1551.

Margueritat, J., Gehan, H., Grand, J., Levi, G., Aubard, J., Felidj, N., Bouhelier, A., and Finot, E. (2011) Influence of the number of nanoparticles on the enhancement

properties of surface-enhanced Raman scattering active area: sensitivity versus repeatability. *ACS nano*. Volume 5(3): 1630-1638.

Markovic, Z., and Trajkovic, V. (2008) Biomedical potential of the reactive oxygen species generation and quenching by fullerenes (C_{60}). *Biomaterials*. Volume 29(26): 3561-3573.

Martin, P., Spagnoli, D., Marmier, A., Parker, S. C., Sayle, D. C., and Watson, G. (2006) Application of molecular dynamics DL_POLY codes to interfaces of inorganic materials. *Molecular Simulation*. Volume 32(12-13): 1079-1093.

Masurkar, S. A., Chaudhari, P. R., Shidore, V. B., and Kamble, S. P. (2011) Rapid biosynthesis of silver nanoparticles using *Cymbopogan citratus* (lemongrass) and its antimicrobial activity. *Nano-Micro Letters.* Volume 3: 189-194.

Mateo-Alonso, A., Bonifazi, D., and Prato, M. (2006) Functionalization and applications of C_{60} fullerene. *Carbon nanotechnology: Recent developments in chemistry, physics, materials science and device applications*.

Maynard, A., and Michelson, E. (2007) A nanotechnology consumer products inventory. Woodrow Wilson International Center of Scholars. Available from: www.nanotechproduct.org/consumerproducts.

McLamore, E. S., Shi, J., Jaroch, D., Claussen, J. C., Uchida, A., Jiang, Y., Zhang, W., and Porterfield, D. M. (2011) A self referencing platinum nanoparticle decorated enzyme-based microbiosensor for real time measurement of physiological glucose transport. *Biosensors and Bioelectronics*. Volume 26(5): 2237-2245.

Meng, L., Jin, J., Yang, G., Lu, T., Zhang, H., and Cai, C. (2009) Nonenzymatic electrochemical detection of glucose based on palladium-single-walled carbon nanotube hybrid nanostructures. *Analytical Chemistry*. Volume 81(17): 7271-7280.

Messina, E., Cavallaro, E., Cacciola, A., Iat ì M. A., Gucciardi, P. G., Borghese, F., Denti, P., and Marago, O. M. (2011).o Plasmon-enhanced optical trapping of gold nanoaggregates with selected optical properties. *ACS nano*. Volume 5(2): 905-913.

Michalet, X., Pinaud, F. F., Bentolila, L. A., Tsay, J. M., Doose, S., Li, J. J., Li, G., Sundaresan, A. M., Wu, A. M., Gambhir, S. S., and Weiss, S. (2005) Quantum dots for live cells, in vivo imaging, and diagnostics. *Science*. Volume 307(5709): 538-544.

Milone, M. C. (2012) Analytical Techniques used in Therapeutic Drug Monitoring. *Therapeutic Drug Monitoring: Newer Drugs and Biomarkers*, 49.

Miroux, B. and Walker, J. E. (1996) Over- production of proteins in *Escherichia coli*: mutant hosts that allow synthesis of some membrane proteins and globular proteins at high levels. *Journal of Molecular Biology*. Volume 260: 289-298.

Mishra, B., Patel, B. B., and Tiwari, S. (2010) Colloidal nanocarriers: a review on formulation technology, types and applications toward targeted drug delivery.*Nanomedicine: Nanotechnology, biology and medicine*. Volume 6(1): 9-24.

Mizote, T., Tsuda, M., Smith, D. D., Nakatama, H. and Nakazawa, T. (1999) Cloning and characterization of the *thiD/J* gene of Escherichia coli encoding a thiamin-synthesizing bifunctional enzyme, hyroxymethylpyrimidine kinase/ phosphomethylpyrimidine kinase. *Microbiology.* Volume 142: 1969-1974.

Mokhtari, N., Daneshpajouh, S., Seyedbagheri, S., Atashdehghan, R., Abdi, K., Sarkar, S., Minaian, S., Shahverdi, H. R., and Shahverdi, A. R. (2009) Biological synthesis of very small silver nanoparticles by culture supernatant of *Klebsiella pneumonia*: The effects of visible-light irradiation and the liquid mixing process. *Materials Research Bulletin*. Volume 44(6): 1415-1421.

Muller, K. M., Arndt, K. M., Bauer, K., and Pluckthun, A. (1998) Tandem immobilized metal-ion affinity chromatography/immunoaffinity purification of his-tagged proteins- evaluation of two anti-his-tag monoclonal antibodies. *Analytical Biochemistry*. Volume 259: 54-61.

Mondal, A. K., Mondal, S., Samanta, S., and Mallick, S. (2011) Synthesis of Ecofriendly Silver Nanoparticle from Plant Latex used as an Important Taxonomic Tool for Phylogenetic Inter-relationship. *Synthesis*. Volume 31: 33.

Morett, E., KOrbel, J. O., Rajan, E., Saab- Rincon, G., Olvera, L., Olvera, M., Schmidt, S., Snel, B., and Bork, P. (2003) Systematic discovery of analogous enzymes in thiamin biosynthesis. *Nature Biotechnology*. Volume 21:790-795.

MubarakAli, D., Thajuddin, N., Jeganathan, K., and Gunasekaran, M. (2011) Plant extract mediated synthesis of silver and gold nanoparticles and its antibacterial activity against clinically isolated pathogens. *Colloids and Surfaces B: Biointerfaces*. Volume 85(2): 360-365.

Mujoriya, R., Singh, D., Bodla, R. B., and Dhamande, K. (2011) Niosome: A Novel Drug Delivery System. *Innovative Systems Design and Engineering*. Volume 2(3): 237-244.

Mukherjee, P., Roy, M., Mandal, B. P., Choudhury, S., Tewari, R., Tyagi, A. K., and Kale, S. P. (2012) Synthesis of uniform gold nanoparticles using non-pathogenic bio-control agent: evolution of morphology from nano-spheres to triangular nanoprisms. *Journal of Colloid and Interface Science*. Volume 367(1): 148-152.

Mukherjee, P., Roy, M., Mandal, B. P., Dey, G. K., Mukherjee, P. K., Ghatak, J., Tyagi, A. K., and Kale, S. P. (2008) Green synthesis of highly stabilized nanocrystalline silver particles by a non-pathogenic and agriculturally important fungus *T. asperellum. Nanotechnology*. Volume 19(7): 075103.

Muller, I. B., Hyde, J. E., & Wrenger, C. (2010) Vitamin B metabolism in *Plasmodium falciparum* as a source of drug targets. *Trends in Parasitology*. Volume 26(1): 35-43.

Muller, I. B., Wu, F., Bergmann, B., Knockel, J., Walter, R. D., Gehring, H., and Wrenger, C. (2009) Poisoning pyridoxal 5-phosphate-dependent enzymes: a new strategy to target the malaria parasite *Plasmodium falciparum*. *PLoS One*. Volume 4(2): e4406.

Muller, S., and Kappes, B. (2007) Vitamin and cofactor biosynthesis pathways in *Plasmodium* and other apicomplexan parasites. *Trends in Parasitology*. Volume 23(3): 112-121.

Na, J. H., Koo, H., Lee, S., Min, K. H., Park, K., Yoo, H., .Lee, S. H., and Kim, K. (2011) Real-time and non-invasive optical imaging of tumor-targeting glycol chitosan nanoparticles in various tumor models. *Biomaterials*. Volume 32(22): 5252-5261.

Nair, B., and Pradeep, T. (2002) Coalescence of nanoclusters and formation of submicron crystallites assisted by *Lactobacillus strains*. *Crystal Growth and Design*. Volume 2(4): 293-298.

Nanotechnology Fights Infection.Medical Editing, Medical Writing, Healthcare Communication, and Engineering Technical Writing. http://angiebiotech.com/nanotechnology-nanoparticle-fight-infection/

Nakonechny, F., Firer, M. A., Nitzan, Y., and Nisnevitch, M. (2010) Intracellular antimicrobial photodynamic therapy: a novel technique for efficient eradication of pathogenic bacteria. *Photochemistry and Photobiology*. Volume 86(6): 1350-1355.

Nash, M. A., Yager, P., Hoffman, A. S., and Stayton, P. S. (2010) Mixed stimuli-responsive magnetic and gold nanoparticle system for rapid purification, enrichment, and detection of biomarkers. *Bioconjugate Chemistry*. Volume 21(12): 2197-2204.

Neidhardt, F. C., Curtiss, R., Ingraham, J. L., Lin, E.C.C., Low, K.B., Magasanik, B., Reznikoff, W.S., Rilley, M., Schaechter, M., Umbarger, H.E. (1996) *Escherichia coli* and *Salmonella*: Cellular and molecular biology, 2nd edition. ASM Press, Washington, DC.

Ndiaye, J. L., Faye, B., Gueye, A., Tine, R., Ndiaye, D., Tchania, C., Ndiaye, I., and Gaye, O. (2011) Repeated treatment of recurrent uncomplicated *Plasmodium falciparum* malaria in Senegal with fixed-dose artesunate plus amodiaquine versus fixed-dose artemether plus lumefantrine: a randomized, open-label trial. *Malaria Journal* Volume 10(237): 1475-2875.

Ni, W., Ba, H., Lutich, A. A., Jäckel, F., and Feldmann, J. (2012) Enhancing Single-Nanoparticle Surface-Chemistry by Plasmonic Overheating in an Optical Trap. *Nano Letters*. Volume 12(9): 4647-4650.

Niikura, K., Nagakawa, K., Ohtake, N., Suzuki, T., Matsuo, Y., Sawa, H., and Ijiro, K. (2009) Gold nanoparticle arrangement on viral particles through carbohydrate

recognition: a non-cross-linking approach to optical virus detection. *Bioconjugate chemistry*. Volume 20(10): 1848-1852.

Nosaka, K. (2006). Recent progress in understanding thiamin biosynthesis and its genetic regulation in *Saccharomyces cerevisiae*. *Applied Microbiology and Biotechnology*. Volume 72(1): 30-40.

Nosten, F., McGready, R., dAlessandro, U., Bonell, A., Verhoeff, F., Menendez, C., Thenonest, M., and Brabin, B. (2006) Antimalarial drugs in pregnancy: a review. *Current Drug Safety*. Volume 1(1): 1-15.

Oehler, S., Amouyai, M., Kolkhof, P., Wilckenbergmann, B., Muller, H. B. (1994) Quality and position of the three *lac* operators of *E. coli* define efficiency of repression. *The EMBO Journal*. Volume 13: 3348-3355.

Oliveira, M. L. S., Neto, J. C., Krieger, J. E., Raw, I. and Ho, P. L. (2001) Sitedirected mutagenesis of bovine FGF-2 cDNA allows the production of the human-form of FGF- 2 in *Escherichia coli*. *Biotechnology Letters*. Volume 23: 1151-1157.

Olliaro, P. L., Haynes, R. K., Meunier, B., and Yuthavong, Y. (2001) Possible modes of action of the artemisinin-type compounds. *Trends in Parasitology*. Volume 17(3): 122-126.

Ong, L., Dagastine, R. R., Kentish, S. E., and Gras, S. L. (2011) Microstructure of milk gel and cheese curd observed using cryo scanning electron microscopy and confocal microscopy. *LWT-Food Science and Technology*. Volume 44(5): 1291-1302.

Orbach, R., Mironi-Harpaz, I., Adler-Abramovich, L., Mossou, E., Mitchell, E. P., Forsyth, V. T., Gazit, E., and Seliktar, D. (2012) The Rheological and Structural Properties of Fmoc-Peptide-Based Hydrogels: The Effect of Aromatic Molecular Architecture on Self-Assembly and Physical Characteristics. *Langmuir*. Volume 28(4): 2015-2022.

Oza, G., Pandey, S., Shah, R., and Sharon, M. (2012) A Mechanistic Approach for Biological Fabrication of Crystalline Gold Nanoparticles Using Marine Algae, *Sargassum wightii*. *European Journal of Experimental Biology*. Volume 2(3): 505-512.

Pacchioni, G., and Freund, H. (2012) Electron Transfer at Oxide Surfaces. The MgO Paradigm: from Defects to Ultrathin Films. *Chemical Reviews*.

Papp, T., Schiffmann, D., Weiss, D., Castranova, V., Vallyathan, V., and Rahman, Q. (2008) Human health implications of nanomaterial exposure. *Nanotoxicology.* Volume 2(1): 9-27.

Parag, D., and Ashish, B. (2005) The nanoscope, Encyclopedia of Nanoscience and Nanotecnology. *Pentagon press.*Volume1**:** 250-276.

Parikh, R. P., Singh, S., Prasad, B. L. V., Patole, M. S., Sastry, M., and Shouche, Y. S. (2008) Extracellular synthesis of crystalline silver nanoparticles and molecular evidence of silver resistance from *Morganella sp.*: towards understanding biochemical synthesis mechanism. *ChemBioChem.* Volume 9(9): 1415-22.

Park, H. H., Park, S., Ko, G., and Woo, K. (2013) Magnetic hybrid colloids decorated with Ag nanoparticles bite away bacteria and chemisorb viruses. *Journal of Materials Chemistry B.*

Partha, R., and Conyers, J. L. (2009) Biomedical applications of functionalized fullerene-based nanomaterials. *International Journal of Nanomedicine*. Volume 4: 261.

Parveen, S., Misra, R., and Sahoo, S. K. (2012) Nanoparticles: a boon to drug delivery, therapeutics, diagnostics and imaging. *Nanomedicine: Nanotechnology, Biology and Medicine*. Volume 8(2): 147-166.

Paudel, H. P., and Leuenberger, M. N. (2012) Light-controlled plasmon switching using hybrid metal-semiconductor nanostructures. *Nano Letters*. Volume 12(6): 2690-2696.

Perez-Juste, J., Pastoriza-Santos, I., Liz-Marzan, L. M., and Mulvaney, P. (2005) Gold nanorods: Synthesis, characterization and applications. *Coordination Chemistry Reviews.* Volume 249: 1870-1901.

Petersen, L. A., Downs and D. M. (1997) Identification and characterization of an operon in *Salmonella typhimurium* involved in thiamine biosynthesis. *Journal of Bacteriology*. Volume 179: 4894–4900.

Polte, J., Erler, R., Thunemann, A. F., Sokolov, S., Ahner, T. T., Rademann, K., .Emmerling, F., and Kraehnert, R. (2010) Nucleation and growth of gold nanoparticles studied via in situ small angle X-ray scattering at millisecond time resolution. *Acs Nano*. Volume 4(2): 1076-1082.

Poon, L., Zandberg, W., Hsiao, D., Erno, Z., Sen, D., Gates, B. D., and Branda, N. R. (2010) Photothermal Release of Single-Stranded DNA from the Surface of Gold Nanoparticles Through Controlled Denaturating and Au−S Bond Breaking. *ACS nano*. Volume 4(11): 6395-6403.

Pozun, Z. D., Tran, K., Shi, A., Smith, R. H., and Henkelman, G. (2011) Why Silver Nanoparticles Are Effective for Olefin/Paraffin Separations. *The Journal of Physical Chemistry C*. Volume 115(5): 1811-1818.

Prabhu, N., Divya, T. R., and Yamuna, G. (2010) Synthesis of silver phyto nanoparticles and their antibacterial efficacy.*Digest Journal of Nanomaterials and Biostructures.* Volume 5: 185-189.

Prathna, T. C., Chandrasekaran, N., Raichur, A. M., and Mukherjee, A. (2011) Biomimetic synthesis of silver nanoparticles by *Citrus limon* (lemon) aqueous extract and theoretical prediction of particle size. *Colloids and Surfaces B: Biointerfaces*. Volume 82(1): 152-159.

Pryce, I. M., Kelaita, Y. A., Aydin, K., and Atwater, H. A. (2011) Compliant metamaterials for resonantly enhanced infrared absorption spectroscopy and refractive index sensing. *ACS nano*. Volume 5(10): 8167-8174.

Railsback, J. G., Johnston-Peck, A. C., Wang, J., and Tracy, J. B. (2010) Size-dependent nanoscale Kirkendall effect during the oxidation of nickel nanoparticles. *ACS nano*. Volume 4(4): 1913-1920.

Rajasekharreddy, P., Rani, P. U., and Sreedhar, B. (2010) Qualitative assessment of silver and gold nanoparticle synthesis in various plants: a photobiological approach. *Journal of Nanoparticle Research*. Volume 12(5): 1711-1721.

Ralph, S. A., Van Dooren, G. G., Waller, R. F., Crawford, M. J., Fraunholz, M. J., Foth, B. J., Tonkin, C. J., and McFadden, G. I. (2004) Tropical infectious diseases:

metabolic maps and functions of the *Plasmodium falciparum* apicoplast. *Nature Reviews Microbiology*. Volume 2(3): 203-216.

Ramos, C. R. R., Abreu, P. A. E., Nascimento, A. L. T. O. and Ho, P. L. (2004) A high- copy T7 *Escherichia coli* Expression vector for the production of recombinant proteins with a minimal N-terminal His-tagged fusion peptide. *Brazilian Journal of Medical and Biological Research*. Volume 37: 1103-1109.

Rangappa, D., Sone, K., Ichihara, M., Kudo, T., and Honma, I. (2010) Rapid one-pot synthesis of LiMPO4 (M= Fe, Mn) colloidal nanocrystals by supercritical ethanol process. *Chemical Communications*. Volume 46(40): 7548-7550.

Ranjan, S. (2012) Liposome Nanoparticles for Targeted Drug and Gene Delivery and Magnetic Imaging. *Proceed With Caution: Concept and Application of the Precautionary Principle in Nanobiotechnology*, 225.

Rapala-Kozik, M., Olczak, M., Ostrowska, K., Starosta, A., and Kozik, A. (2007) Molecular characterization of the thi3 gene involved in thiamine biosynthesis in Zea mays: cDNA sequence and enzymatic and structural properties of the recombinant bifunctional protein with 4-amino-5-hydroxymethyl-2-methylpyrimidine (phosphate) kinase and thiamine monophosphate synthase activities. *The Biochemical Journal*. Volume 408(Pt 2): 149.

Raut, R. W., Kolekar, N. S., Lakkakula, J. R., Mendhulkar, V. D., and Kashid, S. B. (2010) Extracellular synthesis of silver nanoparticles using dried leaves of *Pongamia pinnata* (L) pierre. *Nano-micro Letter*. Volume 2(2): 106-113.

Ringe, E., McMahon, J. M., Sohn, K., Cobley, C., Xia, Y., Huang, J., George, C. S., Laurence, D. M. and Van Duyne, R. P. (2010) Unraveling the effects of size, composition, and substrate on the localized surface plasmon resonance frequencies of gold and silver nanocubes: a systematic single-particle approach. *The Journal of Physical Chemistry C*. Volume 114(29): 12511-12516.

Rivera_Gil, P., Clift, M. J., Rutishauser, B. R., and Parak, W. J. (2012) Methods for Understanding the Interaction between Nanoparticles and Cells. In *Nanotoxicity* (Page 33-56). Humana Press.

Salkar, R. A., Jeevanandam, P., Aruna, S. T., Koltypin, Y., and Geddanken, A. (1999) The sonochemical preparation of amorphous silver nanoparticles. *Journal of Materials Chemistry*. Volume 9: 1333-1335.

San, C. Y., and Don, M. M. (2012) Characterization of Ag Nanoparticles Produced by White-Rot Fungi and Its in vitro Antimicrobial Activities. *The International Arabic Journal of Antimicrobial Agents*. Volume 2(3).

Savalia, D., Robins, W., Nechaev, S., Molineux, L., Severinov, K. (2010) The role of the T7 Gp2 inhibitor of host RNA polymerase in phage development. *Journal of Molecular Biology*. Volume 402: 118-126.

Schmitt, J., Hess, H. and Stunnenberg, H. G. (1993) Affinity purification of histidine-tagged proteins. *Molecular Biology Reviews.* Volume 18: 223-230.

Shahverdi, A. R., Fakhimi, A., Shahverdi, H. R., and Minaian, S. (2007) Synthesis and effect of silver nanoparticles on the antibacterial activity of different antibiotics against *Staphylococcus aures* and *Escherichia coli*. *Nanomedicine: Nanotechnology, Biology and Medicine.* Volume 3: 168-471.

Shin, H., Yang, H., Kim, S., and Lee, M. (2004) Mechanism of growth of colloidal silver nanoparticles stabilized by polyvinyl pyrrolidone in ɣ-irradiated silver nitrate solution. *Journal of Colloid and Interface Science.* Volume 274: 89-94.

Sivaraman, S. K., Elango, I., Kumar, S., and Santhanam, V. (2009) A green protocol for room temperature synthesis of silver nanoparticles in seconds. *Current science*. Volume 97(7): 1055-1059.

Staniewicz, L., Donald, A. M., Stokes, D. J., Thomson, N., Sivaniah, E., Grant, A., Bulmer, D., and Khan, A. (2012) The Application of STEM and In situ Controlled Dehydration to Bacterial Systems Using ESEM. *Scanning*. Volume 34(4): 237-246.

Rai, M., Yadav, A., and Gade, A. (2009) Silver nanoparticles as a new generation of antimicrobials. *Biotechnology Advances*. Volume 27(1): 76-83.

Ray, A. (2012) Fullerence (C60) Molecule–A Review. *Asian Journal of Pharmaceutical Research*. Volume 2(2): 47-50.

Raymond, F., Ho, H. A., Peytavi, R., Bissonnette, L., Boissinot, M., Picard, F., Leclerc, M., Bergeron, M. (2005) Detection of target DNA using fluorescent cationic polymer and peptide nucleic acid probes on solid support. *BMC Biotechnology*. Volume 5(1): 10.

Rebecca, M., Hsing-Lin, W., Jun, G., Srinivas, I., Gabriel, M. A., Jennifer, M., Andrew, S. P., and Rashi, I. (2009) Impact of physicochemical properties of engineered fullerenes on key biological responses. *Toxicology and Applied Pharmacology*. Volume 234(1): 58-67.

Reina, A., Jia, X., Ho, J., Nezich, D., Son, H., Bulovic, V., Dresselhaus, M. S., and Kong, J. (2008) Large area, few-layer graphene films on arbitrary substrates by chemical vapor deposition. *Nano Letters*. Volume 9(1): 30-35.

Renggli, K., Baumann, P., Langowska, K., Onaca, O., Bruns, N., and Meier, W. (2011) Selective and responsive nanoreactors. *Advanced Functional Materials*. Volume 21(7): 1241-1259.

Ringe, E., McMahon, J. M., Sohn, K., Cobley, C., Xia, Y., Huang, J., Schatz, G. C., Marks, L. D., and Van Duyne, R. P. (2010) Unraveling the effects of size, composition, and substrate on the localized surface plasmon resonance frequencies of gold and silver nanocubes: a systematic single-particle approach. *The Journal of Physical Chemistry C*. Volume 114(29): 12511-12516.

Rivera-Gil, P., Jimenez De Aberasturi, D., Wulf, V., Pelaz, B., Del Pino, P., Zhao, Y., Jesus, M., De La, F., and Parak, W. J. (2012) The Challenge To Relate the Physicochemical Properties of Colloidal Nanoparticles to Their Cytotoxicity. *Accounts of Chemical Research*.

Rivera-Gil, P., Oberdorster, G., Elder, A., Puntes, V., and Parak, W. J. (2010) Correlating physico-chemical with toxicological properties of nanoparticles: the present and the future. *ACS nano*. Volume 4(10): 5527-5531.

Rizzo, A., Li, Y., Kudera, S., Della Sala, F., Zanella, M., Parak, W. J., Cingolani, R., Manna, L., Gigli, G. (2007) Blue light emitting diodes based on fluorescent CdSe/ZnS nanocrystals. *Applied Physics Letters*. Volume 90(5): 051106-051106.

Rosarin, F. S., and Mirunalini, S. (2011) Nobel metallic nanoparticles with novel biomedical properties. *Journal of Bioanalysis and Biomedicine*. Volume 3: 085-091.

Rosenberg, M., and Petrie, T. A. (2012) Theoretical study on the possible use of SiC microparticles as photothermal agents for the heating of bacteria. *Nanotechnology*. Volume 23(5): 055103.

Rosler, A., Vandermeulen, G. W., and Klok, H. A. (2001) Advanced drug delivery devices via self-assembly of amphiphilic block copolymers. *Advanced Drug Delivery Reviews*. Volume 53(1): 95-108.

Rozendaal, J. A. (1997) *Vector control: methods for use by individuals and communities*. World Health Organization.

Sadeghi, B., Jamali, M., Kia, S., Amininia, A., and Ghafari, S. (2010) Synthesis and characterization of silver nanoparticles for antibacterial activity. *International Journal of Nano Dimension.* Volume 1: 119-124.

Sagawa, H., Ohshima. A., Kato, I. (1996) A tightly regulated expression system in *Escherichia coli* with SP6 RNA polymerase.*Gene*. Volume 168: 37-41.

Saitoh, Y., Miyanishi, A., Mizuno, H., Kato, S., Aoshima, H., Kokubo, K., and Miwa, N. (2011) Super-highly hydroxylated fullerene derivative protects human keratinocytes from UV-induced cell injuries together with the decreases in intracellular ROS generation and DNA damages. *Journal of Photochemistry and Photobiology B: Biology*. Volume 102(1): 69-76.

Sanchez, S., Roldan, M., Perez, S., and Fabregas, E. (2008) Toward a fast, easy, and versatile immobilization of biomolecules into carbon nanotube/polysulfone-based biosensors for the detection of hCG hormone. *Analytical Chemistry*. Volume 80(17): 6508-6514.

Santos-Magalhaes, N. S., and Mosqueira, V. C. F. (2010) Nanotechnology applied to the treatment of malaria. *Advanced Drug Delivery Reviews*. Volume 62(4): 560-575.

Sathishkumar, M., Sneha, K., and Yun, Y. S. (2010) Immobilization of silver nanoparticles synthesized using *Curcuma longa* tuber powder and extract on cotton cloth for bactericidal activity. *Bioresource Technology*. Volume 101(20): 7958-7965.

Satoh, M., Matsuo, K., Takanashi, Y., and Takayanagi, I. (1995) Effects of acute and short-term repeated application of fullerene C_{60} on agonist-induced responses in various tissues of guinea pig and rat. *General Pharmacology: The Vascular System*. Volume 26(7), 1533-1538.

Sau, T. K., and Rogach, A. L. (2010) Nonspherical Noble Metal Nanoparticles: Colloid- Chemical Synthesis and Morphology Control. *Advanced Materials*. Volume 22(16): 1781-1804.

Sau, T. K., Rogach, A. L., Jackel, F., Klar, T. A., and Feldmann, J. (2010) Properties and applications of colloidal nonspherical noble metal nanoparticles. *Advanced Materials*. Volume 22(16): 1805-1825.

Scarselli, M., Castrucci, P., and De Crescenz, M. (2012) Electronic and optoelectronic nano-devices based on carbon nanotubes. *Journal of Physic*. Volume 24: 31.

Schrand, A. M., Braydich-Stollel, L. K., Schlager, J. J., Dai, L., and Hussain, S. M. (2008) Can silver nanoparticles be useful as potential biological labels? *Nanotechnology.* Volume 19: 235104.

Scott, C. D., Arepalli, S., Nikolaev, P., and Smalley, R. E. (2001) Growth mechanisms for single-wall carbon nanotubes in a laser-ablation process. *Applied Physics A*, Volume 72(5): 573-580.

Scott, T. C. and Phillips, M. A. (1997) Characterization of Trypanosoma brucei pyridoxal kinase: purification, gene isolation and expression in *Escherichia coli*. *Molecular and Biochemical Parasitology.* Volume 88: 1-11.

Sengar, S. K., and Mehta, B. R. (2012) Size and alloying induced changes in lattice constant, core, and valance band binding energy in Pd-Ag, Pd, and Ag nanoparticles: Effect of in-flight sintering temperature. *Journal of Applied Physics*. Volume 112(1): 014307-014307.

Settembre, E., Begley, T. P., and Ealick, S. E. (2003).Structural biology of enzymes of the thiamin biosynthesis pathway. *Current Opinion in Structural Biology*. Volume 13(6): 739-747.

Sevene, E., Gonzalez, R., and Menendez, C. (2010) Current knowledge and challenges of antimalarial drugs for treatment and prevention in pregnancy. *Expert Opinion on Pharmacotherapy*. Volume 11(8): 1277-1293.

Shahbazi, M. A., Herranz, B., and Santos, H. A. (2012) Nanostructured porous Si-based nanoparticles for targeted drug delivery. *Biomatter*. Volume 2(4): 0-1.

Shaheen, S. M., Ahmed, F. R. S., Hossen, M. N., Ahmed, M., Amran, M. S., and Anwar-UL-Islam, M. (2006) Liposome as a carrier for advanced drug delivery. *Pakistan Journal of Biological Sciences*. Volume 9(6): 1181-1191.

Shahverdi, A. R., Minaeian, S., Shahverdi, H. R., Jamalifar, H., and Nohi, A. A. (2007) Rapid synthesis of silver nanoparticles using culture supernatants of Enterobacteria: A novel biological approach. *Process Biochemistry*. Volume 42(5): 919-923.

Sharma, N. C., Sahi, S. V., Nath, S., Parsons, J. G., Gardea-Torresde, J. L., and Pal, T. (2007) Synthesis of plant-mediated gold nanoparticles and catalytic role of biomatrix-embedded nanomaterials. *Environmental Science and Technology*. Volume 41(14): 5137-5142.

Sharma, S. K., Chiang, L. Y., and Hamblin, M. R. (2011) Photodynamic therapy with fullerenes in vivo: reality or a dream? *Nanomedicine*. Volume 6(10): 1813-1825.

Shrestha, M. (2012) Nanotechnology to Revolutionize Medicine. *Journal of Drug Delivery and Therapeutics*. Volume 2(5).

Shvedova, A. A., Kagan, V. E., Fadeel, B. (2010) Close encounters of the small kind: adverse effects of man-made materials interfacing with the nano-cosmos of biological systems. *Annual Review of Pharmacology and Toxicology*. Volume 50: 63-88.

Sing, N. Manshian, B., Jenkins, G. J., Griffithes, S. M., Maffeis, T. G., Wright, C. J., and Doak, S. H. (2009) Nano-genotoxicology: the DNA damaging potential of engineered nanomaterials. *Biomaterials*. Volume 30: 3891-3914.

Singaravelu, G., Arockiamary, J., Ganesh, K., and Govindaraju, K. (2007) A novel extracellular synthesis of monodisperse gold nanoparticles using marine alga, *Sargassum wightii* Greville. *Colloids Surf B Biointerfaces.* Volume 57: 97-101.

Singh, M., Kumar, M., Kalaivani, R., Manikandan, S., and Kumaraguru, A. K. (2012) Metallic silver nanoparticle: a therapeutic agent in combination with antifungal drug against human fungal pathogen. *Bioprocess and Biosystems Engineering*. Volume 2012: 1-9.

Singh, R., Gupta, N., Sadie, J. A., Poole, K. F., Ballato, J., and Hwu, S. J. (2010).Challenges and opportunities of manufacturing the next generation of integrated photonics. In *MOEMS-MEMS* (Page 75910N-75910N). International Society for Optics and Photonics.

Singh, S. K., Shrivastava, S., and Dash, D. (2011) Metallic Nanoparticles: Biological Perspective. In *Metal Nanoparticles in Microbiology* (Page 285-298). Springer Berlin Heidelberg.

Sivaraman, S. K., Elango, I., Kumar, S., and Santhanam, V. (2009) A green protocol for room temperature synthesis of silver nanoparticles in seconds. *Current Science*. Volume 97(7): 1055-1059.

Slocik, J. M., Naik, R. R., Stone, M. O., and Wright, D. W. (2005) Viral templates for gold nanoparticle synthesis. *Journal of Materials Chemistry*. Volume 15(7): 749-753.

Smalley, R. E., and Yakobson, B. I. (1998) The future of the fullerenes. *Solid state communications*. Volume 107(11): 597-606.

Smith, A. M., Duan, H., Mohs, A. M., and Nie, S. (2008) Bioconjugated quantum dots for *in vivo* molecular and cellular imaging. *Advanced Drug Delivery Reviews*. Volume 60(11): 1226-1240.

Smith, B. C. (2011) *Fundamentals of Fourier transform infrared spectroscopy*. CRC press.

Snima, K. S., Jayakumar, R., Unnikrishnan, A. G., Nair, S. V., and Lakshmanan, V. K. (2012) O-Carboxymethyl chitosan nanoparticles for metformin delivery to pancreatic cancer cells. *Carbohydrate Polymers*.

Solis Jr, D., Willingham, B., Nauert, S. L., Slaughter, L. S., Olson, J., Swanglap, P., Pal, A., Chang, W. S., and Link, S. (2012) Electromagnetic Energy Transport in Nanoparticle Chains via Dark Plasmon Modes. *Nano Letters*. Volume 12(3): 1349-1353.

Solomon, S. D., Bahadory, M., Jeyarajasingam, A. V., Rutkowsky, S. A., and Boritz, C. (2007) Synthesis and Study of Solver Nanoparticles. *Journal of Chemical Education.* Volume 84(2): 322-325.

Song, J. Y., Jang, H. K., and Kim, B. S. (2009) Biological synthesis of gold nanoparticles using *Magnolia kobus* and *Diopyros kaki* leaf extracts. *Process Biochemistry*. Volume 44(10): 1133-1138.

Song, J. Y., Kwon, E. Y., and Kim, B. S. (2010) Biological synthesis of platinum nanoparticles using *Diopyros kaki* leaf extract. *Bioprocess and Biosystems Engineering*. Volume 33(1): 159-164.

Sprenger, G. A., Schorken, U., Wiegert, T., Grolle, S., De Graaf, A. A., Taylor, S. V., Tadhg, P. B., and Sahm, H. (1997). Identification of a thiamin-dependent synthase in *Escherichia coli* required for the formation of the 1-deoxy-D-xylulose 5-phosphate precursor to isoprenoids, thiamin, and pyridoxol. *Proceedings of the National Academy of Sciences*. Volume 94(24): 12857-12862.

Sperling, R. A., Gil, P. R., Zhang, F., Zanella, M., and Parak, W. J. (2008) Biological applications of gold nanoparticles. *Chemical Society Reviews*. Volume 37(9): 1896-1908.

Stern, S. T., and McNeil, S. E. (2008) Nanotechnology safety concerns revisited. *Toxicological Sciences*. Volume 101(1): 4-21.

Stojanovic, D. B., Brajovie, L., Orlovic, A., Dramlic, D., Radmilovic, V., Uskokovic, P. S., and Aleksic, R. (2012) Transparent PMMA/silica nanocomposites containing silica nanoparticles coating under supercritical conditions. *Progress in Organic Coatings*.

Strackharn, M., Stahl, S. W., Puchner, E. M., and Gaub, H. E. (2012) Functional Assembly of Aptamer Binding Sites by Single-Molecule Cut-and-Paste. *Nano Letters*. Volume 12(5): 2425-2428.

Su, L., Jia, W., Zhang, L., Beacham, C., Zhang, H., and Lei, Y. (2010) Facile Synthesis of a Platinum Nanoflower Monolayer on a Single-Walled Carbon Nanotube Membrane and Its Application in Glucose Detection. *The Journal of Physical Chemistry C*. Volume 114(42): 18121-18125.

Sugai, T., Yoshida, H., Shimada, T., Okazaki, T., Shinohara, H., and Bandow, S. (2003) New synthesis of high-quality double-walled carbon nanotubes by high-temperature pulsed arc discharge. *Nano Letters*. Volume 3(6): 769-773.

Suresh, A. K. (2012) Introduction to Nanocrystallites, Properties, Synthesis, Characterizations, and Potential Applications. In *Metallic Nanocrystallites and their Interaction with Microbial Systems* (Page 1-23). Springer Netherlands.

Suri, S. S., Fenniri, H., and Singh, B. (2007) Nanotechnology-based drug delivery systems. *Journal of Occupational Medicine and Toxicology*. Volume 2(1): 16.

Sweeney, R. Y., Mao, C., Gao, X., Burt, J. L., Belcher, A. M., and Georgiou, G. (2004) Bacterial biosynthesis of cadmium sulfide nanocrystals. *Chemistry and Biology*. Volume 11:1553-9.

Takagi, A., Hirose, A., Nishimura, T., Fukumori, N., Ogata, A., Ohashi, N., Kitajima, S., and Kanno, J. (2008) Induction of mesothelioma in p53+/-mouse by intraperitoneal application of multi-wall carbon nanotube. *The Journal of Toxicological Sciences*. Volume 33(1): 105-116.

Tan, M. L., Choong, P. F., and Dass, C. R. (2010) Recent developments in liposomes, microparticles and nanoparticles for protein and peptide drug delivery. *Peptides*. Volume 31(1): 184-193.

Tan, Z., Zhang, F., Zhu, T., Xu, J., Wang, A. Y., Dixon, J. D., Li, L., Zhang, Q., Mohney, S. E., and Ruzyllo, J. (2007) Bright and color-saturated emission from blue light-emitting diodes based on solution-processed colloidal nanocrystal quantum dots. *Nano Letters*. Volume 7(12): 3803-3807.

Tasker, L. H., Sparey-Taylor, G. J., and Nokes, L. D. M. (2007) Applications of nanotechnology in orthopaedics. *Clinical Orthopaedics and Related Research*. Volume 456: 243-249.

Taylor, S. V., Kelleher, N. L., Kinsland, C., Chiu, H. J., Costello, C. A., Backstrom, A. D., Mc Lafferty, F. W. and Begley, T. P. (1998) Thiamine biosynthesis in *Escherichia coli*. Identification of this thiocarboxylate as the immediate sulfur donor in the thiazole formation. *The Journal of Biological Chemistry*. Volume 273: 16555-16560.

Tejera-Garcia, R., Ranjan, S., Zamotin, V., Sood, R., and Kinnunen, P. K. (2011) Making unilamellar liposomes using focused ultrasound. *Langmuir*. Volume 27(16): 10088-10097.

Terrones, M. (2004) Carbon nanotubes: synthesis and properties, electronic devices and other emerging applications. *International Materials Reviews.* Volume 49(6): 325-377.

Thakkar, K. N., Mhatre, S. S., and Parikh, R. Y. (2010) Biological synthesis of metallic nanoparticles. *Nanomedicine: Nanotechnology, Biology and Medicine.* Volume 6(2): 257-262.

Tolaymat,T M., El-Badawy, A. M., Genaidy, A., Scheckel, K. G., Luxton, T. P., and Suidan, M. (2010) An evidence-based environmental perspective of manufactured silver nanoparticles in syntheses and applications: a systematic review and critical appraisal of peer- reviews scientific papers. *Science of Total Environment Journal.* Volume 408: 999-1006.

Toumey, C. (2010) Tracing and disputing the story of nanotechnology. In. *Cheltenham, UK: Edward Elgar*, 46-59.

Trampuz, A., Jereb, M., Muzlovic, I., and Prabhu, R. M. (2003) Clinical review: Severe malaria. *Critical Care-London*. Volume 7(4): 315-323.

Tripathi, J., Keller, J. M., Das, K., Tripathi, S., and Shripathi, T. (2012) Influence of Rhodamine (B) doping on vibrational, morphological and absorption properties of poly (vinyl) alcohol. *Journal of Physics and Chemistry of Solids*.

Tripathi, V. S., Kandimalla, V. B., and Ju, H. (2006) Amperometric biosensor for hydrogen peroxide based on ferrocene-bovine serum albumin and multiwall carbon nanotube modified ormosil composite. *Biosensors and Bioelectronics*. Volume 21(8): 1529-1535.

Turci, F., Ghibaudi, E., Colonna, M., Boscolo, B., Fenoglio, I., and Fubini, B. (2010) An integrated approach to the study of the interaction between proteins and nanoparticles. *Langmuir*. Volume 26(11): 8336-8346.

Vaidyanathan, R., Kalishwaralal, K., Gopalram, S., and Gurunathan, S. (2009) RETRACTED: Nanosilver—the burgeoning therapeutic molecule and its green synthesis. *Biotechnology Advances*. Volume 27(6): 924-937.

Valodkar, M., Nagar, P. S., Jadeja, R. N., Thounaojam, M. C., Devkar, R. V., and Thakore, S. (2011) Euphorbiaceae latex induced green synthesis of non-cytotoxic metallic nanoparticle solutions: a rational approach to antimicrobial applications. *Colloids and Surfaces A: Physicochemical and Engineering Aspects*. Volume 384(1): 337-344.

Van Boxtel, C. J. (2001) Analgesics, Antirheumatics and Drugs for the Treatment of Gout. *Drug Benefits and Risks: International Textbook of Clinical Pharmacology*: 387.

Van Dong, P., Ha, C. H., Binh, L. T., and Kasbohm, J. (2012) Chemical synthesis and antibacterial activity of novel-shaped silver nanoparticles. *International Nano Letters.* Volume 2: 9.

Van Heusden, K., Kunze, K., Kiim, H., Stump, A. D., Schult, A. B., Hampden-Smith, M. J., and Kowalski, M. H. (2010) *U.S. Patent No. 7,749,299*. Washington, DC: U.S. Patent and Trademark Office.

Van Huyssteen, E. (2010) *Efficacy enhancement of the antimalarial drugs, mefloquine and artesunate, with Pheroid TM technology/E. van Huyssteen* (Doctoral dissertation).

Varadan, V. K., Chen, L., and Xie, J. (2008) *Nanomedicine: Design and Applications of Magnetic Nanomaterials, Nanosensors and Nanosystems*. Wiley.

Veerapandian, M., and Yun, K. (2011) Functionalization of biomolecules on nanoparticles: specialized for antibacterial applications. *Applied Microbiology and Biotechnology*. Volume 90(5): 1655-1667.

Vermeij, E. J., Zoon, P. D., Chang, S. B. C. G., Keereweer, I., Pieterman, R., and Gerretsen, R. R. R. (2012) Analysis of microtraces in invasive traumas using SEM/EDS. *Forensic Science International*. Volume 214(1): 96-104.

Vigneshwaran, N., Kathe, A. A., Varadarajan, P. V., Nachanc, R. P., and Balasubramanya, R. J. (2007) Functional fishing of cotton fabrics using silver nanoparticles. *Journal of Nanoscience and Nanotechnology.* Volume7: 1893-7.

Vinod, V. T. P., Saravanan, P., Sreedhar, B., Devi, D. K., and Sashidhar, R. B. (2011) A facile synthesis and characterization of Ag, Au and Pt nanoparticles using a natural hydrocolloid gum kondagogu (*Cochlospermum gossypium*). *Colloids and Surfaces B: Biointerfaces*. Volume 83(2): 291-298.

Virkutyte, J., and Varma, R. S. (2011) Green synthesis of metal nanoparticles: biodegradable polymers and enzymes in stabilization and surface functionalization. *Chemical Science*. Volume 2(5): 837-846.

Vivero-Escoto, J. L. (2013) Nanovehicles for Intracellular Protein Delivery. *Journal of Biotechnology and Biomaterial*. Volume 3: e117.

Von Freymann, G., Kitaev, V., Lotsch, B. V., and Ozin, G. A. (2013) Bottom-up assembly of photonic crystals. *Chemical Society Reviews*.

Wang, B., He, X., Zhang, Z., Zhao, Y., and Feng, W. (2012) Metabolism of Nanomaterials in Vivo: Blood Circulation and Organ Clearance. *Accounts of Chemical Research*.

Wang, C., Zhao, H., Wang, H., Liu, L., Xiao, C., and Ma, D. (2012).The effects of ionic additives on the aqueous-phase Fischer–Tropsch synthesis with a ruthenium nanoparticle catalyst. *Catalysis Today*. Volume 183(1): 143-153.

Wang, H. C., Wu, J. S., Chia, J. C., Yang, C. C., Wu, Y. J., and Juang, R. H. (2009) Phytochelatin synthase is regulated by protein phosphorylation at a threonine residue near its catalytic site. *Journal of Agricultural and Food Chemistry*. Volume 57(16): 7348-7355.

Wang, J., and Musameh, M. (2003) Carbon nanotube/teflon composite electrochemical sensors and biosensors. *Analytical Chemistry*. Volume 75(9): 2075-2079.

Wang, M., and Thanou, M. (2010) Targeting nanoparticles to cancer. *Pharmacological Research*. Volume 62(2), 90-99.

Wang, S., Jiang, S. P., and Wang, X. (2011) Microwave- assisted one-pot synthesis of metal/metal oxide nanoparticles on graphene and their electrochemical applications. *Electrochimica Acta.* Volume 56(9): 3338-3344.

Wang, X., Wu, L., Ren, J., Miyoshi, D., Sugimoto, N., and Qu, X. (2011) Label-free colorimetric and quantitative detection of cancer marker protein using noncrosslinking aggregation of Au/Ag nanoparticles induced by target-specific peptide probe. *Biosensors and Bioelectronics*. Volume 26(12): 4804-4809.

Wasankar, S. R., Faizi, S. M., and Deshmuk, A. D. (2012) Formulation and Development of liposomal gel for topical drug delivery system. *International Journal of Pharmaceutic Sciences Review*.Volume 3(11): 4462-74.

Webb, M. E., Marquet, A., Mendel, R. R., Rebeille, F., and Smith, A. G. (2007) Elucidating biosynthetic pathways for vitamins and cofactors. *Natural Product Reports*. Volume *24*(5): 988-1008.

Wen, J., Arkawa, T. and Philo, J.S. (1996) Size- exclusion chromatography with on-line light-scattering, absorbance, and refractive index detectors for studying proteins and their interactions.*Analytical Biochemistry*. Volume 240: 155-166.

Wells, T. N., Alonso, P. L., and Gutteridge, W. E. (2009) New medicines to improve control and contribute to the eradication of malaria. *Nature Reviews Drug Discovery*. Volume 8(11): 879-891.

Werner, M. E., Foote, M. B., and Wang, A Z. (2012) Chemoradiotherapy of human tumors: novel approaches from nanomedicine. *Current Pharmaceutical Design*. Volume 18(19): 2830-2837.

Wiarachai, O., Thongchul, N., Kiatkamjornwong, S., and Hoven, V. P. (2012) Surface-quaternized chitosan particles as an alternative and effective organic antibacterial material. *Colloids and Surfaces B: Biointerfaces*. Volume 92: 121-129.

Wight, R. and Meacock, P. A. (1971) The *THI5* gene family of *Saccharomyces cerevisiae*: distribution of homologues among the hemiascomycetes and functional redundancy in the aerobic biosynthesis of thiamine from pyridoxine. *Microbiology.* Volume 149: 1447-1460.

Wilkinson, G. N. (1960) Statistical estimations in enzyme kinetics. *Biochemistry Journal.* Volume 80: 324-332.

Wilson, L. and Walker, J. (1994) Practical Biochemistry Principles and Techniques. Fourth Ed. Cambridge University Press, Britain 17: 498-507.

Witte, P. (2008) *Amphiphilic Fullerenes for Biomedical and Optoelectronical Applications*.

Wohlstadter, J. N., Wilbur, J. L., Sigal, G. B., Biebuyck, H. A., Billadeau, M. A., Dong, L., Fischer, A. B., and Wohlstadter, S. J. (2003) Carbon nanotube-based biosensor. *Advanced Materials*. Volume 15(14): 1184-1187.

World Health Organization[1]. (2011) World malaria report 2011. http://www.who.int/malaria/world_malaria_report_2011/9789241564403_eng.pdf

World Health Organization[2].(2006) Guidelines for the treatment of Malaria. http://books.google.co.za/books?hl=en&lr=&id=RMOrOvUkB8C&oi=fnd&pg=PP2&dq=Guidelines+for+the+treatment+of+Malaria.&ots=5ZlmVjpCj5&sig=T76km5VPFBe471nQ0Cfw5yqLsd8#v=onepage&q=Guidelines%20for%20the%20treatment%20of%20Malaria.&f=false

Wrenger, C., Eschbach, M. L., Muller, I. B., Laun, N. P., Begley, T. P., and Walter, R. D. (2006) Vitamin B_1*de novo* synthesis in the human malaria parasite *Plasmodium*

falciparum depends on external provision of 4-amino-5-hydroxymethyl-2-methylpyrimidine. *The Journal of Biological Chemistry.* Volume 387: 41-51.

Wrenger, C., Eschbach, M. L., Muller, I. B., Warnecke, D. and Walter, R. D. (2005) Analysis of the vitamin B6 biosynthesis pathway in the human malaria parasite *Plasmodium falciparum*. *Journal of Biological Chemistry*. Volume 276: 29651-29656.

Wu, H., He, L., Gao, M., Gao, S., Liao, X., and Shi, B. (2011) One-step in situ assembly of size-controlled silver nanoparticles on polyphenol-grafted collagen fiber with enhanced antibacterial properties. *New Journal of Chemistry*. Volume 35(12): 2902-2909.

Xiao, L., Aoshima, H., Saitoh, Y., and Miwa, N. (2010) Fullerene–polyvinylpyrrolidone clathrate localizes in the cytoplasm to prevent Ultraviolet-A ray-induced DNA-fragmentation and activation of the transcriptional factor NF- kappaB. *Journal of Cellular Biochemistry*. Volume 111(4): 955-966.

Xiao, L., Takada, H., and Miwa, N. (2006) The water-soluble fullerene derivative 'Radical Sponge® exerts cytoprotective action against UVA irradiation but not visible-light-catalyzed cytotoxicity in human skin keratinocytes. *Bioorganic and Medicinal Chemistry Letters*. Volume 16(6): 1590-1595.

Xu, X., and Burgess, D. J. (2012) Liposomes as carriers for controlled drug delivery. In *Long Acting Injections and Implants* (Page 195-220). Springer US.

Xu, Z. P., Zeng, Q. H., Lu, G. Q., and Yu, A. B. (2006) Inorganic nanoparticles as carriers for efficient cellular delivery. *Chemical Engineering Science*. Volume 61(3): 1027-1040.

Yadav, B. C., and Kumar, R. (2008) Structure, properties and applications of fullerenes. *International Journal of Nanotechnology and Applications*. Volume 2(1): 15-24.

Yadav, T. P., Yadav, R. M., and Singh, D. P. (2012) Mechanical Milling: a Top Down Approach for the Synthesis of Nanomaterials and Nanocomposites. *Nanoscience and Nanotechnology*. Volume 2(3): 22-48.

Yah, C. S., Iyuke, S. E., and Simate, G. S (2012) A Review of Nanoparticles Toxicity and Their Routes of Exposures. *Pakistan Journal of Pharmaceutical Sciences*. Volume 25(2): 477-491.

Yang, Y., Tsui, H. C. T., Man, T. K., and Winkler, M. E. (1998) Identification and function of the *pdxY* gene, which encodes a novel pyridoxal kinase involved in the salvage pathway of pyridoxal 5′-phosphate biosynthesis in *Escherichia coli* K-12. *Journal of bacteriology*. Volume 180(7): 1814-1821.

Yeung, C. S., Chen, Y. K., and Wang, Y. A. (2011) Theoretical studies of substitutionally doped single-walled nanotubes. *Journal of Nanotechnology*, *2010*.

Yi, Z., Li, X., Xu, X., Luo, B., Luo, J., Wu, W., Yi, Y., and Tang, Y. (2011) Green, effective chemical route for the synthesis of silver nanoplates in tannic acid aqueous solution. *Colloids and Surfaces A: Physicochemical and Engineering Aspects*. Volume 392(1): 131-136.

Yildirimer, L., Thanh, N. T., Loizidou, M., and Seifalian, A. M. (2011) Toxicology and clinical potential of nanoparticles. *Nano Today*. Volume 6(6): 585-607.

Yu, D., Smith, G. A., Enquist, L. W., and Shenk, T. (2002) Construction of a self-excisable bacterial artificial chromosome containing the human cytomegalovirus genome and mutagenesis of the diploid TRL/IRL13 gene. *Journal of Virology*. Volume 76(5): 2316-2328.

Yu, F., Zhang, L., Huang, Y., Sun, K., David, A. E., and Yang, V. C. (2010) The magnetophoretic mobility and superparamagnetism of core-shell iron oxide nanoparticles with dual targeting and imaging functionality. *Biomaterials*. Volume 31(22): 5842-5848.

Yu, H., Krause, C. F., Oyanedel-Craver, V., Fauss, E., Swami, N., and Smith, J. A. (2011) Impact of silver nanoparticle concentration and size in colloidal-silver-impregnated xeramic filters for point-of-use removal of *E. coli* and MS-2 Phage. *Proceedings of the Water Environment Federation*. Volume 2011(3): 72-79.

Yum, K., Na, S., Xiang, Y., Wang, N., and Yu, M. F. (2009) Mechanochemical delivery and dynamic tracking of fluorescent quantum dots in the cytoplasm and nucleus of living cells. *Nano Letters*. Volume 9(5): 2193-2198.

Zasada, F., Piskorz, W., Stelmachowski, P., Kotarba, A., Paul, J. F., Płocinnski, T., Kurzydlowski, K. J., and Sojka, Z. (2011) Periodic DFT and HR-STEM studies of surface structure and morphology of cobalt spinel nanocrystals. Retrieving 3D shapes from 2D images. *The Journal of Physical Chemistry C*. Volume 115(14): 6423-6432.

Zhang, B., Watts, K. M., Hodge, D., Kemp, L. M., Hunstad, D. A., Hicks, L. M., and Odom, A. R. (2011) A second target of the antimalarial and antibacterial agent fosmidomycin revealed by cellular metabolic profiling. *Biochemistry*. Volume 50(17), 3570-3577.

Zhang, L., Zhao, J., Zhang, H., Jiang, J., and Yu, R. (2013) Double strand DNA-templated copper nanoparticle as a novel fluorescence indicator for label-free detection of polynucleotide kinase activity. *Biosensors and Bioelectronics*. Volume 44: 6-9.

Zhang, J., Taylor, S.V., Chiu, H. J. and Begley, T. (1997) Characterization of the *Bacillus subtilis* thiC operon involved in thiamine biosynthesis.*Journal of Bacteriology*. Volume 179: 3030-3035.

Zhang, J. Z. (2010) Biomedical applications of shape-controlled plasmonic nanostructures: a case study of hollow gold nanospheres for photothermal ablation therapy of cancer. *The Journal of Physical Chemistry Letters*. Volume 1(4): 686-695.

Zhang, T., Nix, M. B., Yoo, B. Y., Deshusses, M. A., and Myung, N. V. (2006) Electrochemically functionalized single-walled carbon nanotube gas sensor. *Electroanalysis*. Volume 18(12): 1153-1158.

Zhang, Y., Peng, H., Huang, W., Zhou, Y., and Yan, D. (2008) Facile preparation and characterization of highly antimicrobial colloid Ag or Au nanoparticles. *Journal of colloid and interface science*. Volume 325(2): 371-376.

Zhang, Y., Taylor, SV., Chiu, H.J., Begley, T. P. (1997) Characterization of the *Bacillus subtilis* thiC operon involved in thiamine biosynthesis. *Journal or Bacteriology*. Volume 179: 3030–3035.

Zhang, Y. F., Wang, J. C., Bian, D. Y., Zhang, X., and Zhang, Q. (2010) Targeted delivery of RGD-modified liposomes encapsulating both combretastatin A-4 and

doxorubicin for tumor therapy: In vitro and in vivo studies. *European Journal of Pharmaceutics and Biopharmaceutics*. Volume 74(3): 467-473.

Zhou, W. (2013) Principles and Status of Nanoimprint Lithography. In *Nanoimprint Lithography: An Enabling Process for Nanofabrication* (Page 5-32). Springer Berlin Heidelberg.

Appendices

Appendix 1: *Pf*ThzK sequence

```
  1 atgagaaaatataatttttttacaaaaagtcgcttattctctaccttaaccaaaataaat
 61 agcgttaaggaatatcatgatgatataataaagtgcattgagaaagttcgggttattaat
121 cctcttgttcattgtataactaatagagtaaccactgaaaaggtggcaaacagtttattg
181 gcctttggctcttctccggctatgattgataatcctaaggaagttgaagaatttgctaaa
241 atagcttcatgtacttatttcaacttagggttacatacgacgcaggtagaaaatattaat
301 ttattagaaaagttaagaaaagaatgtatgaaagataaatttatgttaattatagatcca
361 atagctgttggagcaacaacctatagaactaatgttattaaagatataatttttaaaatgc
421 caacctaatgtaataaaaggtaatattgctgaaatttattatttagataaaggagaattt
481 ttggggaagggtgtagatagtaataataacaatactcataatgaaacagatgtaattaat
541 agtgccagaaatgttgcattaaaatataattgtgctgtagtagttacatcaaaaacagat
601 tatattgttagtccatgttctcattatgtagccaaaattaattgtgatttaaaaattctg
661 acaaaaattactgggtcaggttgttctgttggtgccctttgtgcagcagctacttcagta
721 tatcctcaaaacccattcatagcatgtatatctgctactcttatatataaattggcagca
781 ttcaaagcatatcaaaaagaaaagtatccaggttccctaagtcataaaattattgatgat
841 atttattactattcacataatcctcattttctcaatttccaaatcgtagatatttacaaa
901 gcagcataa
```

Appendix 2: Media and Buffers

Table A1. Media and Buffers

Luria Broth (LB)	10 g/L tryptone 5 g/L yeast extract 10 g/L NaCl	Autoclave
Luria Agar (LA)	10 g/L tryptone 5 g/L yeast extract 10 g/L NaCl 15 g/L agar	Autoclave
TAE	0.04 M Tris-HCl 1 mM EDTA pH 8.0 0.021 mM glacial acetic acid	
SOB	20 g/L tryptone 5 g/L yeast extract 0.584 g/LNaCl 0.186 g/L KCl 2.034 g/L $MgCl_2$ 2.464 g/L $MgSO_4$	Autoclave
SOC	20 g/L tryptone 5 g/L yeast extract 0.584 g/LNaCl 0.186 g/L KCl 2.034 g/L $MgCl_2$ 2.464 g/L $MgSO_4$	Add 20 ml/L of sterile glucose after autoclave
TB buffer	2.6 g/L HEPES pH6.7 2.203 g/L $CaCl_2$ 18.638 g/L KCl 10.886 g/L$MnCl_2$	Mix all the components except $MnCl_2$, adjust pH to 6.7 with KOH/HCL, then add $MnCl_2$, and filter sterilize (0.22 µm)
Tris-HCl	121.14 g/molTris Powder Hydrochloric acid	Adjust with HCl to desired pH value Dilute with dH_2O to desired concentration
Binding buffer	0.5 M NaCl 20 mM imidazole 20 mMTris-HCl	Adjust pH to 7.5, degas and filter
Elution buffer	0.5 M NaCl 0.5 M imidazole 20 mMTris-HCl	Adjust pH to 7.5, degas and filter
Gel filtration buffer	50 mMNaCl 50 mMTris-HCl	Adjust pH to 7.5, degas and filter
10% Resolving gel	0.972 ml 30% Acrylamide 485 µl 3M Tris, pH8.8 2.188 ml dH_2O 91 µl 10% SDS 12.5 µl 10% APS 2.5 µl TEMED	TEMED should be added last.
4% Stacking gel	0.2 ml 30% Acrylamide 105 µl 0.5M Tris, pH6.8 1.185 ml dH_2O 15 µl 10% SDS 15 µl 10% APS 1.5 µl TEMED	TEMED should be added last.

SDS-PAGE loading buffer	1.6 ml dH_2O 0.5 ml 0.5 M Tris, pH6.8 0.8 ml 50% glycerol 0.8 ml 10% SDS 0.2 ml 2-βmercaptoethanolbromophenol blue 0.1 ml acetic acid	2-βmercaptoethanolbromophenol blue should be added just before use.
SDS-PAGE running buffer	25 mMTris powder 192 mM glycine 0.1% SDS	
Fairbanks A	0.05% Coomassie Blue 25% isopropanol 10% acetic acid	
Fairbanks B	0.005% Coomassie Blue 10% isopropanol 10% acetic acid	
Fairbanks C	0.002% Coomassie Blue 10% acetic acid	
Fairbanks D	10% acetic acid	

Appendix 3: Biospin Gel Extraction Kit Protocol

(BioFlux, Bioer Technology Co., Ltd)

1. **Excise the DNA fragment from the agarose gel with a clean scalpel.**
   Minimize the size of the gel slice by removing extra agarose.
2. **Weigh the gel slice and add 3 volume of Extraction Buffer to 1 volume of gel slice (100 mg=100 μl).**
   Add 300 μl Extraction Buffer to each 100 mg gel, and the gel slice should not be more than 400 mg per test.
3. **Incubate at 50℃ until the gel melts in a heating block and vortex the tube every 2 minutes during the incubation.**
   Usually, it takes 10 min. If the colour of the mixture is purple then add 10 μl of 3 M sodium acetate (pH5.0), and mix. The colour will return to yellow.
4. **Optional: Add 1volume of isopropanol to1 volume of gel and mix.**
   No need to add isopropanol in the case the fragments > 500 bp and < 4 kb.
5. **Apply the sample to Spin column, centrifuge for 1 min at 6,000 × g. Discard the flow-through.**
   If the sample volume is more than 750 μl, simply load and spin again.
6. **Add 500 μl Extraction Buffer to Spin column, centrifuge for 30-60 s at 12,000 × g. Discard the flow-through.**
7. **Add 750 μl Wash buffer to Spin column, centrifuge for 30-60s at 12,000 × g. Discard the flow-through.**
   If the DNA will be used for salt sensitive applications, let the spin column stand for 2-5min after addition of Wash Buffer, before centrifugation.
8. **Centrifuge for an additional 1min at 12,000 × g and transfer the Spin column to a sterile 1.5 ml microcentrifuge tube.**
   Recommend to centrifuge according to this step; otherwise, there will be residual liquid in the column.
9. **Add 30-100 μl Elution Buffer, H_2O or TE Buffer to the Spin column and let it stand for 1 min at room temperature.**

The volume of Elution Buffer could be adjusted according to needs, but no less than 20 μl.

10. **Centrifuge for 1min at 12,000 × g. The buffer in the microcentrifuge tube contains the DNA.**

    The extracted DNA can be used directly for downstream molecular biological experiment. Store at -20℃.

Appendix 4: Biospin Plasmid DNA Extraction Kit Protocol

(BioFlux, Bioer Technology Co., Ltd)

1. **Add 2 ml cultured bacteria to 2 ml microcentrifuge tube.**
2. **Cenrifuge at 10,000 × g for 30 s, and discard the supernatant.**
   Step 1 and 2 could be repeated for more than once to collect enough cells.
3. **Resuspend pelleted bacteria cells in 250 μl Resuspension Buffer and No cell clumps should be visible after resuspension of the pellets.**
4. **Add 250 μl Lysis Buffer and gently invert the tube 4-6 times to mix.**
   Do not vortex, as this will result in shearing of genomic DNA. Do not allow this step for more than 5 min.
5. **Add 350 μl Neutralization Buffer and gently invert the tube 4-6 times to mix.**
   The solution should become cloudy and no local precipitate should be visible.
6. **Centrifuge for 10 min at 13,000 × g until a compact white pellet form.**
7. **Apply the supernatant to the Spin column and centrifuge for 1 min at 6000 × g. Discard the flow-through.**
8. **Add 650 μl Wash Buffer to the Spin column and centrifuge for 1 min at 12,000 × g. Discard the flow-through.**
9. **Repeat step 8.**
10. **Centrifuge for an additional 1 min at 12,000 × g and transfer the Spin column to a sterile 1.5 ml microcentrifuge tube.**
    Recommend to centrifuge according to this step; otherwise, there will be residual liquid in the column.
11. **Add 50 μl Elution Buffer to the Spin column and let it stand for 15 min at 37℃.**
    The volume of Elution Buffer could be adjusted according to needs.
12. **Centrifuge for 1 min at 12,000 × g. The buffer in microcentrifuge tube contains the plasmid DNA.**
13. **The purified plasmid DNA can be used directly for kinds of downstream molecular biological experiments. Store at -20℃.**

Appendix 5: Fairbanks Coomassie Blue Protein Staining and Destaining Protocol

(Fairbanks *et al*., 1971)

1. **After electrophoresis, the gels are placed in a microwavable container, and approximately 100 ml of Fairbanks A staining solution was added.**
2. **The gel in the solution is then heated in a conventional microwave oven on full power until the solution reaches boiling point (about 2 min).**
3. **Cool the gel and solution to room temperature for approximately 5 min with gentle shaking.**
4. **The Fairbanks A solution is then discarded and the gel rinsed in distilled water at room temperature for a few seconds.**

   After this step, protein bands containing 100 ng or more are easily observed.
5. **Add approximately 100 ml of Fairbanks B solution and proceed as in steps 2-4.**

   After this step, protein bands containing 50 ng or more are easily observed.
6. **Add approximately 100 ml of Fairbanks C solution and proceed as in steps 2-4.**

   After this step, protein bands containing 25 ng or more are easily observed.
7. **Add approximately 100 ml of Fairbanks D solution (destaining solution) and repeat steps 2-4.**

   After this step, protein bands containing 5 ng or more are easily observed.

A water- clear background can be achieved by repeating step 7 two or three times, or if the gel is left shaking in the destaining solution for 15 or more minutes.

Also, the procedure can be stopped at any of the steps once the desired results are achieved, followed by destaining as in step 7.

All solutions used here are shown in Appendix 2.

Appendix 6: BCA protein Assay and standard

A. Preparation of diluted BSA Standard, and 1 ml of 2.0 mg/ml albumin was used as stock.

Use Table A2 as a guide to prepare a set of protein standards.

Table A2. Preparation of diluted albumin standards.

Vial	Volume of Diluent (µl)	Volume and source of BSA (µl)	Final BSA concentration (µg/ml)
A	0	300 of stock	2,000
B	125	375 of stock	1,500
C	325	325 of stock	1,000
D	175	175 of vial B	750
E	325	325 of vial C	500
F	325	325 of vial E	250
G	325	325 of vial F	125
H	400	100 of vial G	25
I	400	0	0=Blank

B. Preparation of BCA working reagent (WR)

1. Use the following formula to determine the total volume of WR required:

   (standards + samples) × (3 replicates) × (volume of WR per sample) = WR required

2. Prepare WR by mixing 50 parts of BCA reagent A with 1 part of BCA reagent B (50:1).

C. 2 ml Eppendorf-tube procedure (sample to WR ratio = 1:20)

1. Pipette 50 µl of each standard and unknown sample replicate into 2 ml-eppendorf tube.
2. Add 1ml of the WR to each tube, and mix well.
3. Incubate at 60 ℃ for 30 min, and cool down to room temperature.
4. Read absorbance at 562 nm.

D. BCA standard curve

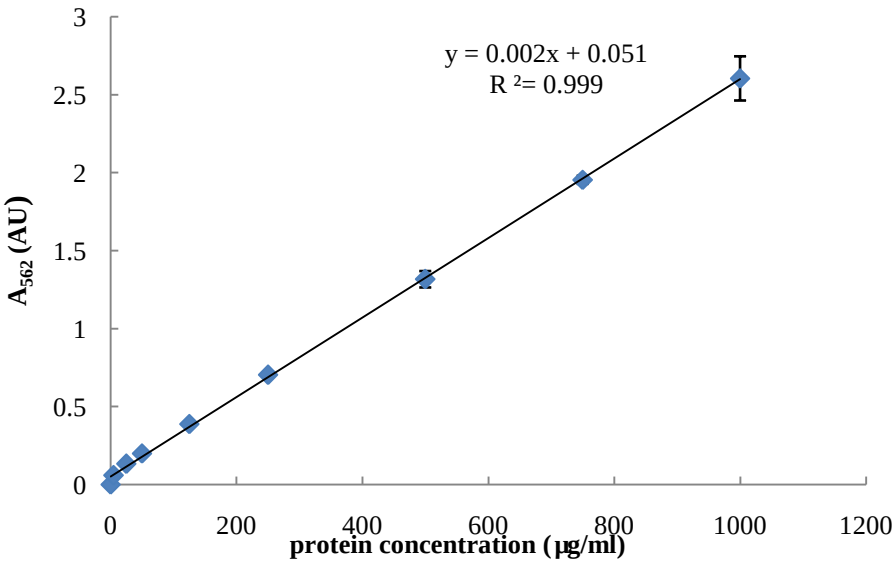

Figure A1. BCA standard curve.

Appendix 7: Ag nanoparticles standard

Preparation of diluted Ag nanoparticles standard as Table A3, and 1 ml of 1 mM Ag NPs was used as stock. The samples were read at 400 nm.

Table A3. Preparation of Ag nanoparticles standard.

	1	2	3	4	5	6
1mM stock (µl)	0	10	20	50	80	100
dH_2O (µl)	1000	990	980	950	920	900
Final concentration (mM)	0	0.1	0.2	0.5	0.8	1.0

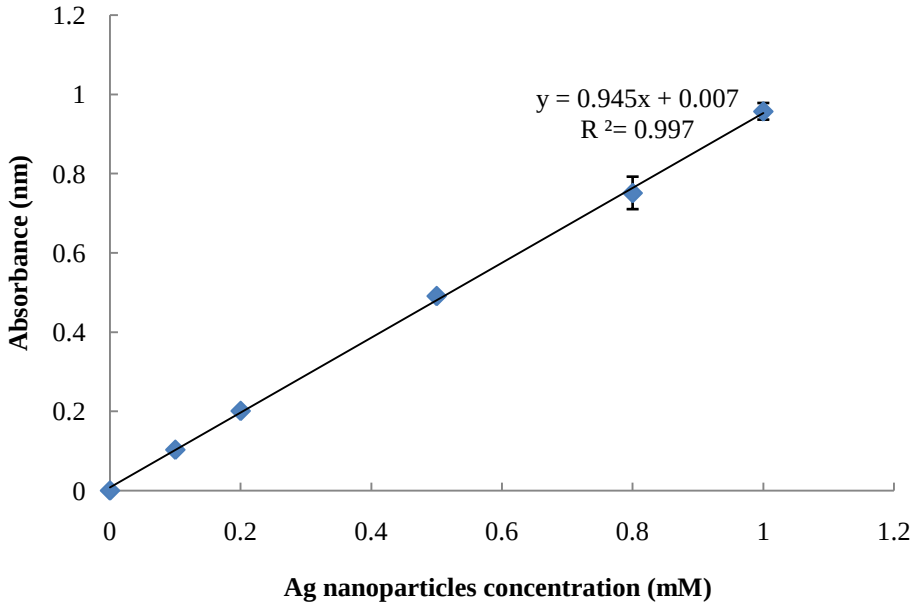

Figure A2. The Ag nanoparticles standard.

Appendix 8: Molybdate assay and phosphate standard

A. Preparation of diluted Na_2HPO_4 Standard as Table A4, and 1 ml of 1 mM Na_2HPO_4 was used as stock.

Table A4. Preparation of diluted Na_2HPO_4.

	1	**2**	**3**	**4**	**5**	**6**	**7**	**8**	**9**	**10**
1mM stock (µl)	0	10	20	30	40	50	80	90	100	120
dH_2O (µl)	1000	990	980	970	960	950	920	910	900	880
Final concentration (µM)	0	10	20	30	40	50	80	90	100	120

B. Preparation of Molybdate assay reagents.

- Reagent A: 2 g of ammonium molybdate is dissolved in 9 ml of concentrated H_2SO_4. This is diluted with 200 ml of dH_2O and make up to 310 ml.
- Reagent B: 9% Ascorbic solution is prepare by dissolving 18 g of L-ascorbic acid in a little quantity of dH_2O, and then fill up to 200 ml.
- Reagent C: prepare just before use by mixing A and B in 4:1 ratio.

C. Protocol of Molybdate assay

- 80 µl of each sample is placed in microtite plate.
- 160 µl of reagent C is added to each sample and allow to stand for 10 min at room temperature for colour development.
- Read absorbance at 700 nm

D. Phosphate standard curve:

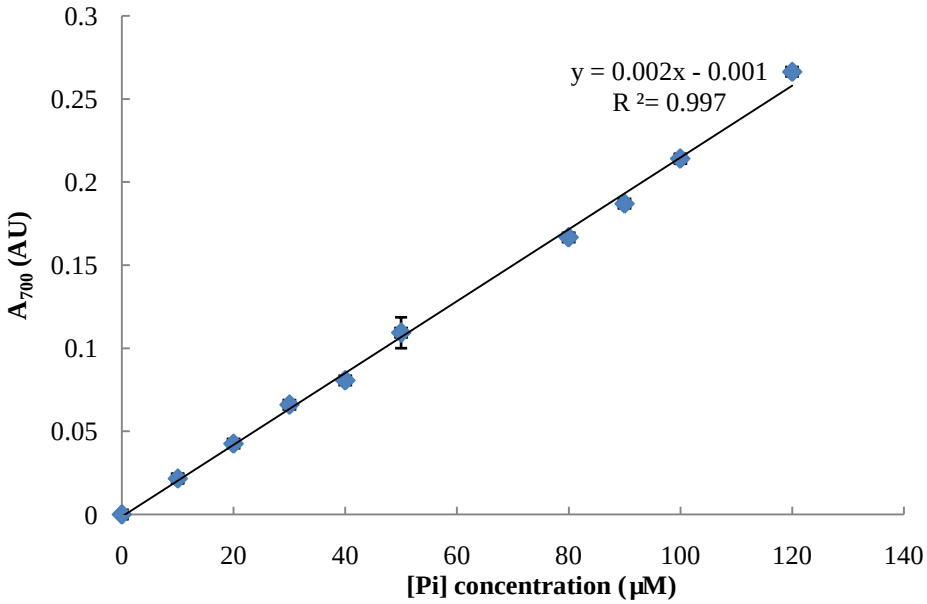

Figure A3. Phosphate standard curve